THE PHYSIOLOGY OF THE BLUE MUSSEL (*MYTILUS EDULIS*, LINNÉ 1758) IN RELATION TO OCEAN ACIDIFICATION

ZUR PHYSIOLOGIE DER MIESMUSCHEL (*MYTILUS EDULIS*, LINNÉ 1758) IM ZUSAMMENHANG MIT DER OZEANVERSAUERUNG

Diplomarbeit

Vorgelegt von Julia Saphörster

Oktober 2008

The physiology of the blue mussel (*Mytilus edulis*, Linné 1758) in relation to ocean acidification

Zur Physiologie der Miesmuschel (*Mytilus edulis*, Linné 1758) im Zusammenhang mit der Ozeanversauerung

Diplomarbeit

vorgelegt von
Julia Saphörster
geb. am 01.12.1983 in Münster

Universität Rostock
Institut für Biowissenschaften
Abt. Meeresbiologie

Oktober 2008

in Zusammenarbeit mit/ in cooperation with:
Universität Rostock, Abteilung Meeresbiologie
Leibniz-Institut für Meereswissenschaften an der Universität Kiel
Exzellenzcluster „Ozean der Zukunft"

Erstgutachter: Dr. Stefan Forster

Zweitgutachter: Prof. Dr. Frank Melzner
IFM-GEOMAR
FB2/BI/ JRG A1
Hohenbergstr. 2
24105 Kiel

Abstract

Anthropogenic CO_2 emissions have already altered ocean chemistry, leading to lower carbonate saturation states, elevated seawater pCO_2 and decreased pH. This scenario will even be enhanced in the future due to rising atmospheric CO_2 levels. Recent studies suggested drastic impacts of increased seawater pCO_2 values especially on the ecophysiological performance of calcifying organisms.

In this study, whole-animal performance of the blue mussel, *Mytilus edulis*, from the Baltic Sea was related to rising pCO_2 levels in order to predict physiological changes on the organism level in a future high CO_2 world. Thus, cardiac performance and activity patterns were observed in adult specimens exposed to different pCO_2 values (380 ppm [39 Pa; pH 8.0], 560 ppm [57 Pa; pH 7.9], 840 ppm [85 Pa; pH 7.8], 1120 ppm [114 Pa; pH 7.7], 1400 ppm [142 Pa; pH 7.6] and 4000 ppm [405 Pa; pH 7.1]) for two weeks.

The results revealed that heart rates and heart rate variability, as well as activity patterns were not significantly affected by CO_2 levels applied in this study. The mean instantaneous heart rate (IHR) was determined using infrared light sensors (plethysmographs). Throughout the experiment, IHR fluctuated around a mean value of 12 beats per minute (BPM). There was also no change in the distribution of beat-to-beat intervals (heart rate variability, HRV). This study examined changes in the HRV by comparing different parameters, including parameters so far only used in humans, composed of mean, median, mode, range, skewness, kurtosis, coefficient of variation (CV), standard deviation of beat-to-beat intervals (SDNN), standard deviation of differences between adjacent beat-to-beat intervals (SDdeltaNN) and root mean square successive differences (RMSSD). Valve and siphon activity was investigated using time lapse images recorded with a set of webcams. The valve and siphon diameter in percentage of their maximum opening per mussel varied around 57 % (Valve) and 46 % (Siphon). On average valve and siphon were open about 50 % of the time even when exposed to CO_2. Since the food was supplied at a continuous rate, cleared algal cells could be measured using a coulter counter. While mussels from all treatment groups <1400 ppm were able to clear a similar percentage of algae cells in their experimental aquaria (49 %), there was a drastic decline in filtration rate in the 4000 ppm treatment, where the mussels were able to remove only 3 % of the supplied algae cells.

Field measurements carried out at the sampling site during the trial period revealed high pCO_2 levels of up to 2345 ppm (238 Pa) and low pH values of even 7.4 at some days probably due to upwelling of undersaturated bottom water. Thus, animals are already confronted with extraordinarily high CO_2 levels in their natural habitat. As they are

probably well adapted to a fluctuating carbonate system, this might partly explain why CO_2 levels in this study were not sufficient to trigger a response in cardiac performance and activity patterns. But on the longer term, inhibition of feeding at very high CO_2 levels will probably lead to a concomitant decrease in heart rates and valve/siphon activity. Due to its low buffering capacity and observed corrosive upwelling events, critical pCO_2 may be reached in the Baltic Sea in the future, if atmospheric carbon dioxide concentrations continue to rise as anticipated.

Zusammenfassung

Anthropogene CO_2 Emissionen haben bereits die chemischen Eigenschaften des Ozeans im Vergleich zu präindustriellen Werten verändert, so dass schon heute verringerte Sättigungsgrade, erhöhte CO_2 Partialdrücke und erniedrigte pH Werte im Meerwasser festgestellt wurden. Ein fortschreitender Anstieg der atmosphärischen CO_2 Konzentration wird dies in Zukunft sogar noch verstärken. Aktuelle Studien weisen darauf hin, dass steigende CO_2 Partialdrücke im Meerwasser drastische Auswirkungen auf marine Lebewesen haben, insbesondere auf die Ökophysiologie von kalzifizierenden Organismen.

Das Ziel dieser Arbeit war es physiologische Veränderungen auf der Organismus Ebene in einer zukünftigen CO_2 reichen Umwelt zu simulieren. Dafür wurde an der Miesmuschel, *Mytilus edulis*, aus der Ostsee die Funktionalität des Organismus in Beziehung zu steigenden pCO_2 Werten gesetzt. Aktivitätsmuster und die kardiologische Leistung adulter Tiere wurden über zwei Wochen bei verschiedenen pCO_2 Werten (380 ppm [39 Pa; pH 8,0], 560 ppm [57 Pa; pH 7,9], 840 ppm [85 Pa; pH 7,8], 1120 ppm [114 Pa; pH 7,7], 1400 ppm [142 Pa; pH 7,6] und 4000 ppm [405 Pa; pH 7,1]) untersucht.

Die Ergebnisse ließen erkennen, dass weder Herzraten und Herzratenvariabilität (HRV) noch Aktivitätsmuster signifikant beeinträchtigt wurden durch die hier verwendeten CO_2 Partialdrücke. Hierfür wurde mit Hilfe von Infrarotlicht-Sensoren die mittlere instantane Herzrate (IHR) bestimmt. Diese fluktuierte während des gesamten Versuchszeitraumes um einen mittleren Wert von 12 Schlägen pro Minute (BPM). Desweiteren konnte keine Beeinflussung der Verteilung der Herzschlagsintervalle (Herzratenvariabilität, HRV) nachgewiesen werden. In dieser Studie wurde zudem das Augenmerk auf den Vergleich mehrerer Parameter gelegt, wobei humanmedizinischer mit eingeschlossen wurden. Diese Parameter bestanden aus Mittel, Median, Modal, Intervallspanne, Skewness, Kurtosis, Variationskoeffizienten (CV), Standardabweichung der Intervalle (SDNN), Standardabweichung der Unterschiede angrenzender Intervalle (SDdeltaNN) und Root Mean Square Successive Differences (RMSSD). Weiterhin wurden Schalen- und Siphonöffnungsmuster durch Zeitrafferaufnahmen bestimmt. Der vertikale Durchmesser der Schalen- und Siphonöffnung schwankte über den ganzen Versuch um einen Mittelwert von 57 % der maximalen Schalenöffnung und 46% der maximalen Siphonöffnung. Im Mittel waren Schale und Siphon ca. 50 % der Zeit geöffnet. Futter wurde kontinuierlich zugeführt und Algenkonzentration im Versuchsaufbau wurde mit Hilfe eines Coulter Counters bestimmt. Während Muscheln in allen Behandlungen bis 1400 ppm die gleiche Zellkonzentration aus ihrem Aquarium filtern konnten (49%), wurde eine drastische

Abnahme der Filtrationsrate (3 % filtrierte Algenzellen) in der 4000 ppm Behandlung beobachtet.

Feldmessungen am Probenort während des Versuchszeitraumes ergaben, dass an bestimmten Tagen sehr hohe pCO_2 Werte bis zu 2345 ppm (238 Pa) und sehr niedrige pH Werte bis 7.4, wahrscheinlich als Resultat von lokalen Auftriebsphänomenen auftraten. Die Tiere scheinen demnach schon mit außergewöhnlich hohen CO_2 Konzentrationen in ihrem natürlichen Habitat konfrontiert zu werden und sind somit möglicherweise auch schon gut an große Fluktuationen im Karbonatsystem adaptiert. Dies könnte erklären, warum die in dieser Studie benutzen pCO_2 Werte nicht ausreichten, um eine Reaktion hinsichtlich des Aktivitätsmusters und der kardiologischen Leistung zu erzeugen. Auf längere Sicht, könnte sich die beobachtete Limitierung der Filtrationsrate bei hohen CO_2 Konzentrationen jedoch negativ auf die Herzraten und die Schalen-/Siphon-Aktivität auswirken. Falls die CO_2 Konzentrationen in der Atmosphäre jedoch weiter ansteigen, wie erwartet, könnten solche kritische pCO_2 Werte möglicherweise in der Ostsee auftreten, da die Ostsee zusätzlich zu den genannten Auftriebsphänomenen eine geringe Pufferkapazität aufweist. Dies ändert womöglich die Verteilung der Miesmuscheln in der Ostsee und könnte somit Verschiebungen der dominanten Arten des Ökosystems zur Folge haben.

Contents

Figures

Pictures

Tables

Equations

Abbreviations

Ω	saturation state of calcium carbonate
ANOVA	analysis of variations
A_T	total alkalinity
BPM	beats per minute
C_T	dissolved inorganic carbon
CV	coefficient of variation
HR	heart rates
HRV	heart rate variability
IHR	instantaneous heart rate
NN interval	Normal heart beat-to beat interval
pH_e	extracellular (haemolymph) pH
pH_i	intracellular pH
RMSSD	root mean square successive differences
SDdeltaNN	standard deviation of the differences between adjacent intervals
SDNN	standard deviation of normalized intervals

1 Introduction

Atmospheric pCO_2 have already increased dramatically during the last 200 years from a preindustrial value of 280 ppm to a current value of 380 ppm mostly due to deforestation and burning of fossil fuels (Siegenthaler and Sarmiento 1993, Fabry et al. 2008). As indicated by data taken from ice-cores, this increase is greater than any other observed during the last 420000 years (Petit et al. 1999).

Further increases in the surface ocean ranging from 490 to 1250 ppm by the year 2100 (Houghton et al. 2001) and up to 1900 ppm by the year 2300 (Caldeira und Wickett 2003, figure 1.1) are expected. Although atmospheric CO_2 concentrations had already exceeded more than 7500 ppm during the past 300 Myr, those changes developed slowly and over millions of years (Crowley and Berner 2001). The expected rapid changes may, therefore have devastating effects on the marine biota.

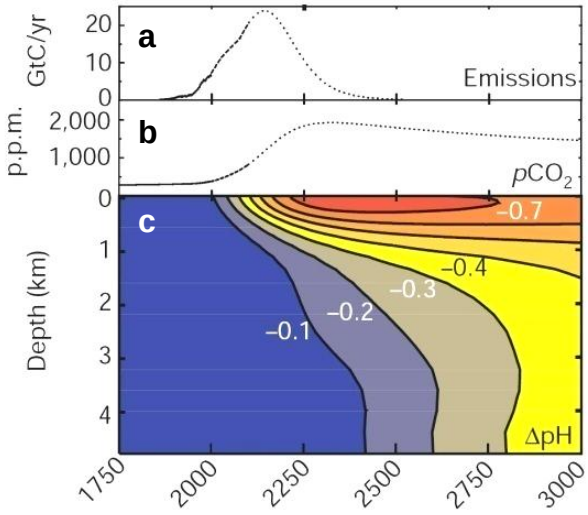

Figure 1.1 Past and future emissions [GtC/yr] (a), atmospheric pCO_2 levels [ppm] (b) as well as changes in ocean pH (c). Future values are predicted from modelled emission scenarios. Changes in pH are horizontally averaged. Adopted from Caldeira and Wickett (2003).

About one third of the anthropogenic CO_2 emissions so far has been stored in the ocean (Sabine et al. 2004), leading to a decrease in seawater pH of 0.1 units from 8.2 to 8.1 pH since preindustrial levels (Haugan and Drange 1996, Orr et al. 2005). If a "business-as-usual scenario" is assumed, a further decrease of about 0.77 units to a pH of even 7.3 is expected until the year 2300 (Caldeira and Wickett 2003, figure 1.1).

1.1 The Marine Carbonate System

Total dissolved inorganic carbon

The ocean is in equilibrium with the atmosphere following Henry's law (equ. 1.1), where the concentration of a gas in the ocean ($[G]_{ocean}$) is dependent on the partial pressure of the gas in the atmosphere (pG_{atm}) and the solubility coefficient (α). The solubility coefficient itself is a function of temperature and salinity, where a decrease in either of these parameters leads to an increase in the solubility of the gas (Weiss 1974).

Equ. 1.1 Henry's law

$$[G]_{ocean} = \alpha * pG_{atm}$$

$[G]_{ocean}$ = concentration of gas in the ocean [mol/m³]
H_G = solubility coefficient [mol/(m³ Pa)]
pG_{atm} = partial pressure of gas in atmosphere [Pa]

In contrast to most other gases, carbon dioxide not only dissolves physically but also reacts chemically with the water molecules (equ.1.2, Dickson 2007) forming carbonic acid (H_2CO_3). Since it is a diprotic acid, it first releases a proton, thereby dissociating to bicarbonate (HCO_3^-), which again releases a proton dissociating to carbonate (CO_3^{2-}). These three different inorganic carbon species (dissolved carbonate, bicarbonate and carbon dioxide) are overall referred to as C_T (total dissolved inorganic carbon; synonyms in the literature are DIC, TCO_2 or $\sum CO_2$).Their equilibrium concentration in sea water is dependent on pH, pressure, temperature and salinity determined by their thermodynamic equilibrium constants K^*_1 and K^*_2.

Equ. 1.2 Dissolution of CO_2 in water

$$CO_2\,(g) \leftrightarrow CO_2\,(aq) + H_2O \leftrightarrow \underset{\textit{carbonic acid}}{H_2CO_3} \overset{K1}{\leftrightarrow} H^+ + \underset{\textit{bicarbonate}}{HCO_3^-} \overset{K2}{\leftrightarrow} 2H^+ + \underset{\textit{carbonate}}{CO_3^{2-}}$$

K^*_1, K^*_2 = dissociation constants

Temperature, pH and the C_T components are all strongly correlated. This relationship is usually shown in a Bjerrum plot (Figure 1.2). At today's ocean pH of about 8.0, 9% of the C_T is made up of carbonate, whereas bicarbonate accounts for 90% (Zeebe and Gladrow 2001). Rising atmospheric pCO_2 values, leading to an increased oceanic uptake, change the

pH and the equilibrium concentration of the components of the carbonate system, because a change in pH is buffered by conversion of the carbon species into each other. As described above uptake of CO_2 leads to the formation of carbonic acid and release of a proton, this acidic reaction is buffered by the reaction of carbonate with H^+ and formation of bicarbonate. Therefore, if pCO_2 continues to rise the carbonate surface-water concentration will decline by about 60% in 2100, even though the C_T will rise by 12%, visible in an increase in carbon dioxide and bicarbonate concentration (Feely et al. 2004).

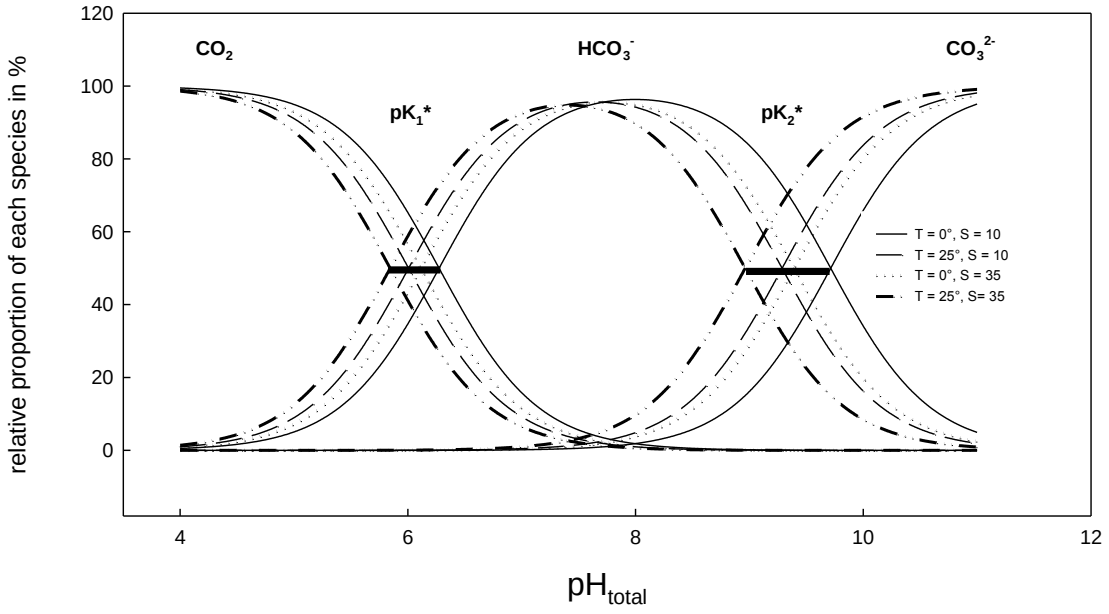

Figure 1.2 Bjerrum plot: Speciation of $[CO_2]_{aq}$, $[HCO_3^-]$ and $[CO_3^{2-}]$ as a function of pH for different temperatures and salinities. Dissociation constants were taken from Roy et al. (1993) pK1* and pK2* are the negative common logarithms of K_1* and K_2*, respectively. This transformation makes the constants directly comparable with the pH where $[CO_2]$ and $[HCO_3^-]$ for pK_1* and $[HCO_3^-]$ and $[CO_3^{2-}]$ for pK_2* occur in equal proportions. The range of pK_1* and pK_2* are indicated by thick black lines. Straight line: T=0 °C, S=10; Dashed line: T=25 °C, S=10; Dotted line: T=0 °C, S=35; Dashed-dotted line: T=25 °C, S=35. Graphic was kindly provided by Lennart Bach.

Saturation state

This decline affects calcifying organisms relying on the formation of calcium carbonate. In today's ocean the carbonate concentration is higher than expected, thus the ocean is supersaturated with $CaCO_3$. This is expressed as a saturation state (Ω) higher than one. Ω is calculated after Mucci (1983) using the ion product of the in-situ concentration of calcium and carbonate divided by the stoichiometric solubility product (K^*_{sp}) (equ. 1.3): K^*_{sp}, on the other hand, is defined as the ion product at that concentration, at which precipitation of calcium carbonate takes place.

Equ. 1.3 Saturation state

$$\Omega = \frac{[Ca^{2+}] * [CO_3^{2-}]}{K_{sp}^*}$$

Ω = saturation state
K_{sp} = stoichiometric solubility product

At Ω values below 1 the water is undersaturated in respect to carbonate. Hence, physical dissolution of calcium carbonate structures takes place. There are two main polymorphs of calcium carbonate: (1) Calcite is characterized by a hexagonal structure being found for example in coccolithophores, foraminifera and the prismatic shell layer of *M. edulis*, whereas (2) aragonite possesses a more rhombic structure and occurs for example in pteropoda, corals and the nacre shell layer of *M. edulis*. Furthermore, Ω is dependent on temperature, salinity and pressure, calcite being the more stable form. Since calcium is a conservative element changing only in proportion to salinity, the more important factor influencing Ω in seawater is carbonate, which changes with temperature, salinity, pressure and pH (see Bjerrum plot figure 1.2). Decreasing carbonate concentrations at higher pCO_2 values will, therefore, lead to the lowering of Ω. As a result, high latitude surface-waters are expected to become corrosive for aragonite by the end of this century potentially leading to dissolution of polar pteropod shells (Orr et al. 2005).

Alkalinity

The natural buffer of the ocean is described as the total alkalinity (A_T). A_T is the excess amount of weak bases in water, which are capable of accepting a proton. A weak base is characterized as being a proton acceptor with a dissociation constant (K) $\leq 10^{-4.5}$ at 25 °C (Dickson 1981) and, therefore, A_T can be defined as follows (equ.1.4):

Equ. 1.4 Total alkalinity (AT)

$$\begin{aligned} A_T = {} & [HCO_3^-] + 2[CO_3^{2-}] + [B(OH)_4^-] + [OH^-] + [HPO_4^{2-}] + 2[PO_4^{3-}] \\ & + [SiO(OH)_3^-] + [NH_3] + [HS^-] + \dots \\ & - [H^+]_F - [HSO_4^-] - [HF] - [H_3PO_4] - \dots \end{aligned}$$

Carbonate and bicarbonate concentration have a strong effect on A_T, since they are the main components being described as the carbon alkalinity (A_C, equ.1.5), where the carbonate concentration counts twice due to its double negative charge.

Equ. 1.5 Carbon alkalinity (A_C) $$A_C = [HCO_3^-] + 2[CO_3^{2-}]$$

A_T is measured by titration with a strong acid, since it dissociates completely in aqueous solutions.

In nature, the charge of ions in the ocean displays an excess of cations over anions (2140 µmol/kg SW at a salinity of 35), which is exactly compensated by A_T. This is also the reason why less saline waters like the Baltic Sea possess a lower A_T as a result of overall reduced ion concentrations, which lessen the charge difference (Zeebe and Gladrow 2001).

Parameters

The carbonate system is characterized by altogether six variables including [C_T], [A_T], [HCO_3^-], [CO_3^{2-}], pH and pCO_2 and four equations (including equations for K^*_1, K^*_2 equ. 1.3 and 1.5). Changing one of these parameters influences at least some of the other variables. Only two of the parameters [C_T], [A_T], pH and pCO_2 have to be known, to calculate the whole carbonate system at a particular temperature, salinity and pressure, provided, that the solubility and equilibrium constants are known.

1.2 Specific Features of the Baltic Sea

The Baltic Sea is a landlocked sea characterized by brackish water. Due to its high river runoff in the east and its connection to the North Sea, a decrease in salinity from 17 in the western parts to 5-3 in the north-eastern parts is observed. The mean salinity of 15 at the sampling site in the western Baltic Sea is, therefore, strongly dependent on saline deep water transport from the North Sea and river runoff at the surface. Hence, a halocline separates bottom and surface water in summer and autumn, as already reported for the Eckernförde Bay (Hansen et al. 1999).

As indicated above alkalinity is highly dependent on salinity and, thus, the same trend from west to east is expected. However, rivers transport carbonates into the Baltic Sea and alter the alkalinity independent of salinity (Hjalmarsson et al. 2008). At the sampling site in Kiel Bight, the mean surface alkalinity varies from 1800 to 2000 µmol/kg SW (Rodhe 1998). During summer time heating leads to the formation of a thermohaline, which combines with the halocline to a pycnocline at 15 m water depth. This has already been observed in the Eckernförde Bay (Hansen et al. 1999). In the bottom water oxygen is consumed due to decomposition of organic material leading to oxygen saturation values as low as 5% until the water column is mixed again in autumn due to stronger winds and cooling of surface waters.

The Baltic Sea is a relatively young sea (12,000 yr) and, thus, there are only a few endemic brackish water species. Furthermore, due to its low alkalinity it also possesses a low buffering capacity exhibiting only small protection against pH changes than full strength saline oceans. As a result, effects due to CO_2 increases may have an even stronger impact on marine biota in the Baltic Sea.

1.3 Effects on Marine Biota

Thus, decreasing ocean pH and carbonate concentration along with increasing undersaturation and global warming, happening faster than ever before, will probably have a great impact on marine fauna particularly in the Baltic Sea. A change in ecosystem community structure due to elevated seawater pCO_2 (=hypercapnia) has already been observed in ocean areas with naturally increased pCO_2 levels. Around Ischia Island, CO_2 is released from volcanic activity (Hall-Spencer et al. 2008). In this area a decline in calcification was observed leading to shell dissolution in gastropods at pH 7.4. Reduced calcification in response to elevated pCO_2 levels has been described for many organisms e.g. phytoplankton (Riebesell et al. 2000) and mollusks (Orr et al. 2005). Furthermore, Hall-Spencer et al. (2008) revealed a change in community structure, since there was a decline in the abundance of two sea urchin species at pH 7.5. On the other hand, it was also observed that elevated CO_2 had beneficial effects on plants, which are often CO_2 limited. As a result, sea-grass production was highest in an area with a pH of 7.6.

Furthermore, the long-term survival of organisms in an acidified future ocean is mostly dependent on the response of larvae, fecundity and fertilization at low pH. For the sea urchin, *Hemicentrotus pulcherrimus*, a retardation of pluteus larval growth as a result of hypercapnia has already been revealed (Kurihara et al. 2004). And in veliger larvae of the oyster, *Crassostrea gigas,* a higher amount of larval malformations was observed at elevated pCO_2 levels (Kurihara et al. 2007).

Sensitivity towards ocean acidification largely depends on the way animals cope with extra- and intracellular acid-base disturbances (see review by Pörtner et al. 2004). Organisms like fish (e.g. Michaelidis et al. 2007) and most crustaceans (e.g. Spicer et al. 2007) are able to compensate their extracellular pH (pH_e) after an initial drop. This is achieved by active transport mechanisms. This behavior is an adaptation to pCO_2 values, which naturally occur during respiratory acidosis. On the other hand, organisms with lower metabolic rates deal with decreasing pH by increasing the bicarbonate concentration, probably resulting from dissolution of the shell or testes, as a buffer substance. This has been observed in many marine invertebrates like sipunculids (Pörtner et al. 1998),

echinoderms (Miles et al. 2007) and bivalves (Booth et al. 1984, Walsh et al. 1984, Lindinger et al. 1984). But the accumulation of bicarbonate not fully recovers pH_e. On the other hand, the intracellular pH (pH_i) is regulated independently. An initial drop in pH_i is completely compensated within a few days in mussels and sipunculids (Lindinger 1984, Pörtner et al. 1998, Michaelidis 2005). But due to different non-bicarbonate buffer values, resulting from different concentrations of proteins and phosphates, the response of pH_i can even vary in different tissues.

Abiotic stresses like those induced by increasing CO_2 levels lead to the downregulation of energy demanding processes on a cellular level, thereby reducing the demand of ATP. This process is called metabolic depression (Guppy et al. 1994, Boutillier 2001). The key signal involved could be pH_e (Reipschläger and Pörtner 1996). Measurements of oxygen consumption and Na^+/K^+-ATPase activity already revealed that hypercapnia is able to initiate metabolic depression in *Sipunculus nudus* (Pörtner et al. 2000, Langenbuch et al. 2002). And even in *Mytilus galloprovincialis* a reduction in oxygen consumption was observed during hypercapnia, which also indicates metabolic depression (Michaelidis et al. 2005).

Therefore, it is crucial to investigate whole-animal physiological parameters such as heart rates and activity patterns, since they most probably will be influenced by a suppression of metabolic rates, maybe even before metabolic depression occurs.

1.4 Physiology and Ecology of *Mytilus edulis*

The common blue mussel, *Mytilus edulis* (Linné 1758), (figure 1.3) is the dominant benthic organism covering the hard-bottom benthos in the Baltic Proper, making up 95% of the total animal biomass (Kautsky 1982a, Kautsky and van der Maarel 1990). Baltic Sea blue mussels possess thinner shells and smaller shell lengths than North Sea mussels probably due to the reduced salinity (Bøhle 1972, Seed 1968). Its shell is composed of three layers: The first layer is the thin and organic periostracum, which covers the calcific prismatic layer. The inner nacre layer is composed of aragonite. (Wilbur 1972). The aragonite to calcite ratio is very variable ranging from 32 to 83% aragonite, as measured in the Tay estuary, Scotland (Hubbard et al. 1981). Furthermore, *M. edulis* is an important ecosystem engineer. It provides a habitat for other animals due to its hard shell and also by forming dense mussel beds (Gutiérrez et al. 2003). This is important especially in areas,

Figure 1.3 Habitus of the blue mussel, *Mytilus edulis*. Adopted from Meyer and Möbius (1872).

which most other animals cannot assess, such as the Wadden Sea. Furthermore, they are filter feeders ingesting phytoplankton and suspended particles. Thereby they change the inorganic nutrient pool available for phytoplankton through regeneration and storage of nutrients in mussel biomass (Prins et al. 1998). Hence, mussels were found to be a natural eutrophication control as has been shown for the San Francisco bay (Officer et al. 1982) and the Bay of Brest (Hily 1991). As a result, they produce faeces and pseudofaeces, which settle to the seafloor. This process, known as biodeposition, accounts for 1.8 g shell free dry mass, (SFDM), 0.33 g ash free dry mass (AFDM), 0.13 g carbon, $1.7*10^{-3}$ g nitrogen and $2.6*10^{-4}$ g phosphorus per g mussel and year in the Baltic Proper (Kautsky and Evans 1987). The increased sedimentation has a significant impact on benthic fauna (Ragnarsson and Raffaelli 1999) and can reduce erosion by 10-fold (Widdows and Brinsley 2002). In addition, mussels also play a major role in the global aquaculture production accounting for 391,210 t in 2005 (Food and Agriculture Organization of the United Nations 2006)

Thus, physiological changes in *M.edulis* due to ocean acidification might not only affect the mussel community, but the whole ecosystem. In this study, cardiac performance and activity patterns as whole animal stress indicators were investigated.

1.4.1 Physiology of the Heart

The bivalve heart is composed of a median ventricle and two lateral auricles being enclosed in the pericardial cavity (figure 1.4a). It is situated on the mid-dorsal line behind the posterior termination of the hinge. The colourless plasma, called haemolymph, serves as 'blood' and contains different cells (referred to as haemocytes or phagocytes). Blue mussels do not possess a respiratory pigment. Therefore, the oxygen-carrying capacity of the haemolymph is equal to that of seawater. The haemolymph leaves the ventricle via a single anterior aorta and is further carried to the rest of the body through different arteries. The blood system of *Mytilus edulis* is open meaning that the haemolymph is collected in three different sinuses, from which it is distributed to the kidneys, then the gills and back to the heart by a major vein. Even though, the haemolymph does not necessarily have to pass the gills. To maintain a constant heart rhythm, the rigidity of the pericardium, which is supported by the shell, is a prerequisite. As the 'constant-volume' hypothesis (Krijgsman and Divaris 1955) implies, the pericardium is considered to be a closed chamber. During contraction of the heart, called systole, pressure in the pericard is reduced leading to the following filling of the heart, called diastole (for further reading see Bayne 1976, pp. 207-223). Therefore, there are two ways of regulating blood circulation: (1) by regulating the beat frequency or (2) by regulating the stroke volume.

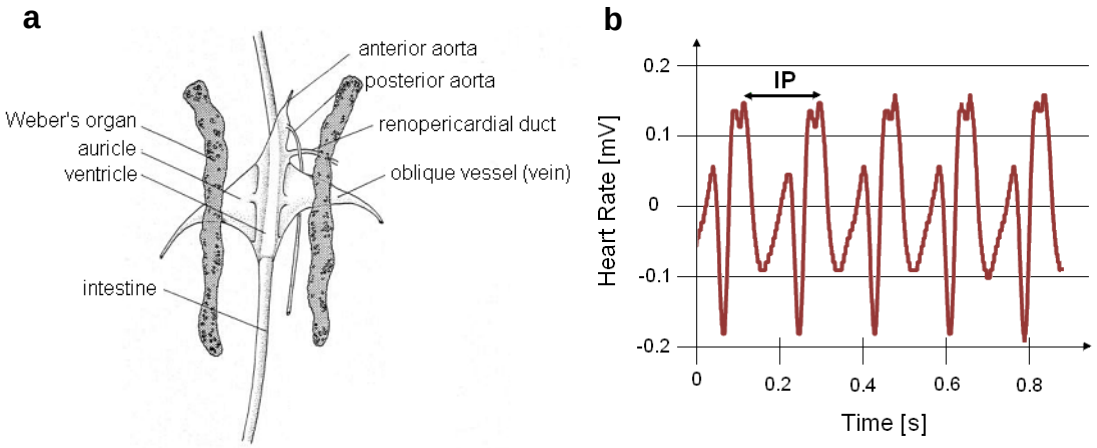

Figure 1.4 Cardiac morphology (a) and heart rate tracing (b) of *Mytilus edulis.* a) Dorsal view on the pericardium. Graphic was kindly provided by Baldo Marinovic, University of California, Santa Cruz. b) Heart rate recording [mV] as a function of time [s]. IP = interpulse duration.

1.4.2 Basics of Heart Rate Variability

Changes in heart beat pattern (figure 1.4b) can be observed by directly investigating the heart rate or by analyzing alterations in the beat-to-beat (= interpulse or interval) duration or heart rate variability (HRV). In this study, heart rate is calculated directly from the interpulse durations as a function of time. This way the beat-by-beat heart rate, called instantaneous heart rate (IHR), in beats per minute (BPM) is yielded. But changes in the interpulse duration can be observed even before changes in the mean heart rate become visible (Depledge et al. 1996). As a result, HRV is used as a more sensitive and reliable indicator. In human and mammals, HRV is strongly influenced by the autonomous nervous system and ventilation (Task Force 1996, Berntson et al. 1997, Kleiger 1995). Therefore, many studies have been conducted lately using HRV in different branches of medicine, e.g. cardiovascular disease, neurology, Diabetes mellitus and others (see review by Ravenswaaij-Arts et al. 1993). Since HRV cannot be quantified using only one parameter, many HRV parameters have been developed during recent years. Therefore, the Task Force of the European Society of Cardiology and the North American Society of Pacing and Electrophysiology (1996) published a document including appropriate standards for use in humans. Two major methods of measuring HRV are known: (1) time domain measurements, where the intervals between successive heart beats are determined, and (2) frequency domain measurements, which are not included in this study.

1.4.3 Physiology of Valve and Siphon Gape

The paired bivalve shells are connected by a dorsal connation, the ligament or hinge, which is responsible for passive gaping of the valves. To regulate the valve gape and to close the shells, two adductor muscles are involved: (1) the posterior adductor muscle (PAM) and (2) the anterior adductor muscle (AAM), named after their insertion with the shells. The muscles are capable of sealing bivalve hermetically over weeks, applying a force of 12 kg/cm² in oysters (Gruner et al. 1993).

The inner organs are covered by ventrally drooping epidermic structures, the mantle lobes, descending from the dorsal side. These are connected at the posterior side forming an opening, the exhalant siphon (figure 1.5.a and b), whereas the ventral and loose part of the mantle lobes are called the inhalant siphon. Water and particles enter the gills through the inhalant siphon, which also contains light sensitive and other sense organs. Following passage through the gills, the exhausted water and faeces are ejected again through the exhalant siphon.

Biological monitoring of the valve and siphon opening has already been successfully used as an indicator for water quality (e.g. Kramer et al. 1989) or in response to stressors, such as copper (Curtis et al. 2000).

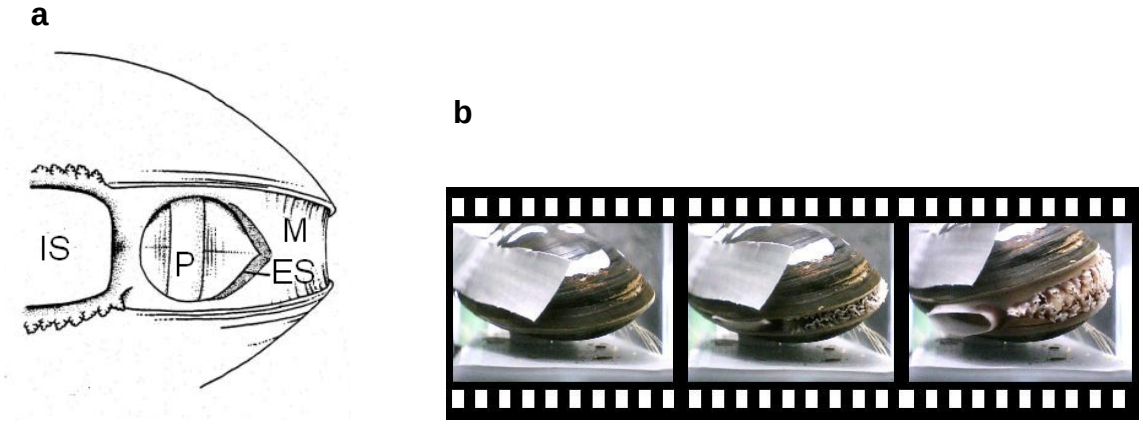

Figure 1.5 Morphology (a) and time lapse images (b) of the exhalant mantle region of *Mytilus edulis*. a) Lateral view on the exhalant mantle region. M=mantle, ES=exhalant siphon, P=posterior adductor muscle, IS=inhalant siphon (also called inhalant opening). Graphic was kindly provided by Baldo Marinovic, University of California, Santa Cruz. B) Time lapse images of valve and siphon opening. The exhalant siphon is displayed on the left and the inhalant siphon on the right side.

1.5 Hypotheses

The proposed work was aimed at investigating whole-animal performance of the blue mussel, *Mytilus edulis*, in the Baltic Sea in response to ocean acidification. Therefore, cardiac performance and activity patterns were monitored at in mussels exposed to different future ocean pCO_2 levels of up to 1400 ppm lying in the range of predicted values for the year 2300 (Caldeira and Wickett 2003). In order to gain a more mechanistic understanding of increased pCO_2 values on the organismic level, a higher value of 4000 ppm CO_2 was also employed. In addition this treatment served to trigger well-defined physiological responses, which might otherwise remain hidden in low pCO_2 treatments under the high variability typical for any physiological measurement. The objective of this study was to gain more insight into how mussels might be affected by further increasing carbon dioxide levels in the future. But it needs to be noted, that pCO_2 values in nature will change relatively slowly, possibly leaving sufficient time for species with a low generation time to adapt. Thus, this work can only give insight into short-term (two weeks) responses of one generation of adult mussels to elevated seawater pCO_2. With a lifespan of 20 years (Bayne 1976) present day mussel population will only experience maximum average surface pCO_2 values of 408 ppm changing on average about 1.4 ppm/yr (calculated from data of monthly mean CO_2 rise at Mauna Loa provided by U.S. Department of Commerce). Due to a low generation time of 2 years (Newell 1989), there will be possibly sufficient genetic variation in future mussels population to allow for adaptation.

The hypotheses for this investigation are outlined as follows:

1. *Heart rates are reduced at high* pCO_2 *levels.*

Abiotic stresses are able to initiate metabolic depression (Guppy et al. 1994) and the elicitor is considered to be low pH_e (Reipschläger and Pörtner 1996). Low pH_e as a result of environmental hypercapnia has already been investigated in *M. edulis* (Lindinger et al. 1984). Hence, high levels of hypercapnia should be able to trigger metabolic depression in blue mussels. Depression of metabolic rate is combined with a marked slowing of the heart rate (Storey and Storey 2004) as has also been observed for Mytilids (Bayne 1976). Therefore, heart rate should be reduced at high carbon dioxide levels.

2. *The distribution of interpulse durations is increasingly altered with rising* pCO_2 *levels.*

Distribution of beat-to-beat interval durations is normally very uniform in blue mussels (Curtis et al. 2000) indicating favourable HRV. The interaction of inhibitory and excitatory nerves under stress results, therefore, in a wider distribution. This study aims at comparing

a whole range of HRV indicators in mussels, as have already successfully been used in humans and mammals. Since the HRV has been shown to react before a change in the mean heart rate is visible in blue mussels (Depledge et al. 1996), a greater variety in HRV is expected even in the lower CO_2 treatments.

3. *Valve closure is more often initiated with rising* pCO_2.

Metabolic depression, as described under part 1, is accompanied not only by slowing of the heart beat, but also by valve closure in marine bivalves such as *Mytilus galloprovincialis* (Anestis et al. 2007). Even in the absence of metabolic depression, blue mussels often close their shells in response to unfavourable environmental conditions such as low food supply (Riisgård et al. 2003). In addition to the rate of valve opening, mussels also regulate the valve position (gape diameter) (Wilson et al. 2005). Hence, with higher pCO_2 lower rates of valve opening as well as a lower gape diameters expected.

4. *The siphon opening decreases with rising* pCO_2.

When the valve is open, the inhalant/exhalant siphons can also be controlled independently. Closing the exhalant siphon while the shell is open allows the mussel to maintain its salinity in brackish water, while providing a higher exposed mantle cavity volume for oxygen supply (Shumway 1977, Newell et al. 2001). Furthermore, regulation of the siphon opening is used to adjust pumping and associated feeding rates in blue mussels (Newell et al. 2001). Under stress, energy consuming processes like filtration are probably the first processes to be compromised. Therefore, decreasing siphon opening rates and diameters with increasing pCO_2 values are expected to occur under hypercapnic conditions.

2 Materials and Methods

2.1 General concept

Three laboratory experiments were performed during the course of this study in order to assess the effects of different seawater pCO_2 values on heart rates as well as valve and siphon opening status of a model bivalve organism. Furthermore, a flow-through aquarium system for long-term carbonate system manipulation experiments was designed and tested.

After an initial acclimation period in this system, animals were exposed to an altered carbonate system for two weeks. During this time period, heart rates were measured continuously and valve/siphon opening status was monitored during daytime. At the end of the incubation period, extracellular pH and pCO_2, haemolymph ion composition and mantle tissue Na^+/K^+ ATPase activity were measured (overview of methods see table 2.1).

Table 2.1 Overview of methods. The frequency of sampling and the method used for each parameter are listed. Text in brackets indicates author or company. Parameters marked with an asterisk (*) were measured by Jörn Thomsen (University of Kiel) in his Diplomarbeit.

Parameter	*Sampling*	*Method*
Heart Rates	continuously	Photoplethysmograph (Depledge 1984)
Valve/Siphon opening status	every hour during the light hours	Webcams (Logitech)
Algae concentration	once in every experiment	Coulter Counter (Beckmann)
Temperature Salinity pH	daily daily daily	Salinometer (WTW) Salinometer (WTW) PH meter (WTW)
DIC	beginning, middle and end of each experiment	Photometrical (Stoll et al. 2001) Coulometrical (Dickson et al. 2007)
Alkalinity	beginning, middle and end of each experiment	Potentiometric titration (Gran 1952, Dickson et al. 2007)
* Extracellular pH	end of the experiment	Micro-optodes (Presens)
* Haemolymph pCO_2	end of the experiment	CO_2 analyzer (Corning 965)
* Haemolymph ion composition	end of the experiment	Ion chromatography (Dionex)
* Na^+/K^+ ATPase	end of the experiment	Photometric enzyme assay (Allen and Schwarz 1969)
Length and wet mass	beginning and end of each experiment	Calliper and scale

2.2 Sampling

Mussels of the species *Mytilus edulis* (Linné 1758) were collected at the West Shore of Kiel Fjord (54°19.8`N; 10°9.0`E), Germany, near the Leibniz Institute of Marine Sciences (IFM-GEOMAR, Figure 2.1).

Figure 2.1 Location of the sampling site. The red spot marks the position of sampling near the IFM-GEOMAR campus. © Google Earth

Animals were scraped off the wooden pier from sub tidal depth (approximately 2 m) with aid of a rake on March 19th, April 16th, and June 16th, 2008. Only individuals belonging to the size group of 70 to 85 mm shell length were kept.

2.3 Cultivation and Acclimation

After cleaning the shells to avoid contributions of epibionts, specimens were immediately transferred to a 150 l maintenance tank, in which they were kept for 2 – 4 weeks. The tank was continuously flushed with coarse filtered Baltic seawater originating from 4 – 6 m depth nearby the sampling site at about 5-10 l/min. Temperature, salinity and pH were checked every day. To exclude the effect of fluctuating air temperature, cultivation took

place in a 10 °C cooling chamber at the IFM-GEOMAR. During cultivation, animals were fed 50 ml phytoplankton diet each day (DT's Live Marine Plankton Premium Blend). The tank was aerated with air stones. Two weeks prior to experimentation, mussels were slowly acclimated to 12 °C. For warm acclimation of the animals, the water temperature was increased by the addition of heaters which had a total power of up to 650 watt. With increasing water temperature of the Fjord above 12 °C these heaters were successively removed and afterwards a cooler (TITAN 1500, Aqua Medic) was installed. Findings by Widdows and Bayne (1971) indicate that this period was sufficient for thermal acclimation.

To minimize the movement of mussels during experimentation, they were fixated onto a podium as described in chapter 2.4.3. Mussels were allowed to recover from stress caused by connection and to acclimate to the podium for one week prior to experimentation. Afterwards, animals were connected to the heart rate sensors (section 2.4.3) and transferred to the experimental setup, where they were kept under control conditions for a few days in order to recover from handling stress and to assure that animals form different aquaria displayed comparable activity and heart rate patterns. This phase also served as a reference period before exposure to higher carbon dioxide levels.

2.4 Experimental Setup

Experiments were performed in a specifically designed open flow-through system (Figure 2.2) in a 10 °C cooling chamber at the IFM-GEOMAR, where an artificial day (14 hours) and night (10 hours) rhythm was simulated. In general, the experimental setup consisted of six aquaria filled with Fjord water from a storage tank and enriched with different carbon dioxide levels. To minimize disturbances caused by moving around in the chamber, the system was separated from the rest of the room using a black curtain. The experimental temperature of 12 °C was chosen as an intermediate according to environmental temperatures during the trial periods, which ranged normally from approximately 5 to 15 °C (Federal Maritime and Hydrographic Agency, BSH). Following the initial aeration period (below referred to as *phase I*) with pressurized air for 4 to 7 days (about 380 ppm CO_2), aquaria were acidified by aerating the seawater with different gas mixtures (see table 2.2) for two weeks (*phase II*), while a control aquarium continued to be aerated with pressurized air. Filtered seawater from Kiel Fjord (from 6-8 m depth at the sampling site) was continuously pumped into a storage tank of 300 l volume. Filtration consisted of a coarse sand filter to remove big particles and subsequent 50, 20 and 5 µm polyester filter cartridges to remove most of the smaller particles.

Table 2.2 Desired pCO_2 values in [ppm] and [Pa] used in the aquaria. An x marks the treatment employed in the respective experiment (n=6) and a check mark (✓) indicates the measurement of activity patterns and cardiac performance (n=4). CO_2 exposure periods are stated.

Aquarium #	p*CO 2 [ppm]*	p*CO 2 [Pa]*	*Experiment I 29.04 - 16.05.08*	*Experiment II 28.05 -12.06.08*	*Experiment III 02.07.- 18.07.08*
1	380	38.5	x ✓	x ✓	x
2	560	56.7	x	x	
3	840	85.1	x	x	x
4	1120	113.5	x	x	x
5	1400	141.9	x ✓	x ✓	x
6a	4000	405.3		x	x ✓
6b	4000	405.3			x ✓

Temperature in the tank was kept constant with the aid of a flow-through cooler (TITAN 1500, Aqua Medic) connected to a pump (universal pump 1260, Eheim). An overflow kept the water level constant. The water was aerated with pressurized air using air stones and mixed by a circulatory pump (universal pump 1260, Eheim), which also fed a header tank. Fully aerated water from the header tank was then supplied to the six different experimental aquaria via plastic tubing (4 mm inner diameter, Eheim) by means of gravity. To ensure a continuous supply of food, an algae suspension was constantly pumped (1 ml/min) into the header tank using a peristaltic pump (chapter 2.4.1). The header tank and each aquarium also possessed an overflow. The water outflow was directly opposite to an air stone hanging in front of the inflow ensuring sufficient mixing of fresh water and food. Flow rate to each experimental aquarium was set at 100 ml/min using two way valves. It was established in preliminary experiments that this flow rate was sufficient to prevent accumulation of mussel waste products (ammonia, CO_2), while at the same time not compromising the carbonate system parameters. Each CO_2 treatment was carried out in a separate aquarium with a volume of 16 l each. The aquaria were continuously equilibrated with CO_2-enriched air at a rate of 0.8 l/min according to the pCO_2 values mentioned using a central automatic five channel CO_2 mixing system (Linde Gas, HTK Hamburg). Consisting of computer controlled valve systems, addition of pure CO_2 gas to pressurized air is regulated by measuring the pCO_2 in air and opening the valve of a CO_2 gas bottle according to this value until the desired concentration is reached. In the first experiment the first channel of the CO_2-mixing equipment was used as a control (380 ppm CO_2) instead of the 4000 ppm treatment, thus only five aquaria were used instead of six. During the other experiments pressurized air served as a control. In the third experiment the 560 ppm channel was not used and instead a second aquarium was treated with 4000 ppm CO_2 as to fully exploit the capacity of the PowerLab for this pCO_2.

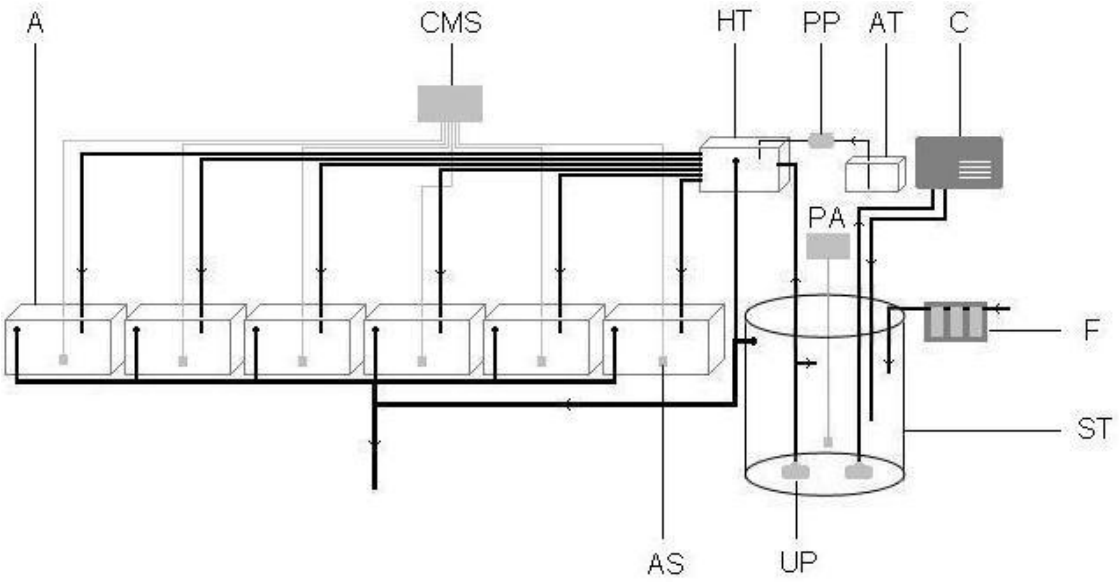

Figure 2.2 Schematic drawing of the experimental setup. For further detail see picture 2.1.

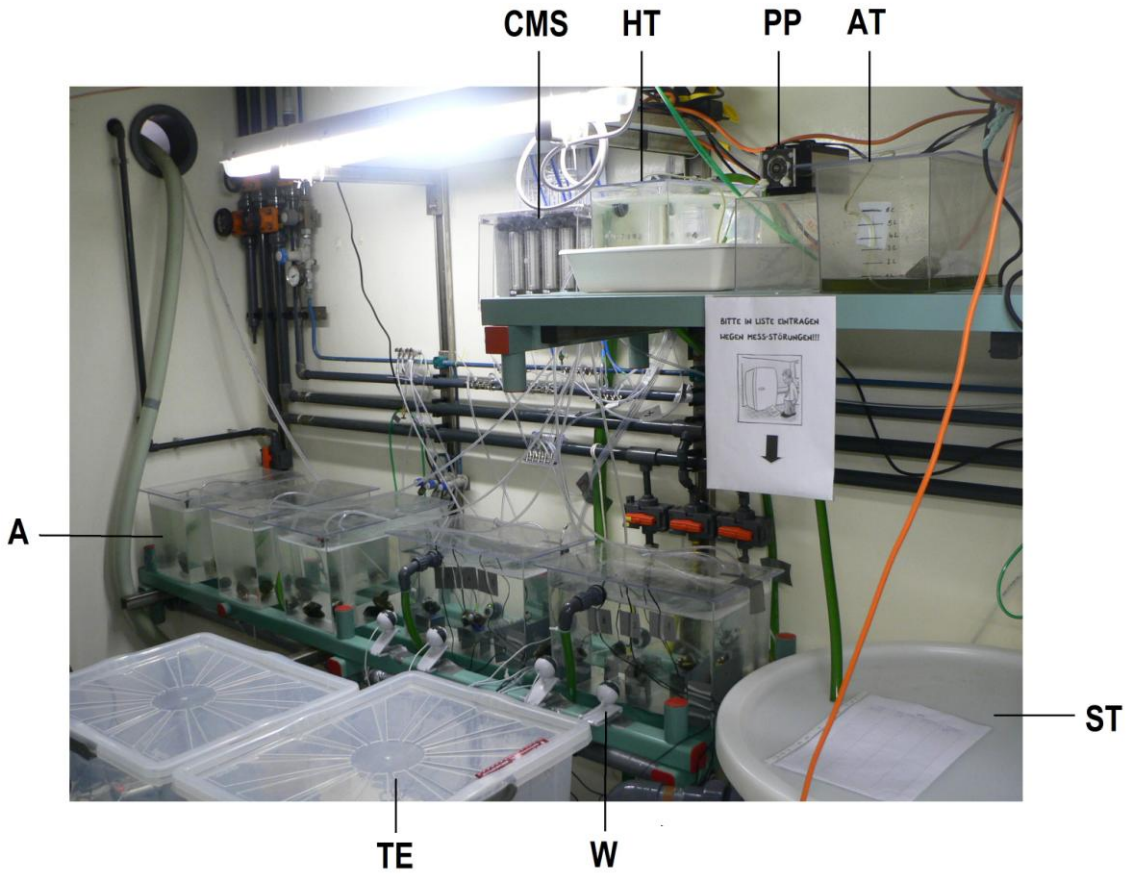

Picture 2.1 Experimental Setup. Filtered Baltic Sea water flowed from the storage tank (ST) to a header tank (HT), where it was mixed with phytoplankton suspension and from where it was distributed to the different aquaria (A). Temperature is kept constant with a cooler (C). Each aquarium is aerated with a different pCO_2 value ranging from 380 to 4000 ppm. Arrows indicate direction of water flow. AS: air stone, AT: algae tank, CMS: carbon dioxide mixing system, PP: peristaltic pump, TE: box containing the technical equipment including the computer and the PowerLab, UP: universal pump, W: webcam.

2.4.1 Feeding

Mussels were fed DT's Live Marine Phytoplankton Premium Blend consisting of 40% *Nannochloropsis oculata*, 40% *Phaeodactylum tricornutum* and 20% *Chlorella* sp. In the past good results have been obtained with this kind of food. Espinosa and Allam (2006) demonstrated that juvenile hard clams, *Mercenaria* sp., displayed the best growth rates and lowest mortality when fed DT's Phytoplankton in contrast to other phytoplankton diets.

To avoid low food supply as seen in a study by Berge et al. (2006), the phytoplankton diet was continuously added using a peristaltic pump (Meredos, Norten Hardenberg) transferring the algae suspension from a small storage aquarium to the header tank. The suspension was aerated and renewed every week to avoid sedimentation.

As was described by Riisgård et al. (2003), mussels were maximal open at a constant phytoplankton concentration of 1000 to 4000 *Rhodomonas* cells/ml (equivalent to 1000-30,000 *Phaeodactylum tricornutum* cells/ml, Riisgård and Randløv 1981). Below this concentration, valve closure was triggered due to lack of food and above this concentration the gut was shown to become saturated. The aim was to relate any possible change in the valve opening to CO_2 exposure and not to lack or surplus of food. Furthermore, at this level Riisgård (1991) observed maximal growth rates. Therefore, a concentration of 3750 cells/ml was chosen to keep all algae species present in the mixture close to optimum concentrations. The final mixture in the experimental aquaria was adjusted to 1500 *Phaeodactylum*, 1500 *Nannochloropsis* cells/ml and 750 *Chlorella* cells/ml.

In order to achieve a constant algal concentration in the flow-through aquaria the water inflow rate and the mussel filtration rate had to be known. The inflow of water was kept constant at 100 ml/min. The mussel filtration rate was also assumed to be constant and was estimated with the following equation (Møhlenberg and Riisgård 1979, equ. 2.1):

Equ. 2.1 Estimation of filtration rate $F = a * W^b$

F = filtration rate [l/h]
W = dry flesh mass [g]
range 0.11 – 1.36
a = 7.45
b = 0.66

The dry flesh mass was calculated using a biometric conversion factor for Baltic Sea blue mussels determined by Rumohr et al. (1987), which states that the shell free dry mass (SFDM) is approximately 5 % of the wet mass (WM). Thus, the amount of algae, which had to be constantly added to achieve an equilibrium concentration of approximately 3750 cells/ml, was calculated using equation 2.2.

Equ. 2.2 $$A = \frac{c * in + c * nF}{P}$$

A	=	aquarium concentration [cells/ml]
c	=	algae tank concentration [cells/ml]
in	=	inflow [ml/min]
n	=	number of mussels
F	=	filtration rate [ml/min]
P	=	peristaltic pump flow rate [ml/min]

Algae concentration was checked during each experiment using a coulter counter (Z2 Coulter® Particle count and size analyzer, Beckman Coulter ™). This device consists of two electrodes, one inside (cathode) and one outside (anode) a tube being connected by an opening of a defined size, the aperture. After positioning the electrodes in the cell suspension and applying an electric current (I), particles are sucked into the tube by applying a vacuum. While passing the aperture, the impedance (R) at the aperture rises. Since the current intensity is kept constant, the measurable voltage pulse (Δ U) is proportional to the particle volume according to Ohm's law (Equation 2.3).

Equ. 2.3 Ohms' law $$\Delta U = I * R$$

Δ U	=	voltage pulse
I	=	intensity of current
R	=	impedance

A count of the number of pulses yields the concentration of particles in the sample. According to the phytoplankton size in the feeding suspension and the sensitivity of the counter, particles from 3-20 µm were counted. Therefore, 50 ml samples were taken from all aquaria, the header tank and the storage tank. Each measurement was performed in triplicate, from which the mean was calculated.

2.4.2 Podium

In order to obtain interference-free recordings of activity and heart rates mussels were held in place by a podium. The podium was built by softening a piece of PVC with aid of a hot air gun and then bending it twice at the same length (figure 2.3 and picture 2.2). A hole was then drilled into the middle of the top side, into which a small plastic screw was inserted. By means of underwater glue (Orca, Aquarium Münster, Pahlsmeier GmbH), the mussel was glued to the plastic screw and after the glue had dried, it was fixed on the podium by tightening the connection with a screw nut. To enhance the construction double-sided self adhesive butyl tape (Tecoband 140, Technoplast GmbH) was wrapped between mussel and podium. Where needed, dental wax (HEKO GmbH) was added for support.

2.4.3 Monitoring of Heart Rates

Heart rates (*HR*) were measured continuously via a photoplethysmograph according to Depledge (1984). We used the same sensors Frederich (1999) developed in cooperation with isiTEC GmbH (Bremerhaven, Germany) to measure the heart rate of the spider crab, *Maja squinado*. The sensors function in seawater and can be glued directly to the shell.

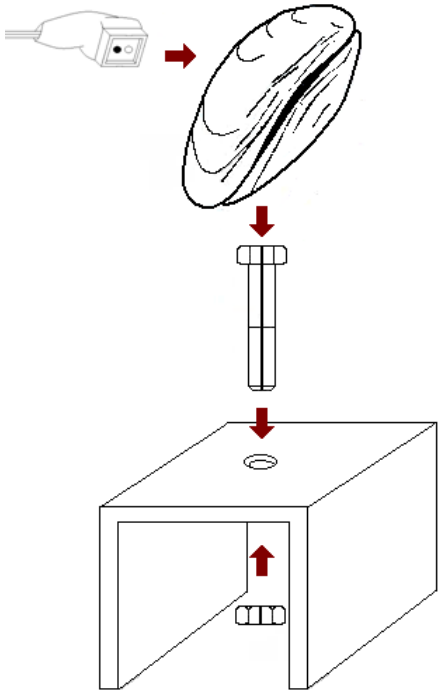

Figure 2.3 Podium Connection Scheme. To keep mussels from moving around, they were glued to a plastic screw and fixed to a podium by a screw nut. Plethysmographs, shown in the left corner, are connected later on.

Picture 2.2 Mussel attached to podium and plethysmograph

Since these devices are weightless in water and there is no need to make direct contact with the heart, this technique is non-invasive and handling of the animals is minimal.

As the Greek word "plethysmos" (=increase) indicates, this device detects the change in haemolymph volume caused by heart contractions. The plastic housing contains a low intensity light bulb and an extremely sensitive photo sensor. The ventricle and the paired auricles reflect differing amounts of light depending on the stage in the heart cycle (for example diastole and systole). The photo sensor detects the reflected light and converts it into a proportional voltage signal.

Before mussels could be connected to their photoplethysmographs, the shell above the cardiac region/pericardial chamber was smoothed using a multifunction rotary tool (Dremel®). This has two advantages: First, the plethysmograph could be attached more easily, since asperities due to growth rings have been removed, and second, the signal amplitude is higher since the light can more easily penetrate the thinned down shell.

To connect shell and sensor, a square piece of double-sided adhesive tape, with a 5 x 5 mm square hole in the centre, was pasted to the shell above the cardiac region. The sensor was then adhered to the tape with additional aid of instant adhesive glue, while it was ensured that the photo sensor and the light bulb were placed over the cut-out in order to maximize the signal. To really tighten the connection between shell and sensor, double-sided self adhesive butyl tape (Tecoband 140 made by Technoplast GmbH, Germany) was wrapped around the sensor after the glue had dried. Furthermore, stripes of duct tape (Tesa®) gave additional stability. This careful procedure was necessary to prevent sensor displacement at low water temperatures for long (two weeks) trial durations, although sensor detachment occurred in only a few cases. Detached sensors were quickly reattached within five minutes.

Each sensor was connected to a signal amplifier (HSA100, isiTEC GmbH) creating a larger output voltage. Each amplifier had its own power supply and communicated with a data acquisition and analysis system by using a BNC connection (PowerLab 8/30, ML870, AD Instruments). Since the PowerLab possesses 8 BNC signal input sockets on the front panel, 8 mussels were measured simultaneously. A USB cable linked the PowerLab to a laptop (HP Compaq, Win XP, SP 2, AMD Turion 64 X2 Mobile), which recorded the data (100 data points/s, Range 50 mV) using Chart™ 5 Pro software (v5.5.5, AD Instruments).

2.4.4 Recording of Valve and Siphon Opening Status

Valve and Siphon opening status were recorded simultaneously with the heart rate measurements using eight webcams (Logitech, Quick Chat). Recording took place during 14 hours each day given by the light hours of the artificial circadian rhythm (6 am to 8 pm). Webcams were placed 10-15 cm away from the mussels outside of the aquarium. Cam 1 and 2 were connected directly to the laptop, which also contained the PowerLab. Cam 3-5 were linked to the same laptop via a USB hub (equip®). Cam 6-8 were attached to an additional PC to ensure all webcams and the PowerLab had enough memory left to operate. Pictures were taken every five minutes using the Vision GS PE (v 2.00 beta) time lapse program.

2.5 Test procedure

Six mussels were randomly distributed in each aquarium on April 25th (Experiment I), May 21st (Experiment II) and June 16th (Experiment III) after shell length in mm and wet mass in g had been determined. The amount of total biomass was approximately the same in all aquaria within each experiment. At the end of the experiments the specimens' wet masses and lengths were determined again.

Heart rates and valve/siphon opening of four mussels in the control and in the 1400 ppm treatment during experiments I and II and of eight mussels in the 4000 ppm treatment during experiment III were measured (table 2.2). All other organisms were used by Jörn Thomsen to determine extracellular pH, CO_2 partial pressure and ion composition in the haemolymph, as well as to carry out Na^+/K^+ ATPase activity measurements.

During the trial period daily measurements of pH, salinity and temperature were conducted. PH was determined with a pH meter (WTW 340i pH-analyzer, WTW SenTix 81-measuring chain) which was calibrated daily with Radiometer precision buffers (IUPAC pH buffer 7 and 10, S11M44, S11 M007). Salinity and temperature were measured with a salinometer (WTW cond 315i, WTW TETRACON 325-measuring chain). Water samples for determination of A_T and C_T of the aquaria and the storage tank were taken at the beginning, the middle and the end of every experiment. During the first experiment, C_T was measured photometrically, while in the subsequent experiments it was determined coulometrically.

After each two-week incubation, haemolymph samples were taken by carefully forcing the shells open and withdrawing samples anaerobically with a syringe from the posterior adductor muscle, while the shell was blocked open (using a 1000 µl pipette tip). Tissue samples were collected by cutting the posterior adductor muscle and opening the shell. Samples of gills, mantle, posterior adductor muscle (PAM), foot, and midgut gland were taken within 15 min after removal from the aquaria. The dissection was performed on ice; samples of 100 mg were rinsed in filtered seawater, blotted dry and immediately frozen in liquid nitrogen.

2.5.1 Photometric determination of C_T

The C_T values of the first experiment were determined according to the method of Stoll et al. (2001) using a Bran & Lübbe QUAATRO System Autoanalyzer. Samples were taken from each aquarium and the storage tank using a 10 ml single-use syringe. They were transferred bubble-free into 4 ml sample vials (Rotilabo®) through a 0.2 µm syringe filter (Sarstedt) to remove any particles, which might influence the C_T value by respiration or photosynthesis. More than one vial volume was discarded to rinse the flask. The vial was sealed airtight using a Teflon®-coated septum and a screw cap with hole (both Carl Roth GmbH + Co. KG). To prevent air exchange vials were additionally covered with Parafilm® and stored at 4 °C. During measurement, samples were calibrated versus a certified reference material with the same salinity of known C_T. First, samples were acidified to a pH less than one, forcing all carbonate components included in the carrier stream into the gas

phase. When the carrier stream passes the semipermeable silicone membrane, the gas is absorbed by the detector stream containing an indicator (phenolphthalein), which is discoloured according to the pCO_2. The extinction measured at a wavelength of 550 nm is then proportional to the C_T content in the sample. The advantage of this method is that even small sample volumes of 5 ml can be used, but only with an accuracy of ±2-3 µM.

2.5.2 Coulometric determination of C_T

During the following experiments DIC was determined coulometrically by the method described by Dickson et al. (2007) using a SOMMA Autoanalyzer. For this method, a much higher sample volume of 500 ml was necessary. However, this method is characterized by a higher accuracy (±1.5-2.5 µM) than the previous method. Ground flasks were flooded through a hose from the corresponding aquarium with at least 2 times the bottle volume before they were filled up and poisoned with 100 µl saturated mercury chloride. Afterwards they were closed and tightened with a rubber band. The same sample was used for alkalinity measurements during experiments II and III. A known amount of the sample is acidified and inert gas is added. This way CO_2 is absorbed from the resulting gas stream using ethanolamine. The so formed hydroxyethylcarbamic acid causes the colour of the indicator thymolphthalein to fade and is titrated coulometrically.

2.5.3 Determination of A_T

During the first experiment the samples (500 ml) were filtered (Whatman® GFF 0.2 µm), filled into gas tight Nalgene® bottles and measured on the same day without poisoning. In the subsequent runs using the VINDTA Autoanalyzer the samples (800 ml) were poisoned with $HgCl_2$ on collection to avoid biological alterations. The method used in both cases was described by Dickson et al. (2003) and is accomplished by a potentiometric open-cell titration with hydrochloric acid. The titration takes place in two steps: First, the sample is acidified to a pH between 3.5 and 4.0 with a single addition of titrant and then stirred for some time until the evolving CO_2 had escaped. It is assumed that at this point the C_T is approximately zero, but the media still contains some buffer capacity mainly resulting from the HSO_4^- concentration. The titration is resumed until the pH linearly falls with the acid addition. At this stage all bases have been converted into their conjugate acids and pH is no longer buffered. This way, A_T is calculated from the titration volume. Two replicates of each sample were measured against a known standard (Dickson seawater, Scripps Institute of Oceanography) determined at the beginning and end of each measurement session. Samples were then corrected for the deviation of the standard from its nominal value.

During titration the pH was determined with a pH-meter (Metrohm pH-Meter 713 series 01) using a glass electrode (depending on H^+ ion concentration) and a reference electrode (possessing a constant potential). Placing both electrodes into the sample led to an electromotive force (EMF) according to the principle of a galvanic cell. Thus, pH was determined by comparing the measured EMF with the EMF of calibration buffers with known pH. The dissociation constants of seawater depend on temperature and, therefore, temperature was additionally measured and all involved chemicals and samples were kept at 20 °C using a cooler.

2.6 Analysis

2.6.1 Analysis of Heart Rates and HRV

Mussels often lowered their heart rate until it was not detectable anymore, going along with total valve closure; a process known as metabolic depression (DeZwaan and Wijsman1976, Guppy 2004). Other discontinuities during recording occurred due to technical problems, e.g. computer break down and loosening of sensors. This is why only two hours each day of the highest quality recordings were analyzed in detail. If in only a few cases no continuous recording over two hours was available, the data was cut together to two hours.

After smoothing the data with aid of low and high pass filters, instantaneous heart rate and HRV were determined using the HRV module for Chart (AD Instruments). Since the module was initially designed for human or vertebrate use, it divides peaks in normals (regular beats), ectopics (abnormal beats) and artifacts (disturbances in measurement) by peak-to-peak duration with the longest possible interval being 60,000 ms. These values have not been defined for *Mytilus edulis* yet. Thus, intervals between approximately 2600 ms (lower limit) and 8200 ms (higher limit) were used. However, in some cases they had to be adjusted, since heart beat could be very variable, especially when phases of low HR were encountered during beginning metabolic depression. Therefore no differentiation into normals and ectopics was made in this study and artifacts have been left out. The module directly calculated the instantaneous heart rate and duration of intervals as well as basic HRV parameters. These comprised the SDNN (standard deviation of normalized intervals), SDdeltaNN (standard deviation of the differences between adjacent intervals), and RMSSD (root mean square successive differences), where each difference is squared, then summed, the result averaged and then the square root obtained.

Interval durations were then exported into a statistic program (SPSS 16.0 EV), where Gauss curves were created for each mussel and day. Parameters obtained from the curve

progression include the mean, median, mode, range, skewness (measure of the symmetry) and kurtosis (measure of peakedness).

Furthermore, the CV (coefficient of variation) was calculated from the standard deviation of interpulse duration to the mean (SDNN divided by mean NN interval). The relevance of each measure is explained at the appropriate place later on (see chapter 3.1.2).

2.6.2 Analysis of Valve and Siphon Opening Status

Pictures were analyzed using ImageJ (v 1.40g) software with the Time Series Analyzer plug-in (courtesy of Balaji J, Weil Medical College of Cornell University). Since the contrast was not high enough to write a macro for automatic image analysis, only one picture every hour was utilized. Before choosing this procedure, it had been tested by comparing the curve progression obtained from one picture/hour with the curve for one picture every five minutes, whether omission of the remaining pictures would have a significant effect on the results of the analysis. However, the resulting data showed only minor deviations from one another.

In each experiment a ruler was held next to each mussel and a picture was taken in order to calibrate the image. The most conspicuous characteristics (e.g. barnacle residues) of each mussel were measured to be able to recalibrate the image scale if the mussel had moved. Recalibration was carried out only if the deviation to the original value was higher than 0.5 mm, since values below were classified as measurement errors.

The distance between the valves was determined by drawing a straight line at a right angle (being equal to the shortest possible distance) between upper and lower valve. This was done at the position between inhalant and exhalant siphon (picture 2.2). Siphon diameter was measured vertically and horizontally by drawing a straight line through the maximum opening.

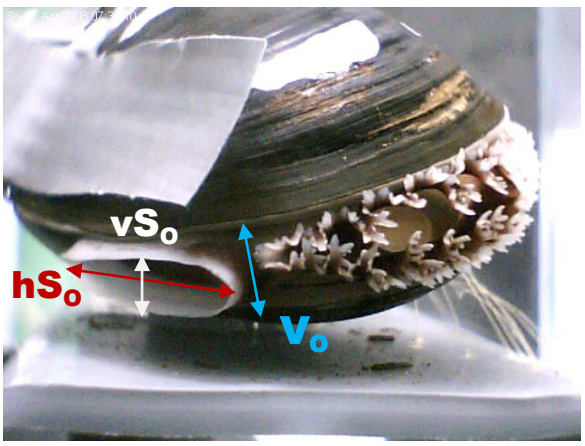

Picture 2.2 Position of transects. Locations are shown, where valve opening (V_O), vertical siphon opening (vS_O) and horizontal siphon opening (hS_O) are measured.

The valve and siphon opening status was obtained by indexing raw data applying the value 1 to open and 0 to closed mussels. Valve opening position was determined as percentage of the maximum opening per mussel and experiment excluding intra-species variations due to e.g. size. For the siphon position, in addition to percentage data, metric data was also included in the analysis since it was also used for the calculation of the siphon area. The area was calculated using the equation of an ellipse (πab) involving the horizontal (a) and the vertical siphon diameter (b).

2.6.3 Analysis of Carbonate System Parameters

After measuring pH, DIC and Alkalinity other carbonate system parameters, consisting of pCO_2 and Ω, were calculated using the program CO2Sys Excel Macro (E. Lewis and D. Wallace 1998). Measured DIC and alkalinity were used as input parameters. The constants K_1 and K_2 were chosen according to Mehrbach et al. (1973, refit by Dickson and Millero 1987) and the KSO_4^- dissociation constant according to Dickson et al (1990). The NBS scale [mol/kg H_20] was used. Total silicate and phosphate were obtained from a time series of annual variation at the sampling site (Stuhr et al. unpublished data).

2.7 Statistical methods

Data were tested for normality (Kolmogorov-Smirnov), which provides the basis for following statistical analysis. Student t-test (significance levels 95% and 99%) was used to test phase I and II for significant differences. One-Way-ANOVA (significance levels 95% and 99%) was employed to test the different treatments for significance.

If the normality test failed, the Mann-Whitney test (U-test) and the Kruskal-Wallis test (H-test) were carried out accordingly. An arcus-sinus transformation of square root percentage data of the valve/siphon opening was used, as percentages are not normally distributed due to values between 0 and 100. This transformation leads to a normal distribution of the data, which is the requirement for further statistics.

The software SigmaStat version 3.5 (Statistica 8 in corporation) was used for normality tests, student's t-tests, One-Way-ANOVA, U-tests and H-tests. General calculations (means, standard error and CV) were conducted in Excel (Microsoft Office 2007).

3 Results

To indicate whole-animal performance under hypercapnic conditions, cardiac performance (chapter 3.1) and activity patterns (chapter 3.2) of eight mussels in three different carbon dioxide treatments were determined. Experimental results were pooled, since no significant differences were detected between the trials in heart rates as well as in valve siphon opening state and position ($p>0.05$; ANOVA). Furthermore, in all six treatments carbonate system parameters (chapter 3.4), phytoplankton concentration (chapter 3.3) and other abiotic parameters (chapter 3.5) were measured to monitor the stability of external influencing factors. No animal losses occurred during the experiments.

3.1 Cardiac Performance

Two indicators for cardiac performance under CO_2 stress were obtained from heart rate recordings: Instantaneous heart rate (IHR) in beats per minute [BPM] was derived directly from the recorded peak patterns (chapter 3.1.1) and the heart rate variability (HRV) was calculated in several ways from the interpulse duration (chapter 3.1.2). For both indicators only two hours of high cardiac activity per day were analysed. One animal (mussel M4A6aE3, 4000 ppm) had to be excluded from calculations due to an instrumental error.

3.1.1 Instantaneous Heart Rate

The mean IHR did neither differ between phases ($p>0.05$; t-test) nor between treatments ($p>0.05$; ANOVA; figure 3.1). The overall mean IHR derived from all treatments and phases was 12.03 BPM (±0.48 SE).

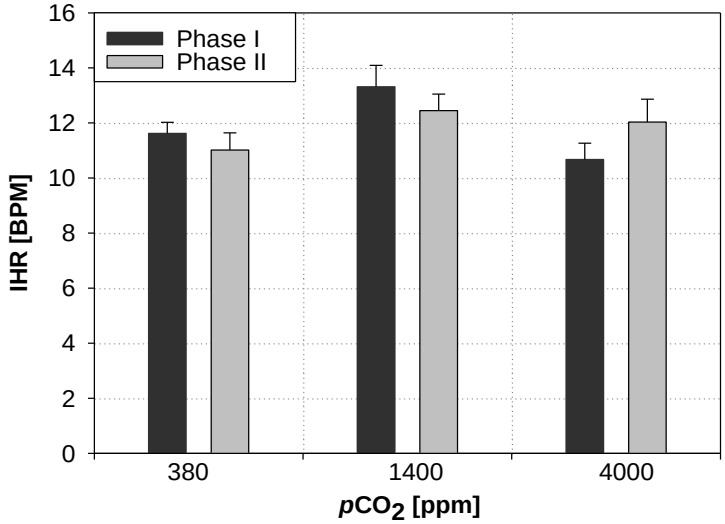

Figure 3.1 Instantaneous heart rates (IHR [BPM]) at three different pCO_2 levels [ppm]. IHR were averaged over the tested animals (n=7-8) under normocapnia (*Phase I*) and hypercapnia (*Phase II*) for each treatment. Mussels in the control group were kept under normocapnia during Phase I. No significant differences between the treatments (ANOVA, $p>0.05$) and between the different phases were observed (t-test, $p>0.05$). Error bars indicate standard error.

3.1.2 Heart Rate Variability

When characterising HRV, many factors have to be taken into consideration to adequately depict the variations between heart beats. In this work the beat-to-beat interval duration was used to calculate mean [ms], median [ms], mode [ms], SDNN (standard deviation of normalized intervals [ms]), SDdeltaNN (standard deviation of the differences between adjacent intervals [ms]), RMSSD (square root of the mean of the squared differences between adjacent intervals), CV (coefficient of correlation), range [ms], skewness and kurtosis.

Box plots with mean values over the tested animals in each phase for the mean, the median, the range and the SDNN were employed (figure 3.2) to demonstrate that there were no significant differences between the phases ($p>0.05$; t-test) and between different treatments ($p>0.05$; ANOVA). The mean (on average 5061.05 ms ±106.52 SE) and the median interval durations (on average 5018.41 ±121.45 SE) were nearly equal indicating a symmetric distribution and consequently no distinct skewness (with exception of phase I in the 4000 ppm treatment). This was additionally supported by mean skewness values close to zero (on average 0.46 ±0.26 SE) and, hence, no significant trend ($p>0.05$; ANOVA; t-test) in skewness was observed.

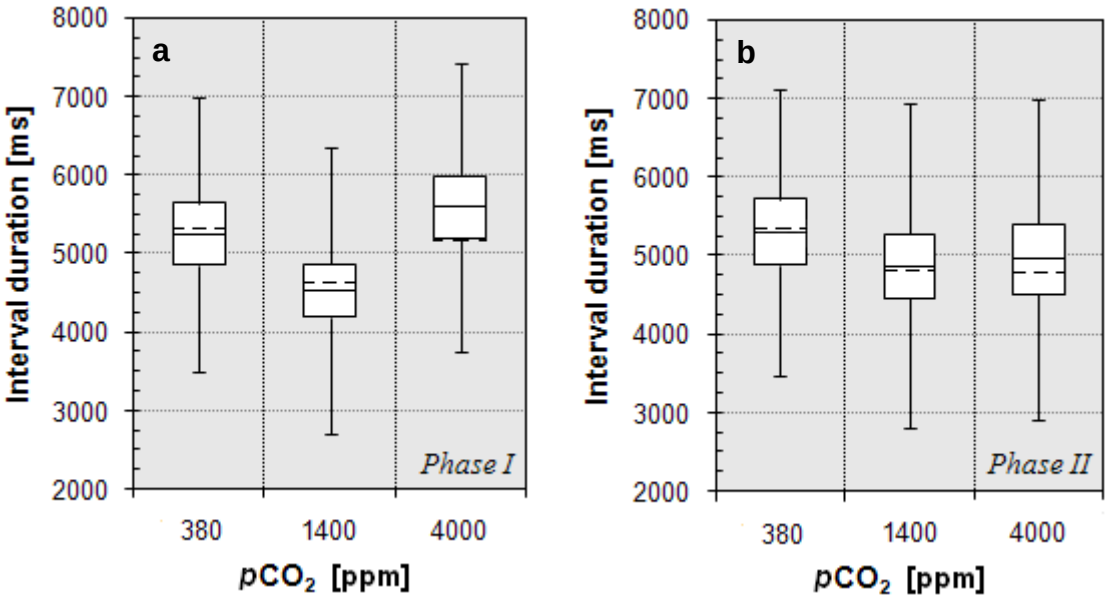

Figure 3.2 Box plots displaying average values for mean, median, range and standard deviation (SDNN) of normalized heart beat intervals [ms] during phase I (a) and phase II (b) in three different carbon dioxide treatments [ppm]. Averages were calculated from all animals per phase and treatment (n=7-8). Solid lines display the mean whereas dashed lines display median values. Boxes indicate SDNN and whiskers mark the range. No significant differences between treatments (ANOVA, $p>0.05$) and between phases were observed (t-test, $p>0.05$). Note that the y-axis scale only covers the range from 2000 to 8000 ms.

Furthermore, kurtosis was used to display how the interval distribution differs from a normal distribution and during the course of the experiment. In every case, mean values for kurtosis, ranging between 5 and 24, were greater than zero (figure 3.3) indicating that the intervals cluster more and have longer tails than expected according to a typical normal distribution. Moreover, a trend towards lower kurtosis was observed from phase I to phase II in all treatments, even though the difference was not large enough and variance to great to detect any significant differences ($p>0.05$; U-test). There were also no differences between the treatments ($p>0.05$; H-test), although the 1400 ppm treatment was characterized by higher fluctuations of kurtosis than the other treatments.

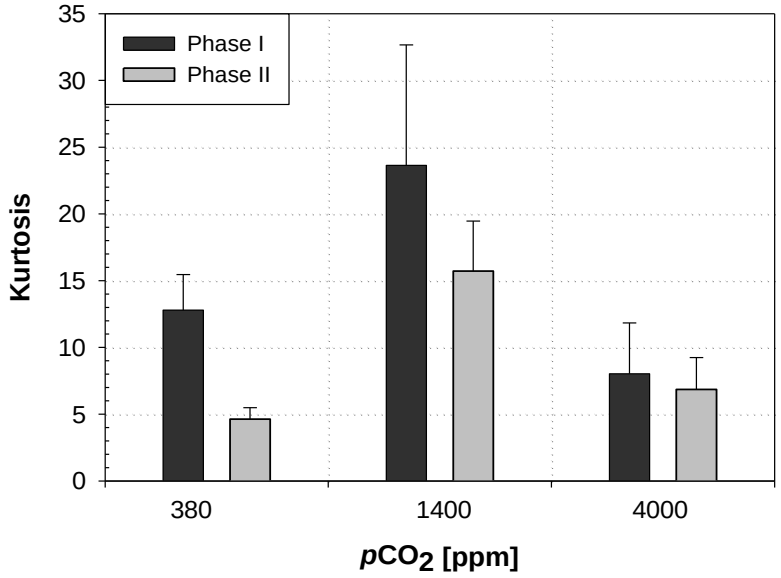

Figure 3.3 Mean kurtosis of beat-to-beat interval distribution in the three treatments [ppm]. For calculation of mean kurtosis animals were averaged accordingly (n=7-8). No significant differences between the treatments ($p>0.05$; H-test) and between the different phases were observed ($p>0.05$; U-test). Error bars indicate standard error.

The mode of the interval distribution was calculated to further reveal deviations from a normal distribution, in which the mode equals the mean and the median. But as well as observed in the mean and median values, the mode values were not found to be significantly different form one another ($p>0.05$; ANOVA; t-test; figure 3.4). The mean mode value in all treatments varied around 4876 ms (±162 SE).

Another factor, the coefficient of variation (CV), was employed as a measure of the ratio of the standard deviation of interpulse duration to the mean. Since the CV is a dimensionless number it was used to compare the results with data from other studies. While the CV increased slightly from phase I to phase II and with rising treatment level in phase II (figure 3.5), no significant results were yielded by comparing both phases ($p>0.05$; U-test) and the three treatments ($p>0.05$; H-test). Overall, CV varied around 0.080 (± 0.004 SE).

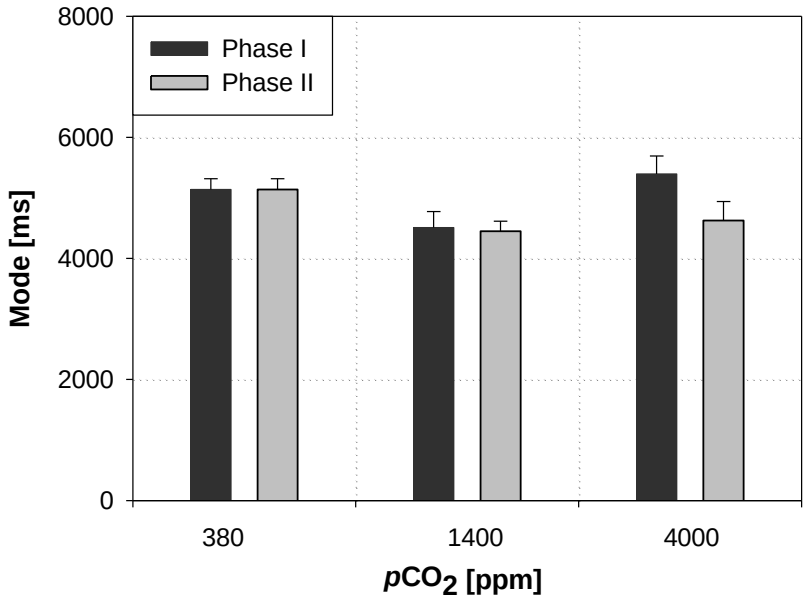

Figure 3.4 Mode of interpulse duration [ms] at three carbon dioxide levels [ppm]. No significant deviations were observed between the treatments ($p>0.05$; ANOVA) and between both phases ($p>0.05$; t-test). Mode values were averaged over the experimental animals per treatment and phase (n=7-8). Error bars indicate standard error.

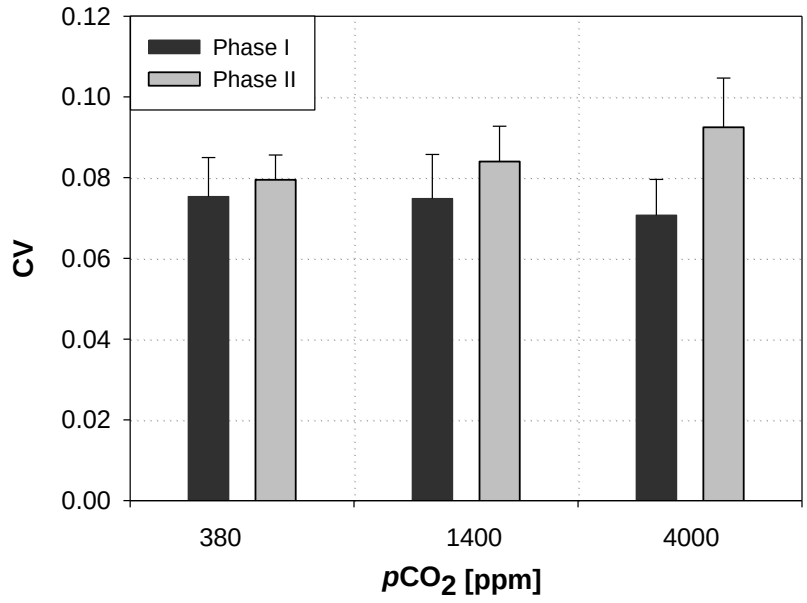

Figure 3.5 Coefficient of variation (CV) of interpulse durations at three carbon dioxide levels [ppm]. For calculation of the CVs the mean values and the standard deviation of NN intervals of the tested animals in each phase were averaged (n=7-8). No significant differences between the treatments ($p>0.05$; H-test) and between the different phases were observed ($p>0.05$; U-test). Error bars indicate standard error.

Further standardized measures of short term changes in HRV include the examination of differences between adjacent intervals. For this reason SDdeltaNN and RMSSD were employed in this study. Both parameters differed only slightly from each other (less than 0.5%) and therefore the same increasing trend from phase I to phase II (figure 3.6) from on average 353 (±31 SE) to 1146 (± 216 SE) was observed. But despite this increase, no statistical significance was obtained between phases ($p>0.05$; U-test), as well as between treatments ($p>0.05$; H-test).

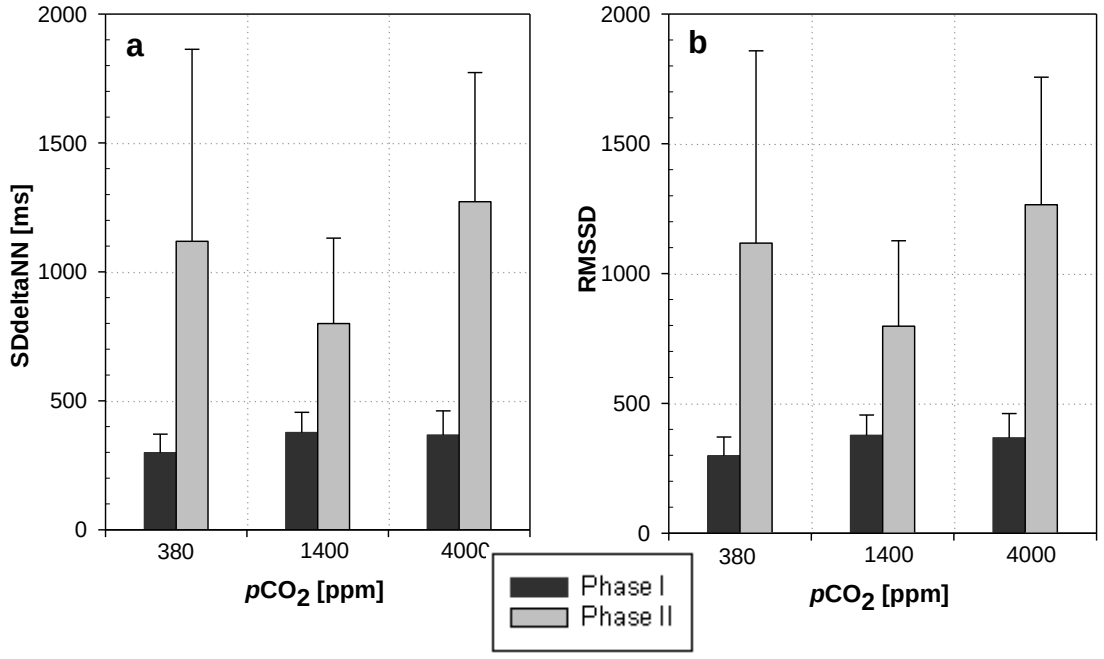

Figure 3.6 Standard measures of HRV versus three pCO_2 levels [ppm]. a) The mean of the standard deviation [ms] of the differences between adjacent intervals (SDdeltaNN) and b) the square root of the mean of the squared differences between adjacent intervals (RMSSD). No significance was detected ($p>0.05$; U-test). The treatments as well did not differ distinctly from each other ($p>0.05$; H-test). Mean values of the experimental animals in each phase were averaged (n=7-8). Error bars indicate standard error.

To summarise the findings described above it has to be noted that no significant results were yielded and therefore only trends can be discussed. The mean IHR remained constant during the experiment throughout the treatments. This was also the case with the mean, the median and the mode of interpulse duration, which all varied around a similar mean value. In the same way, no significant changes were revealed in the SDNN and the range of interpulse duration. Observed skewness values close to zero indicated no deviations from a normal distribution, whereas observed kurtosis values greater than zero did. Furthermore, kurtosis decreased from phase I to phase II. On the contrary, SDdeltaNN and the likewise RMSSD as well as the CV increased from phase I to phase II. The CV even rose with higher pCO_2 values during phase II. The next chapter analyses whether these trends could also be found in the activity pattern of the tested animals.

3.2 Activity Pattern

As measures for activity at different seawater pCO_2 values, valve and siphon opening patterns were investigated. For this purpose, the valve and siphon opening status [open/closed] as well as their vertical opening in % of the maximal opening were determined (chapter 3.2.1). Furthermore, the horizontal diameter [mm] of each siphon was obtained from a random sample during phase II and used with the vertical siphon diameter [mm] for calculation of the siphon area [mm^2] (chapter 3.2.2). Note that activity was obtained from time lapse pictures taken only every hour during light hours (14 hours) and positions were determined only from open mussels.

3.2.1 Valve and Siphon Opening

The opening status of valve and siphon was estimated using indexed values; 1 was assigned to open mussels and 0 to closed mussels. No significant differences were revealed between phases ($p>0.05$), except when comparing siphon opening status of the 1400 ppm treatment ($p<0.05$; t-test), where mussels were closed (index 0.42 ±0.02 SE) more often in phase II than in phase I (index 0.058 ±0.06 SE). Interestingly, a trend towards lower valve/siphon opening state from phase I to phase II was also observed in all other treatments. On average, the valve opening state decreased from 0.67 ±0.04 SE to 0.52 ±0.03 SE and the siphon opening state from 0.58 ±0.04 SE to 0.44 ±0.03 SE. Comparing all pCO_2 levels no significant difference was found between the different treatments ($p>0.05$; ANOVA). Despite non existing significances, a trend towards increased valve and siphon opening states (figure 3.7a and b) was visible in phase II for all treatments, from the control (Valve: 0.47 ±0.04 SE; Siphon: 0.40 ±0.05 SE) to the 4000 ppm group (Valve: 0.56 ±0.05 SE; Siphon: 0.50 ±0.06 SE). But this could also be the case in phase I of the siphon opening state increasing from 0.54 (±0.08 SE) to 0.61 (±0.05 SE). Although the siphon was closed more often than the valve (Siphon: 0.51 ±0.02 SE; Valve: 0.59 ±0.03 SE) a high correlation was obvious ($r = 0.8$). Thus, similar trends were observed in both parameters.

This correlation was not as obvious ($r = 0.4$) in the valve and vertical siphon positions of open mussels (figure 3.7 c and d) as in the opening status. Whereas no significant difference ($p>0.05$; ANOVA; t-test) was revealed in the valve position with values closely ranging around a mean value of 57 % (±1 SE), the siphon position was fluctuating around a mean value of 46 % (±1 SE). Even though in the 1400 ppm treatment the mean siphon position of 39 % (± 4 SE) in phase I indicated a significant deviation from the other treatments ($p<0.05$; ANOVA; Holm-Sidak), there was no significant difference to phase II in the same treatment ($p>0.05$; t-test).

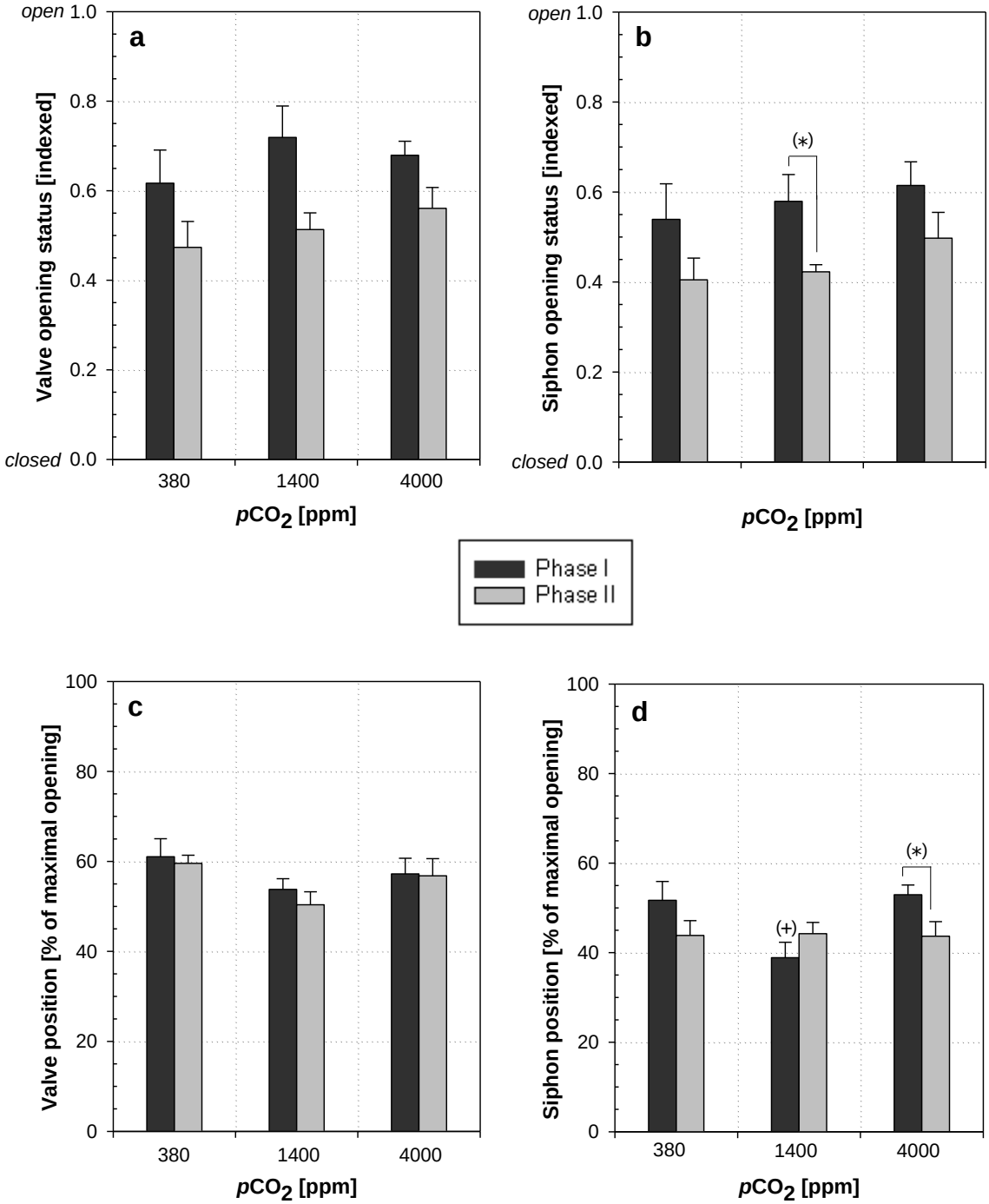

Figure 3.7 Valve and Siphon opening patterns in relation to pCO_2 [ppm]. a) Valve opening status and b) siphon opening status were determined by assigning the number 1 to open mussels and 0 to closed mussels. **c) Valve position and d) vertical siphon position of open mussels expressed as percentage of the maximum opening.** Note that positions were only included when the valve was open. An asterisk in brackets (*) indicates that there is a statistical significant difference between the two phases of one treatment ($p<0.05$; t-test), but not between the same phase of the other treatments ($p>0.05$; ANOVA), e.g. phase I at 1400 ppm in figure 3.7b differs from phase II but not from phase I at 380 and 4000 ppm. A cross in brackets (+) indicates a significant difference between the treatments in one phase ($p<0.05$; ANOVA; Holm-Sidak) but not between the two phases of the same treatment ($p>0.05$; t-test). In this case data at 1400 ppm (figure 3.7d) differs from data at 380 and 4000 ppm in phase I but not from data in phase II at 1400 ppm. Values are means over all mussels in the corresponding phase (n=8). Error bars indicate standard error.

On the other hand, only the 4000 ppm treatment differed between phase I (53 % ±2 SE) and phase II ($p<0.05$; t-test), but not from phase I of the control group (52 % ±4 SE; $p>0.05$; ANOVA). Furthermore, no differences were observed between treatments in phase II ($p>0.05$, ANOVA) varying around a mean value of 44 % (±3 SE).

Looking at opening status and position patterns in figure 3.7, there was no obvious correlation between these two measures (Valve: r = 0.1; Siphon: r = 0.3). As mentioned above, the opening status decreased during the course of the experiment in each treatment, whereas the position remained constant.

3.2.2 Siphon Area and Metric Data

The horizontal siphon diameter of 20 random pictures of each mussel during phase II was employed to estimate the siphon area using the area equation of an ellipse. A clear but insignificant decrease ($p>0.05$; ANOVA) from 120 mm² (±26 SE) to 71 mm² (±12 SE) was observed with rising pCO_2 (figure 3.8).

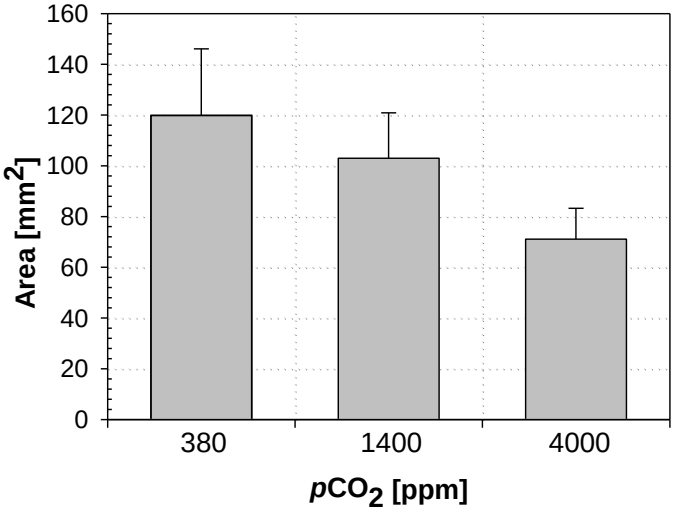

Figure 3.8 Mean siphon area [mm²] versus three carbon dioxide levels [ppm] in phase II. Area was calculated by assuming an elliptic area (πab). No significant differences ($p>0.05$; ANOVA) between treatment levels were detected. Error bars indicate standard error (n=8).

To investigate this decrease more closely, the metric data of the horizontal (figure 3.9a) and the vertical siphon position (figure 3.9b) were examined. The horizontal diameter remained relatively constant (on average 11.1 mm ±0.3 SE) and revealed no significant differences between phases ($p>0.05$; t-test) and treatments ($p>0.05$; ANOVA). The vertical position on the other hand was characterized by a significant decline in diameter from 3.3 mm (±0.4 SE) in the control CO_2 level to 2.0 mm (±0.1 SE) in the 4000 ppm treatment ($p<0.05$; ANOVA; Holm-Sidak). But an insignificant decline was also observed in phase I explaining why no significant deviation between phases were found ($p>0.05$; t-test).

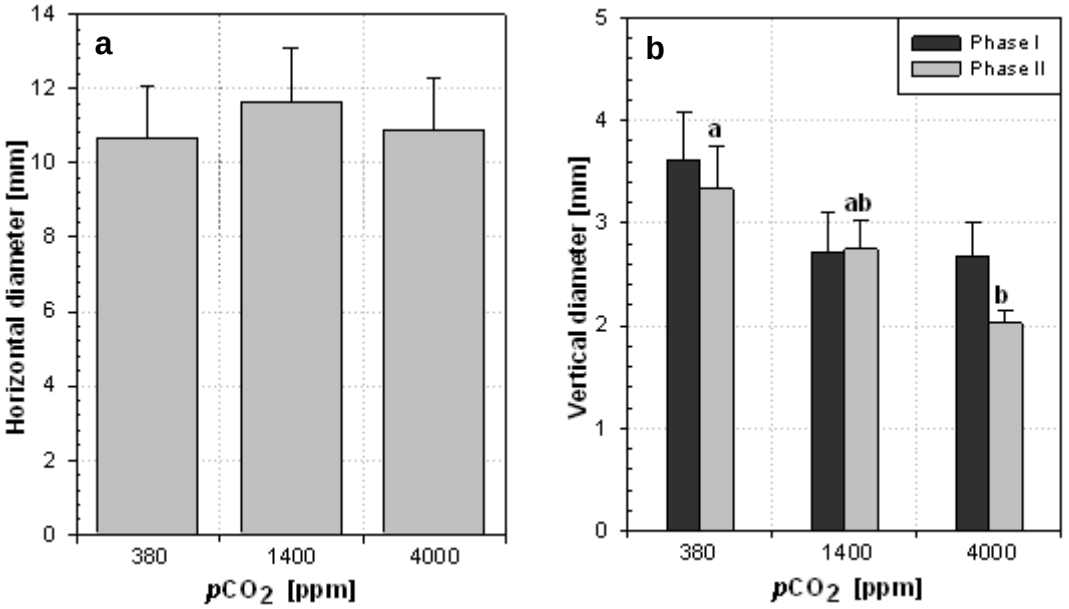

Figure 3.9 Absolute siphon measures [mm] in three pCO_2 treatments [ppm]. In the figures of the **horizontal diameter (a)** and **vertical diameter (b)** different letters indicate a significant difference between the treatments in phase II ($p<0.05$; ANOVA; Holm-Sidak) but no significant differences were observed between the two phases of same treatments ($p>0.05$; t-test). Error bars indicate standard error. Closed mussels were excluded from analysis

To sum it up, a significant trend was never observed in the valve opening patterns, whereas siphon opening patterns possessed significant differences between phases or treatments but never in both. While the valve and siphon opening status decreased from phase I to phase II in each treatment, the positions varied around a mean value. Furthermore, the opening status increased with rising treatment level in phase II. The siphon area as well as the vertical siphon diameter, however, decreased with rising pCO_2 values during phase II, while the horizontal diameter remained constant.

3.3 Phytoplankton Concentration

The algae cell concentration was determined in each aquarium, the header tank and the storage tank. Thus, sufficient food supply at a steady state concentration could be maintained in order to ensure maximal valve and siphon opening as well as growth.

During experimentation there was a constant sigmoidal increase in algae cells [cells/ml] from 941 cells/ml (±78 SE) to 6609 cells/ml (±871 SE) in the storage tank (figure 3.10), which was responsible for an increasing food supply leading to a rising steady state concentration from 1696 (±178 SE) in the first part of experiment I to 4811 cells/ml (±905 SE) in experiment III. Hence, steady-state algae concentration in experiment I was still in the optimum range but lower than expected, rising above the calculated level of 3500 cells/ml during the study period.

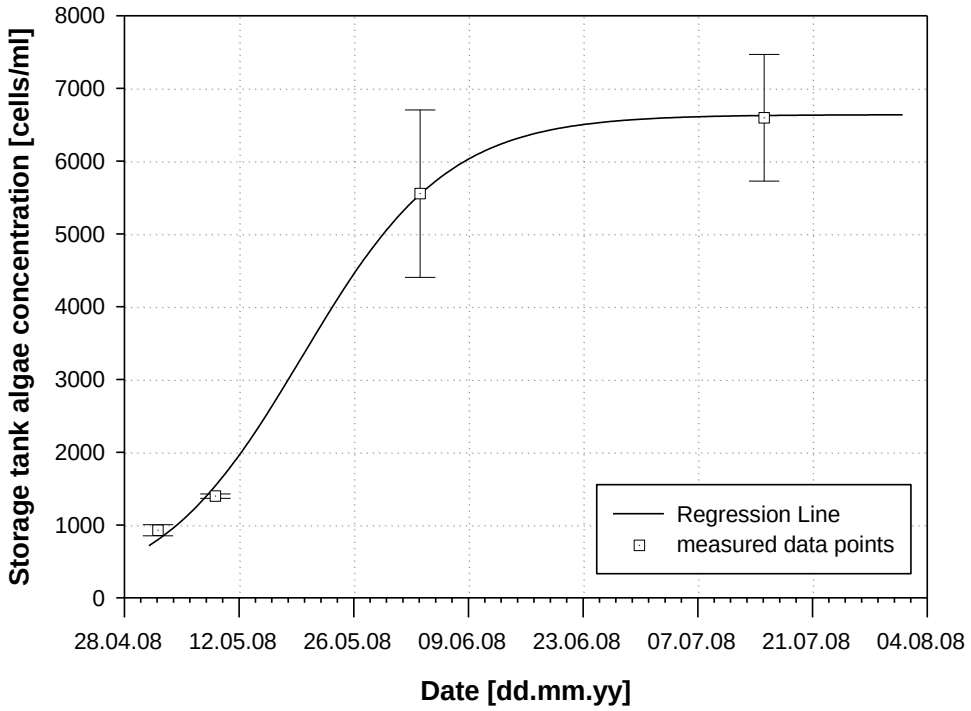

Figure 3.10 Algae concentration [cells/ml] in the storage tank during experimentation. Error bars indicate standard error (n=3).

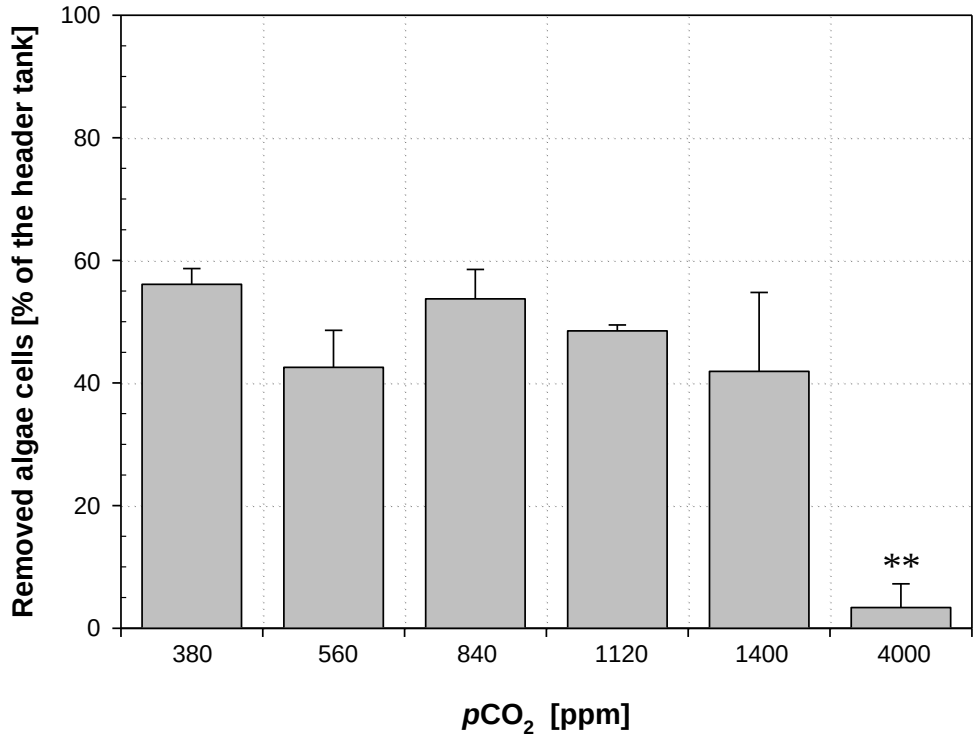

Figure 3.11 Percentage of removed algae in six different CO_2 treatments [ppm] during phase II. The concentration in the header tank was set to a 100 % and the percentaged concentration in the aquaria was subtracted. Significant different groups are indicated by asterisks (** $p<0.01$; ANOVA; Holm-Sidak; n=3-4). Error bars indicate standard error.

In order to compare experiments with one another, the removed algae concentration in the aquaria was expressed as percentage of the header tank algae cell concentration. However, during the course of the three experiments a markedly lower amount was removed at 4000 ppm CO_2 ($p<0.01$; ANOVA; Holm-Sidak). In this treatment level on average only 3 % (±3 SE) of the algae cells were cleared by the experimental animals, whereas in all other treatments on average 49 % (±2 SE) were removed. This was consistently observable among both experiments and in both aquaria used in the last experiments.

Since sufficient food for growth was supplied, wet mass and length of the animals were compared before and after the experiment observing no distinct growth ($p>0.05$; t-test). On average experimental mussels used were 76.1 mm in total length. But some important variations were observed between the experiments (figure 3.12). Differences in the length of the tested animals were encountered by comparing experiment I to experiment III ($p<0.05$; ANOVA; Holm-Sidak), where a slight increase was detected. On the other hand wet mass differed highly significant in all experiment ($p<0.01$; H-test; Dunn's) with a linear increase of about 7.3 g from experiment to experiment.

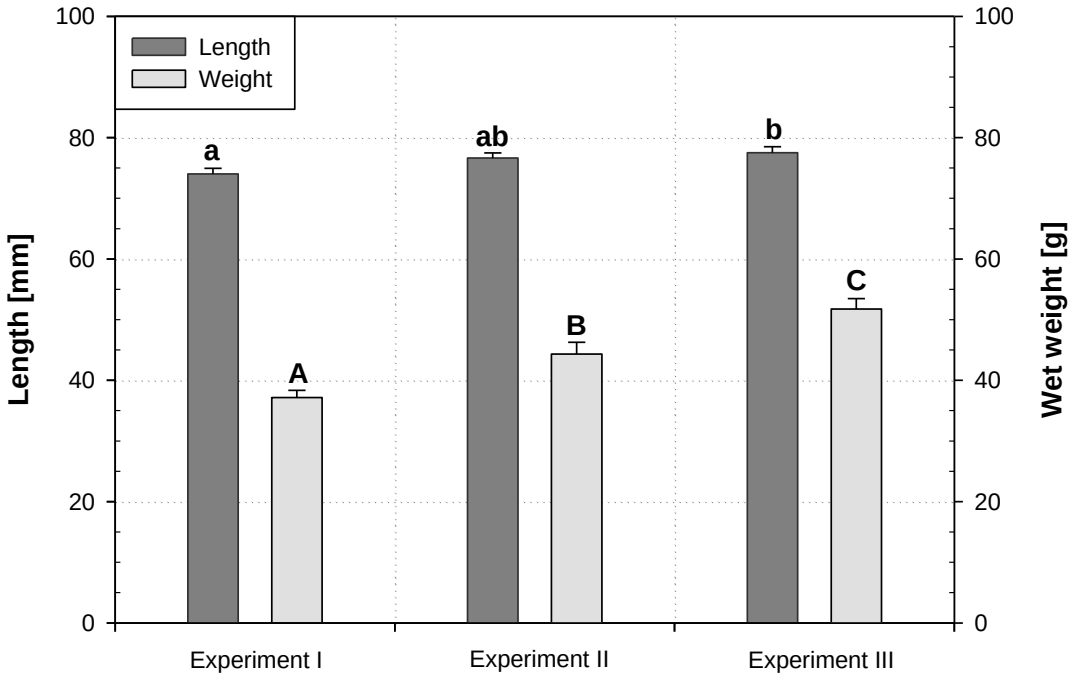

Figure 3.12 Length [mm] and wet mass [g] of tested animals before placement into the experimental setup. Length differed highly significant in the first experiment from the third ($p<0.05$; ANOVA; Holm-Sidak; n=30-36), whereas wet mass differed significantly in all experiments ($p<0.01$; H-test; Dunn's). Length and wet mass were analyzed separately. Note that the scale for mass values is displayed on the right axis. Error bars indicate standard error.

In short, removed algae cells/ml were equal in all treatments except the 4000 ppm treatment, where significantly fewer cells were removed. Algae concentration in the storage tank rose throughout the experiments increasing the food supply. Even though food supply was sufficient no growth was observed. But already at the beginning of the experiments length and weight differed significantly between the trails. To further elucidate the stability of the experimental setup, the next chapter deals with the investigation of carbonate system parameters.

3.4 Carbonate System Parameters

To characterize the carbonate system in the experimental incubations, measurements of total dissolved inorganic carbon (C_T [µmol/kg SW]) and total alkalinity (A_T [µmol/kg SW]) were carried out. Using these measures, further components of the system, i.e. pCO_2 [ppm], $\Omega_{Calcite}$ and $\Omega_{Aragonite}$ were calculated.

The photometric C_T analysis (experiment I) was not included in the investigation of the carbonate system, since at higher pCO_2 values of >1400 ppm out gassing seemed to have occurred, leading to lower C_T concentrations than in the control treatments. Instead, in addition to determination of A_T, pH measurements were used for carbonate system calculations in the first experiment. In the following experiments, the more reliable coulometric C_T analysis was used (figure 3.13).

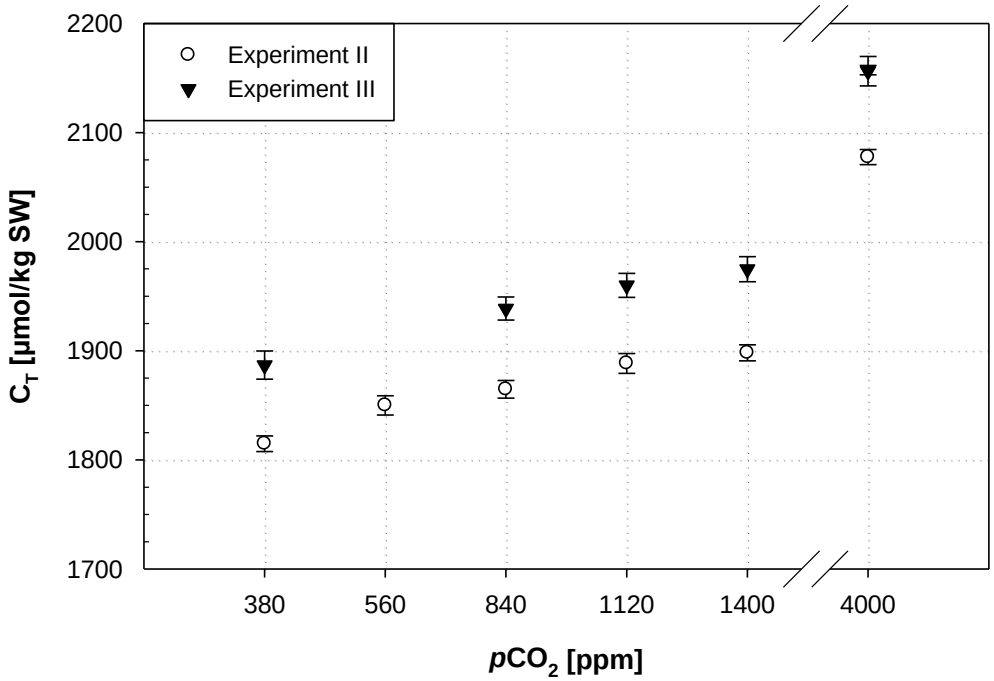

Figure 3.13 Total dissolved inorganic carbon (C_T [µmol/kg SW]) at six different CO_2 levels [ppm]. C_T is consistently rising with increasing pCO_2. Values are shown for the second (○) and the third experiment (▼). Note the break in the x-axis. The y-axis only covers the range from 1700 to 2200 µmol/kg seawater. Error bars indicate standard error (n=3 determinations per experiment and treatment).

C_T concentration showed a clear positive relationship with pCO_2 (r = 0.99) Exactly the same trend was observed in the second and third experiment, but on a much higher level in experiment III, as C_T values were about 80 µmol/kg SW higher than in experiment III. Overall, measured values ranged from 1815 (±7 SE) to 2157 µmol/kg SW (±4 SE).

A_T also differed among experiments with lowest values of on average 1874 µmol/kg SW (±8 SE) in experiment II and highest values of on average 1960 µmol/kg SW (±11 SE) in experiment III (figure 3.14). But also during the course of each experiment fluctuations took place. A_T varied between 1860 (±2 SE) and 1980 µmol/kg SW (± 6 SE) in this study. On the other hand A_T in the different aquaria as well as the storage tank was found to be very constant (± 2.76 SE).

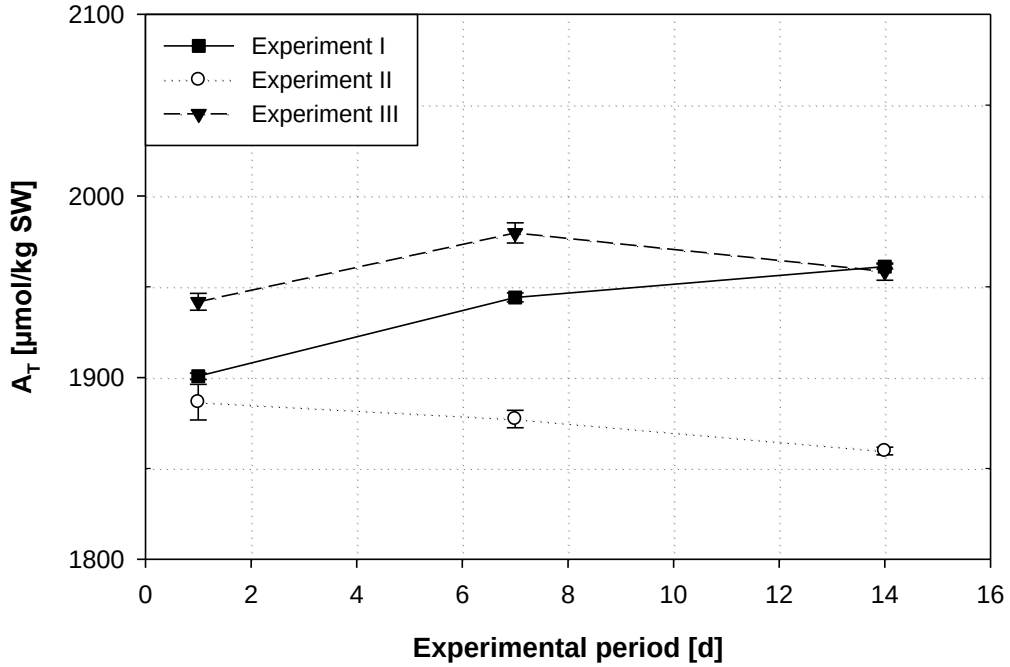

Figure 3.14 Time course [d] of total alkalinity (A_T [µmol/kg SW]). Alkalinity is displayed for the first (■), the second (○) and the third experiment (▼).Note that the y-axis only covers the range from 1800 to 2100 µmol/kg seawater. Error bars indicate standard error (n=3).

In the incoming water pCO_2 values were consistently rising from 402 ppm (± 22 SE) to 789 ppm (± 99 SE) as calculated from values for A_T and C_T/pH in the storage tank (table 3.1). Thus, values close to the third treatment level (840 ppm) were reached in storage tank water coming directly from the fjord. Not surprisingly, even higher pCO_2 values were found during field measurements at the sampling site in Kiel Fjord over the experimental periods (see chapter 3.5.4). The increasing trend in CO_2 level was observed in all treatments during the course of this study (except 1400 ppm in experiment I). Hence, the 'real' experimental pCO_2 values (as calculated from pH, A_T and C_T) were mostly higher than planned.

Table 3.1 Nominal and calculated pCO_2 [ppm] values as calculated from A_T and pH (I) or C_T (II and III). Roman numerals indicate the experiment number. Calculated pCO_2 values differed from desired values (left column, 'treatment'). Standard error (SE) is shown (n=2-3).

Treatment [ppm]	calculated CO_2 level [ppm]							
	I		II		III		Average	
	Mean	SE	Mean	SE	Mean	SE	Mean	SE
380	421.5	±10.6	486.8	±12.3	519.1	±57.5	475.8	±28.7
560	576.0	±20.2	710.3	±15.0			643.1	±54.8
840	716.6	±13.1	823.0	±11.4	852.7	±29.0	797.4	±41.3
1120	958.2	±36.4	1066.5	±22.6	1100.2	±24.2	1041.6	±42.8
1400	1633.2	±39.5	1218.7	±11.3	1248.0	±51.6	1366.6	±133.6
4000			4309.7	±201.2	4455.3	±83.9	4382.5	±72.8
Storage Tank	402.4	±22.4	624.8	±34.4	789.4	±98.8	605.5	±137.3

Furthermore, consistent with rising CO_2 levels from experiment I to III, calcite (table 3.2) and aragonite (table 3.3) saturation state of seawater (Ω) decreased with the study duration in the incoming water from 1.69 (±0.13 SE) to 1.32 (±0.12 SE) with respect to calcite and from 0.97 (±0.07 SE) to 0.78 (±0.07) with respect to aragonite. Rising CO_2 with increasing treatment level also reduced Ω leading to calcite undersaturation ($\Omega_{Calcite}<1$) in treatments above 840 ppm. Interestingly, the water was always undersaturated with respect to aragonite ($\Omega_{Aragonite}<1$), except in the 380 ppm treatment in experiment III.

Table 3.2 Calcite saturation state ($\Omega_{Calcite}$) in the different CO_2 treatments [ppm] during the three experiments. Roman numerals indicate the experiment number. Values above 1 indicate supersaturation, whereas values lower than 1 depict undersaturation. Standard error (SE) is shown (n=2-3).

Treatment [ppm]	$\Omega_{Calcite}$							
	I		II		III		Average	
	Mean	SE	Mean	SE	Mean	SE	Mean	SE
380	1.51	±0.03	1.65	±0.04	1.76	±0.16	1.64	±0.07
560	1.14	±0.07	1.18	±0.03			1.16	±0.02
840	0.92	±0.03	1.02	±0.01	1.11	±0.03	1.02	±0.05
1120	0.71	±0.04	0.82	±0.02	0.89	±0.02	0.81	±0.05
1400	0.44	±0.02	0.72	±0.01	0.79	±0.04	0.65	±0.11
4000			0.22	±0.01	0.24	±0.01	0.23	±0.01
Storage Tank	1.69	±0.13	1.42	±0.06	1.32	±0.12	1.48	±0.11

Table 3.3 Aragonite saturation state ($\Omega_{Aragonite}$) in the different CO_2 treatments [ppm] during the three experiments. Roman numerals indicate the experiment number. Values above 1 indicate supersaturation, whereas values lower than 1 depict undersaturation. Standard error (SE) is shown (n=2-3).

Treatment [ppm]	$\Omega_{Aragonite}$							
	I		II		III		Average	
	Mean	SE	Mean	SE	Mean	SE	Mean	SE
380	0.86	±0.02	0.94	±0.02	1.04	±0.08	0.95	±0.05
560	0.66	±0.04	0.67	±0.02			0.66	±0.01
840	0.53	±0.02	0.58	±0.01	0.65	±0.02	0.59	±0.04
1120	0.41	±0.02	0.47	±0.01	0.53	±0.01	0.47	±0.03
1400	0.25	±0.01	0.41	±0.01	0.47	±0.02	0.38	±0.07
4000			0.12	±0.01	0.14	±0.00	0.13	±0.01
Storage Tank	0.97	±0.07	0.81	±0.04	0.78	±0.07	0.85	±0.06

In summary, C_T increased with rising treatment level and over the experimental duration, while A_T remained fluctuated around a mean value. Calculated pCO_2 values increased over time, especially in the storage tank. Furthermore, the seawater was undersaturated with respect to calcite at ppm values of 840 and higher and always undersaturated with respect to aragonite. But besides the measured carbonate system parameters, other abiotic factors were examined (see next chapter) to control the stability and the influence of external variables.

3.5 Further Abiotic Factors

To assess their possible impact on the experimental animals and the experimental design, abiotic parameters, including pH (chapter 3.5.1), temperature [°C] (chapter 3.5.2) and salinity (chapter 3.5.3) were determined.

3.5.1 pH

Only minor fluctuations in pH were observed within each treatment during the experimental periods, as indicated by the relatively low standard errors (see table 3.4). The pH values decreased with increasing pCO_2, from 8.02 (±0.03 SE) in the control treatment (380 ppm) up to 7.07 (±0.01 SE) in the highest CO_2 treatment (4000 ppm). As C_T and pCO_2 increased in Kiel Bay waters during the experimental period, average pH values decreased from experiment to experiment.

Table 3.4 Mean pH in each CO_2 treatment [ppm] and experiment. Roman numerals indicate the experiment number. Calculated pH is obtained using A_T and C_T measurements from experiment II and III. Standard error (SE) is shown (n=2-3).

Treatment [ppm]	pH								
	I		II		III		Average		calculated
	Mean	SE	Mean	SE	Mean	SE	Mean	SE	pH
380	8.065	±0.006	8.029	±0.006	7.959	±0.019	8.018	±0.031	8.124
560	7.916	±0.008	7.854	±0.004			7.885	±0.031	7.991
840	7.840	±0.004	7.781	±0.004	7.736	±0.007	7.786	±0.030	7.913
1120	7.711	±0.008	7.683	±0.005	7.639	±0.005	7.678	±0.021	7.807
1400	7.504	±0.005	7.614	±0.004	7.584	±0.005	7.567	±0.033	7.752
4000			7.080	±0.005	7.051	±0.007	7.066	±0.014	7.210
Storage Tank	8.065	±0.012	7.930	±0.014	7.751	±0.014	7.915	±0.091	7.995

3.5.2 Temperature

In experiment I water temperature was almost constant (12 °C ±1 SE) in all aquaria. The temperature during the first experimental period slightly fluctuated around 13 °C with a maximum of 14 °C and a minimum of 11 °C (mean values of all aquaria; table 3.5). A slight variation with a maximum of 1 °C/day was visible. The mean temperature of 12 °C (±1 SE) during the second experimental period also fluctuated slightly with a maximum of 1 °C/day. Even in experiment III only small deviations from the mean temperature of 12 °C (±0 SE) were observed (maximal 0.8 °C/day).

In general, the mean temperature was 12 °C in all treatments changing on average only 0.03 °C/day. Maximum and minimum temperatures were less than 2 °C apart from the mean.

Table 3.5 Temperature [°C] in the experiments. Displayed are means, standard error, maximum and minimum values, the mean change per day in each experiment as well as the maximum change per day. Standard errors (SE) are displayed (n=16-17).

	Temperature [°C]					
	Mean	SE	Maximum	Minimum	Mean change [°C/ day]	Maximum change [°C/ day]
Experiment I	12.5	±0.05	13.5	10.9	0.011	-1.140
Experiment II	12.3	±0.05	13.7	11.0	0.042	-1.440
Experiment III	11.8	±0.03	12.6	10.6	0.024	-0.880
All Experiments	12.2	±0.10	13.7	10.6	0.026	-1.440

3.5.3 Salinity

During the first experimental period salinity varied slightly around 12 (±1 SE) (mean values of all aquaria; table 3.6), whereas in experiment II the salinity was a little lower, fluctuating around a value of 11 (±0 SE). In both treatments maximal changes of only 0.8 to 0.3 units/day were detected. On the other hand, during the third experiment a continuously increasing trend from 12 to 18 salinity was observed. This way, the mean value of 16 was more variable in the third experiment than in the other experiments (±0 SE) including a maximum change of 1.3 units.

In the first two experiments salinity was rather constant in contrast to the third experiment, where salinity constantly increased leading to a higher mean value. Therefore, great variations in the overall mean salinity of 13 from a minimum of 11 up to a maximum of 18 occurred.

Table 3.6 Salinity in the experiments. Displayed are means, standard error, maximum and minimum values, the mean change per day in each experiment as well as the maximum change per day. Standard errors (SE) are displayed (n=16-17).

	Salinity					
	Mean	SE	Maximum	Minimum	Mean change [units/ day]	Maximum change [units/ day]
Experiment I	12.4	±0.05	13.7	11.7	-0.063	0.800
Experiment II	11.4	±0.02	11.8	11.0	0.017	0.300
Experiment III	15.9	±0.14	17.8	11.9	0.208	1.280
All Experiments	13.2	±1.35	17.8	11	0.054	1.280

In summary, even though pH was relatively stable within experimental treatments, a decrease in pH was observed from experiment to experiment, especially in the storage tank, which was fed with water drawn from the fjord. Temperature, on the other hand, remained constant throughout the experimental periods leading to similar mean values in the three trials and showing only minor fluctuations. Even less fluctuation in salinity was observed in the first two experiments. This was not the case in the third experiment, where salinity values were rapidly increasing, resulting in a higher mean value in the third experiment than in the previous experiments. To investigate the rise in pCO_2 and the decrease in pH during the study period more closely, environmental parameters at the sampling site in Kiel Fjord were investigated in more detail.

3.5.4 Environmental Parameters

Field measurements at the sampling site were carried out from April to September, 2008, consisting of pH, temperature [°C] and salinity measurements, as well as A_T [µmol/kg SW] and C_T [µmol/kg SW] determinations to gain a better understanding of the carbonate system parameters and other abiotic factors observed in the experiments.

During the experimental periods from April 24th to July 18th 2008, pH decreased, especially between June and July from 8.2 to about 7.7, whereas salinity increased from 11 to 18 (figure 3.15). Temperature, on the other hand, increased strongest from 10 to 15 °C between April and May and varied afterwards rather consistently between 15 and 18 °C, resulting in a mean temperature of 15 °C.

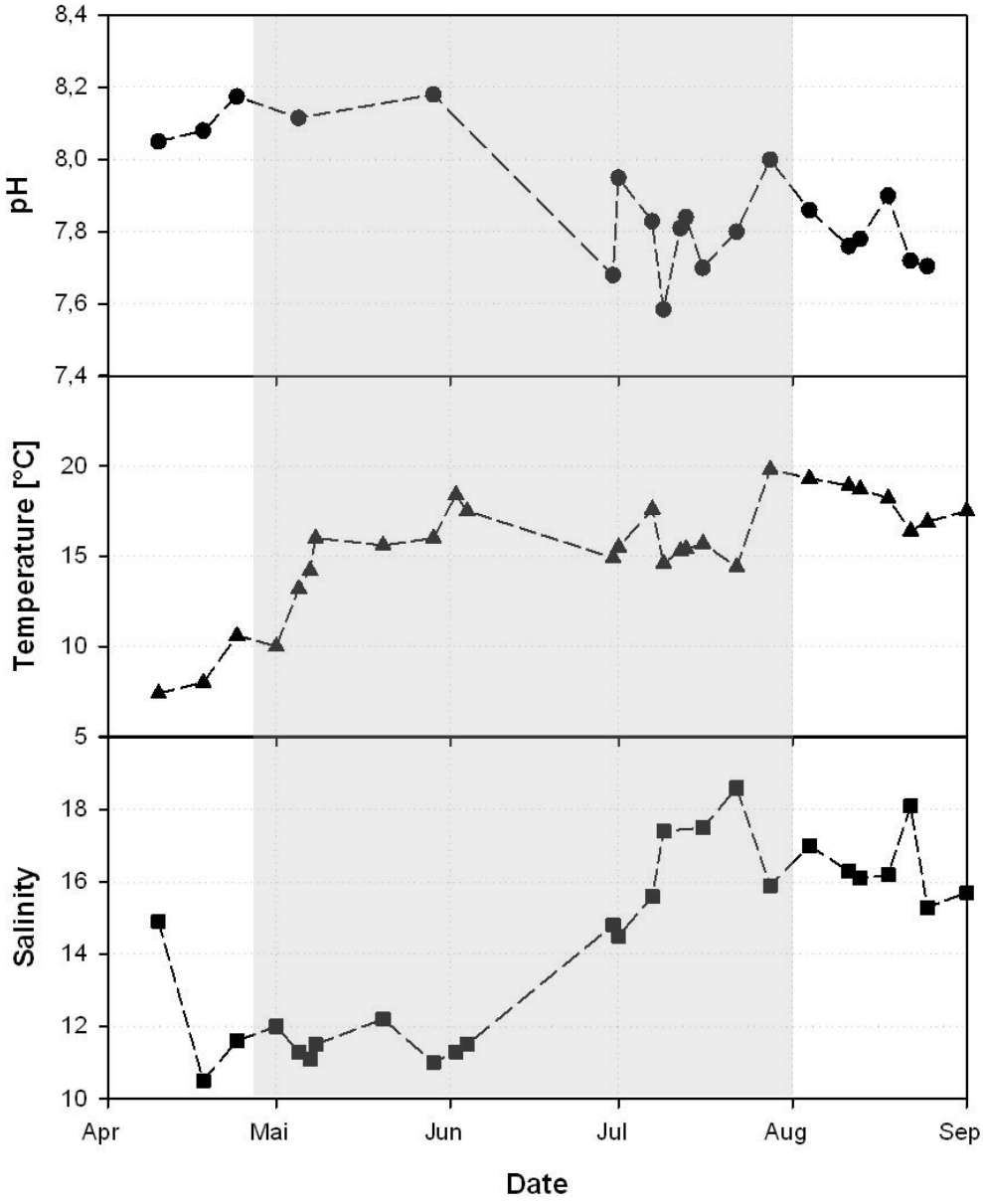

Figure 3.15 Temperature, pH and salinity in the surface water of Kiel Fjord from April to September, 2008. Whereas pH declined temperature and salinity increased during summertime. The time span marked in grey indicates the experiments period.

It is also noteworthy that pH values as low as 7.6 (9th of July ; 1435 ppm), and 7.4 (8th of September; 2345 ppm), were observed at the sampling site, which is comparable to the pH values of the 1400 ppm treatment and even below. For the trend in salinity revealed an inverse relationship to pH values (r = 0.8) whereas temperature behaved independently (r = 0.2) (table 3.7). To further investigate conditions at the sampling site, field samples of A_T and C_T were taken at the mentioned dates and at another day with a higher pH of 7.8. A_T and C_T increased with decreasing pH and, therefore, the calculated parameters exhibited the same trend. Calculated pCO_2 values confirmed the observations made above, that conditions in the Fjord at those two days were above 1400 ppm. Except for calcite on August the 13th (1046 ppm and pH 7.8) the sampling site was undersaturated in respect to calcite and aragonite. Since water pH was measured with an electrode, pH was more precisely calculated using C_T and A_T values, but even after correction values remained markedly low.

Table 3.7 Field measurements at the sampling site at selected dates 2008. Salinity, pH and temperature [°C] were analyzed as well as A_T [µmol/kg SW] and C_T [µmol/kg SW], which both were used to calculate pH and pCO_2, $\Omega_{Calcite}$ and $\Omega_{Aragonite}$. Values for pH on July 9th and September 8th were markedly lower than on August the 13th, 2008.

Date	July 9th, 2008	August 13th, 2008	September 8th, 2008
measured pH	7.585	7.780	7.424
calculated pH	7.683	7.832	7.487
Salinity	17.4	16.1	19.3
Temperature [°C]	14.6	18.7	15.5
A_T [µmol/kg SW]	1955.2	1913.7	2044.9
C_T [µmol/kg SW]	1973.1	1891.5	2106.3
CO_2 concentration [ppm]	1435.0	1046.1	2345.3
$\Omega_{Calcite}$	0.79	1.21	0.58
$\Omega_{Aragonite}$	0.47	0.72	0.35

In summary, salinity was inversely related to decreasing pH values during the experimental period while temperature was not correlated to pH. The most drastic change in salinity and pH was observed between June and July. Temperature, however, increased only at the beginning and in the end of the experimental period remaining constant in between. It stood out, that pCO_2 values greater than those of the 1400 ppm treatment were found at the sampling site on separate days, suggesting that the local mussel population is exposed to elevated pCO_2 in the natural habitat on a regular basis. A_T and C_T increased with lower pH. Since both variables were involved in calculation of Ω, calculated Ω indicated increasing degrees of undersaturation with respect to calcite and aragonite.

4 Discussion

In this thesis, whole-animal performance indicators, such as heart rates and valve/siphon opening patterns of the blue mussel, *Mytilus edulis* from the Baltic Sea were investigated in response to elevated pCO_2 values. The goal was to estimate physiological consequences of future ocean acidification, which is considered to be 1900 ppm in the year 2300 corresponding to a pH of 7.3 (Caldeira and Wickett 2003).

4.1 Whole-animal physiology

Some effects of acidic seawater on systemic physiology of blue mussels are already known. Gazeau et al. (2007) detected that calcification rates declined linearly with increasing pCO_2. These authors observed a cessation of calcification at pCO_2 values of about 1800 ppm in a North Sea population during short-term incubation (<1 week) to elevated seawater pCO_2. Heinemann et al. (unpublished, fig 4.1) detected a similar trend in Baltic *M edulis*, although cessation of calcification was observed at higher pCO_2 values (2500-2700 ppm).

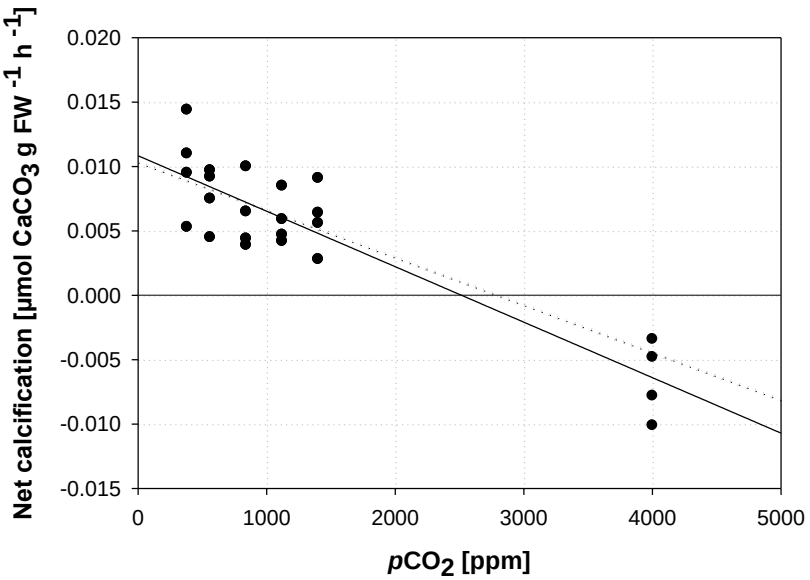

ppm	380	560	840	1120	1400	4000
$\Omega_{Aragonite}$	0.91	0.77	0.74	0.61	0.56	0.31
$\Omega_{Calcite}$	1.53	1.29	1.24	1.01	0.94	0.53

Figure 4.1 Calcification rates per unit fresh mass and hour [µmol $CaCO_3$ g FM^{-1} h^{-1}] in relation to pCO_2 [ppm] in Baltic Sea mussels. Calcification rates were determined using the alkalinity anomality technique after 1, 2, 7 and 14 days (e.g. Gazeau et al. 2007). The intersection of the regression lines with the x-axis at zero marks the onset of shell dissolution. The dotted regression line was calculated without the 4000 ppm treatment data. The table below depicts mean calcium carbonate saturation states at each of the tested pCO_2 treatments. Heinemann et al. unpublished.

Higher pCO_2 values lead to negative rates of calcification, i.e. shell dissolution. The dissolving calcium carbonate shell may therefore contribute to the harmful effects of acidic seawater. This was also suggested by Bibby et al. (2008), who stated that cellular metabolism, function and signalling pathways relying on constant calcium concentrations were disrupted with rising pCO_2 and, hence, had a significant effect on the immune response of *Mytilus edulis*. Furthermore, Berge et al. (2006) observed decreasing growth at pH ≤ 7.4 to 7.1 and virtually no growth at pH 6.7. A pH of less than 6.6 even led to higher mortality.

Experiments conducted by Schlieper (1955b) are the only known experiments investigating the effect of seawater pH and pCO_2 on activity and cardiac performance. He concluded that reduced heart rates (bradycardia), sometimes observed during prolonged valve closure (Woortmann 1926, Helm and Truemann 1966, Coleman and Trueman 1971), are the result of accumulation of CO_2, oxygen depletion (also suggested by Bayne 1971) and resultant proton accumulation, rather than due to the accumulation of metabolic end products or reduced levels of external disturbances (light regime, mechanical disturbances), as predicted by Woortmann (1926). But most of the time before valve closure was triggered, indicating that valve closure and heart rates are not causally related to one another. In addition, Curtis et al. (2000) stated that heart rate variability (HRV) and valve opening status were weakly correlated.

4.1.1 Cardiac performance

Heart rate is a measure of the level of metabolic performance (Schlieper 1955a). Widdows (1973) investigated active and standard metabolic rates by correlating heart rate with ventilation rate and oxygen uptake. Even though he did not find a close relationship between heart rates and metabolic rate, as Lowe and Trueman (1972) did, he observed that heart rate was strongly correlated to disturbances in homeostasis (e.g. due to critical temperatures, starvation). Consequently, the cardiac performance of *Mytilus edulis* has already been successfully used as a whole animal stress indicator in studies dealing with toxins, such as copper (Scott and Major 1976, Curtis at al. 2000) or dimethoate (Lundebye et al. 1997), as well as temperature and salinity effects (Stickle and Sabourin 1979, Bahmet et al. 2005, Braby and Somero 2006).

Methods used for heart rate determinations in the past were direct visual observation, implants or ultrasound stethoskops (see review by Koester et al. 1979). The infrared light sensing method (Depledge 1984) used in this study had the advantage of enabling long-term, non-invasive recordings and, therefore, plethysmographs have been employed in

many recent studies (Frederich et al. 2000, Wedderburn et al. 2000, Bakhmet et al. 2005). Furthermore, the handling stress due to sensor attachment is considered minimal causing only brief disturbances in HRV (≤1 hour; Depledge et al. 1996). Opposed to the CAPMON system (Computer-Aided Physiological Monitoring), an analogue-digital converter that can be used with the plethysmographs invented by Depledge and Andersen (1990), the PowerLab data acquisition system used in this study provided the opportunity to record and analyze data in much more detail. Whereas the CAPMON system displays only means of rate functions (e.g. mean heart and ventilation rate), the PowerLab with its software can even be used to analyze the intervals between heart beats. Therefore, the AIDA system (Automated Interpulse Duration Assessment) was invented by Depledge et al. (1996), which could be used to detect irregularities in cardiac rhythm as well. But in contrast to the AIDA system being specifically designed for measurement using plethysmographs, the PowerLab system provides the ability to measure a whole range of other physiological parameters, e.g. blood pressure, if desired.

Plethysmographic heart rate recordings are non-reliable indicators of heart stroke volume (i.e. the volume of blood that is pumped with each heart beat), because the signal amplitude is affected by surrounding tissues (Koester et al. 1979) and, thus, mainly depends on the placement of the sensor. Furthermore, even the variability within individuals was very high. Sensors were sometimes removed by movements of the mussel and computer break down sporadically occurred. Therefore, only two hours each day were analyzed (as noted in chapter 2). In a previous study by Marshall et al. (2004), investigating HRV in limpets, such a time period has already been proven to be sufficient for a meaningful physiological analysis.

IHR

In this study the mean heart rate of 12 BPM was in good accordance with the predicted heart rate for mussels of this size in the measured salinity and temperature range (Widdows 1973, Bayne 1976, Braby and Somero 2006). Heart rate was not affected by increased carbon dioxide concentrations up to 4000 ppm (=405 Pa). This is in contrast to previous studies on molluscs, where a clear relationship between seawater pCO_2 and heart rates was encountered. Michaelidis et al (1999) found that elevated pCO_2 (100000 ppm/10133 Pa) caused a decrease in heart rate and force of contraction in isolated ventricles of the land snail, *Helix lucorum*, within 60 minutes. Since calcium ions are the essential ions for muscle contraction, these authors suggested that Ca^{2+} competes with protons for binding sites on the sarcolemma. An increasing amount of proton occupied

binding sites, would lead to a decrease in the force of contraction. This was additionally supported by the observation that low calcium levels enhanced the effect of hypercapnia. But on the other hand, elevated calcium levels did not restore the contractility of the heart. Schlieper (1955b) examined the effect of different pCO_2 values on the heart rate and valve opening of blue mussels from Kiel Fjord by direct observation. He found out that concentrations higher than 49998 ppm (5066 Pa) led to cardiac arrest and death within 10 minutes. Mussels exposed to 24999 ppm (=2533 Pa) survived during the 30 minutes exposure period. However, distinct decreases in heart beat amplitude and frequency were observed. The exposure levels used by Schlieper (1955b) and Michaelidis et al. (1999) were extremely high compared to the values used in the present study and the exposure period only lasted 30-60 minutes, but since the mussels used were much smaller (10-13mm), being probably even more sensitive (Sukhotin et al. 2002), these findings might suggest the high stress tolerance level of this species. Furthermore, Schlieper (1955b) also investigated the influence of a more realistic pH of 7.0 by manipulating seawater through addition of HCl. He observed a marked slowing of heart rate immediately after transferring the animal into the acidified seawater. This result stands in contrast to the results yielded in this study, since the measured pH in the highest treatment was also 7.0, but heart rate remained unchanged. However, the pH calculated via CO2SYS using A_T and C_T indicated a higher 'true' pH value of 7.2, which may be not be sufficient to trigger a response in heart rate. But above all, it has to be noted that mussel in the study by Schlieper (1955b) encountered an additional stress, since they were exposed to modified seawater simply by transferring them rapidly from normocapnic water into acidified water. In this study, however, mussels were slowly exposed to CO_2 (desired values were reached in about one day). On the other hand it is more likely that results gained by Schlieper (1955b) and Michaelidis et al. (1999) do not reflect physiological responses normally occurring in nature. Extremely short exposure periods to exceptionally high pCO_2 levels do not pose an opportunity for species to acclimate.

HRV

To determine the sensitivity of blue mussels to ocean acidification more closely, it has to be pointed out that HRV is considered a more sensitive indicator of physiological stress. Depledge et al. (1996) demonstrated that HRV in blue mussels changed during handling stress, while the heart rate remained unchanged. Furthermore, it has been shown that a 50% decrease in HRV was caused by copper concentrations an order of magnitude lower than the concentration that caused a 50% decrease in heart rate (Curtis et al. 2000). Thus, it

was concluded that the beating pattern reacts to stress before a deviation in the heart rate becomes visible. The variability of interpulse duration in blue mussels is a result of the characteristic of the heart itself. Probably most molluscan hearts are myogenic (Jones 1983); meaning that contraction is initiated by the diffuse pacemaker cells itself. The unstable membrane potential of pacemaker cells leads to a spontaneously opening or closing of ion channels (Irisawa 1967). In addition, inotropic (amplitude of heart beat) and chronotropic (heart rate) control is exerted through nerves coming from the visceral ganglion. Excitatory nerves lead to acceleration and inhibitory nerves lead to depression of heart beat. In addition, some neurotransmitters like serotonin (Koester et al. 1979) are assumed to play a role. The interpulse duration of *Mytilus edulis* in well-aerated seawater is more regular than in mammals because no other function such as ventilation is assumed to influence the IHR of this species (Curtis et al. 2000). This was also shown by Widdows (1973), who stated that there is no nervous coupling between heart and ventilation rate. Thus, stress is indicated by a wider distribution of interpulse duration in histograms (Depledge et al. 1996) other than in mammals, where a high temporal fluctuation in the beating pattern resembles a relaxed and powerful organism (Task Force 1996).

This study is the first to precisely determine HRV in relationship to (environmentally relevant) elevated seawater pCO_2 and corresponding pH values. Since there are no standardized indicators of HRV for mussels in the literature, many different parameters have been tested in this study. The mean, median and mode values did not respond to changes in pCO_2. Furthermore they were nearly equal to one another indicating a close to normal distribution of interpulse durations, which is also supported by zero skewness. In addition to this, elevated pCO_2 did also not affect SDNN or the range beat-to-beat interval distribution. Kurtosis, otherwise, insignificantly decreased from phase I to II, indicating that the first peaky distribution of interpulse durations was approaching a normal distribution closer to zero. But this trend is rather due to the adaptation of the animals to the experimental setup than due to rising CO_2 values, since the effect was also visible in the control group. On the other hand, in the CV, SDdeltaNN and RMSSD an insignificant increase from phase I to phase II was observed, suggesting a trend towards higher degrees of stress in experimental animals with incubation time. These contradictory results might suggest that kurtosis is a less suitable indicator of HRV than the latter indicators (i.e. CV, SDdeltaNN and RMSSD). Furthermore, in the 1400 ppm treatment much higher variations in kurtosis were observed than in the other treatments. These fluctuations, as well as the great standard errors are due to the heavy tails of the distribution, which distort the kurtosis value, if extreme values are included. The CV of the beat-to-beat interval has

already been used in a study by Curtis et al. (2000) using the AIDA System dealing with *Mytilus edulis* exposed to copper. They found rising CVs with increasing copper concentrations. Therefore, CV has already been defined as a suitable HRV indicator. The CV of control mussels in the study of Curtis et al. (2000) was 0.08, being in good accordance with the overall CV value measured in this study of also 0.08 (± 0.004 SE). The CV was the only HRV indicator increasing (but insignificant) with rising CO_2 values in phase II, independent of phase I, indicating a slight trend towards more stress due to increasing carbon dioxide concentrations. Whereas the CV detects changes in the overall variability independent of changes in the mean interval duration, the RMSSD and the SDdeltaNN both reflect short term HRV being independent of any diurnal or other long term trends (Kleiger 1995, Kobayashi et al. 1999). Both parameters were highly correlated (differing not more than 0.5%), which has also been shown by Kleiger et al. (1995). Kim et al. (2007) demonstrated a high degree of correlation between RMSSD and SDdeltaNN even in their sensitivity towards missing interval data.

In summary, no significant changes in HRV were observed with rising pCO_2 in any of the measured parameters. The ordinary distribution of beat-to-beat intervals in *Mytilus edulis* seems to be a close to normal distribution with a more pronounced peak and longer tails than a Gaussian curve, as indicated by the mean, median, mode, skewness and kurtosis values. No trends were observed in the mentioned parameters, except in the latter (i.e. kurtosis), as well as in the SDNN and the range, which are, potentially, more robust measures of HRV than kurtosis. CV showed the only response, which could definitely be related to pCO_2. Hence, it seemed to be a more sensitive parameter. The RMSSD and SDdeltaNN also seem to be more sensible indicators, but should be regarded as surrogates for each other. Even though no significant changes occurred, some parameters displayed minor trends, thus it might be useful to measure more than one variable for HRV at the same time. For future analysis, the following parameters should be determined simultaneously to generate a more complete picture of heart rate variability in mussels:

1. *Mean and SDNN*: easy to obtain and robust
2. *Median*: more robust against outliers than the mean
3. *CV*: sensitive indicator and independent of changes in the mean
4. *SDdeltaNN:* indicates short term HRV and more easily obtained than RMSSD

In contrast to findings in this study, Schlieper (1955b) found an erratic beating pattern at 24999 ppm (=2533 Pa), but, apart from using extremely high pCO_2 values in his study, he did not give a measure of HRV and results have been obtained only by means of visual observation. Ellington (1993), on the other hand, studied ventricular myocytes in the

southern quahog, *Mercenaria campechiensis*, a species that exhibits a mostly sedentary lifestyle (Stanley 1985) similar to that of *Mytilus edulis*. He found intracellular pH (pH_i) in cardiac myocytes not to be affected by extracellular (haemolymph) pH (pH_e) at values ranging from 8.0 to 7.1, similar to pH_e values obtained for the experimental animals from the present study (Thomsen et al. unpublished, figure 4.2). Thus, the decrease in pH_e in this study is considered to be not sufficient to yield a significant response in HRV and heart rates.

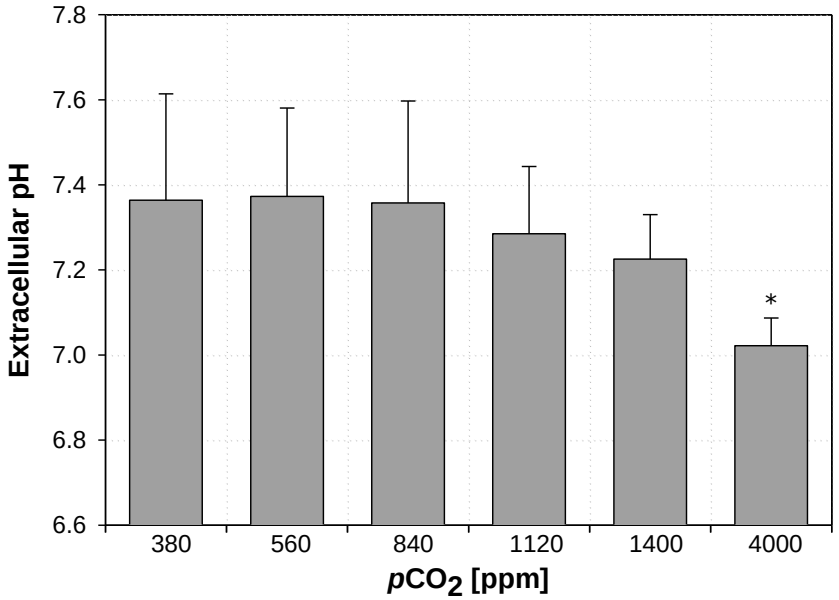

Figure 4.2 Extracellular (haemolymph) pH (pH_e) of Baltic Sea blue mussels at different pCO_2 levels [ppm]. Measurements of pH_e were conducted using fiber-optical sensors (optodes). Values are for the same mussels that were used in the present Diplom thesis. An asterisk (*) marks a highly significant difference ($p<0.01$; ANOVA; Tukey). Thomsen et al. unpublished.

4.1.2 Activity patterns

Valve and siphon opening patterns were examined as indicators for activity. These factors have already been approved of as stress indicators in response to toxins, such as copper (Curtis et al. 2000), or food depletion (e.g. Riisgård and Randløv 1981, Riisgård 1991). Both indicators are necessary because, although there is a weak correlation between siphon and valve, they are not always closely connected (Riisgard et al. 2003). The reason for this is that *M. edulis* is able to alter its pumping rate without altering shell gape by regulating the exhalent siphon area (Davenport and Woolmington 1982, Newell et al. 2001, Maire et al. 2007). Therefore, the siphon area was additionally assessed from the data. Overall, the opening state is considered to be an indicator of periods of active feeding (see chapter 4.1.3) and ventilation (Jørgensen et al. 1986b, Newell et al. 2001).

Results in this study have been obtained by time lapse imaging and computer aided analysis. This had the advantage of obtaining continuous recordings in contrast to direct observations as carried out in older studies (e.g. Davenport and Woolmington 1982). Disadvantages of the method used in this study were that the opening degree was not exactly definable since no visual markers were applied to the shell. Calibration using a ruler also involved additional minor uncertainties due to the right positioning and every time the mussel moved, pixels had to be recalibrated. Even though pictures were obtained every five minutes, only 1 picture/hour was analyzed due to the great expenditure of time while analyzing every picture manually. This problem was overcome by a more recent study by Maire et al. (2007), who invented a new imaging technique using higher contrast and, therefore, were able to obtain results automatically from a computer program. Wilson et al. (2005) used a Hall sensor system to measure valve opening gaining continuous and directly utilisable data, even in the field. A similar method was used in the Musselmonitor-system, which consists of electromagnetic coils (de Zwart 1995). A magnet or electromagnetic coil respectively is glued to one shell half, whereas the Hall sensor or the other coil, acting as receiver, is glued to the other. After calibration, the induced current is proportional to the distance between the shell halves. However, these methods only monitor valve opening status and not the siphon opening, which is the more relevant physiological parameter) and also involved great noise as well as additional stress for the animals due to sensor attachment. Recordings in the present study were obtained only during light hours, avoiding changes in valve opening due to diurnal rhythms as seen by Ameyaw-Akumfi and Naylor (1987) and Wilson et al. (2005). It was observed in these studies that mussels close their shells more often during daylight to avoid predation.

Mussels did not vary their opening degree (valve and siphon position) in response to pCO_2 values applied in this study. The mean valve opening varied around 57 % (±1.33 SE). In contrast, control mussels in the study by Curtis et al. (2000) were 75 % open. However, abiotic factors (15-16 °C, 33 salinity) were different from this study and there was no information about algae cell concentration given. The valve and siphon opening state decreased mostly insignificantly from phase I to phase II, even in the control group, indicating stress due to persisting experimentation as already observed in some HRV parameters. Furthermore, mussels exposed to higher pCO_2 levels opened their shells slightly more often. But this relationship was insignificant and was also found in the siphon opening state before mussels were introduced to higher pCO_2. Therefore, no conclusions should be drawn, besides that valve and siphon positions behaved differently than valve and siphon opening state. The latter parameters are more sensitive indicators in response to

elevated seawater pCO_2. Lower values were observed in the siphon opening state and position than the valve gape, since it was regulated independently as expected and discussed above.

Metric data was not further included in the analysis. Percentage data better reflected the relative mean siphon opening, since metric siphon diameter is strongly dependent on siphon size, shape and orientation to the webcam. Conversion of raw data into percentage or degree of maximum opening is also an approved method in the literature (Curtis et al. 2000, Wilson et al. 2005, Maire et al. 2007).

Significant statistical differences found in siphon opening in this study were disregarded, as either: (1), a treatment differed from the other treatments in phase II but not from its initial control phase indicating that differences were due to individual variability and not a response to CO_2 or (2), mussels behaved differently in phase II than in phase I but no significant difference was found between other treatment groups in the same phase indicating that mussels adjusted to the experimental setup and not to CO_2. In other treatment groups no significances were observed due to higher individual variability.

Results obtained are consistent with Schlieper (1955b), who observed that valves did not react strikingly different at a pCO_2 of even 24999 ppm Pa). Bamber (1990) observed increased gaping of the shells only at a pH $\leq$ 6.6. Below this threshold, mussels appeared to be sedated, as indicated by an abnormal gaping of the valves. This behaviour is probably analogous to narcosis, since high CO_2 concentrations act by paralysing the respiratory centre. In the past CO_2 was often used as an anaesthetic in humans and is still in use for small laboratory animals (Kohler et al. 1999). Hence, the moderate (but environmentally realistic) pCO_2 treatments applied in this study were not sufficient to trigger a response in valve and siphon opening patterns.

4.1.3 Food uptake and growth

The food supply was kept constant during this study as several physiological parameters depend on this crucial factor: valve (Jørgensen et al. 1986a, 1988, Riisgård 1991, Riisgård et al. 2003) and siphon opening state (Newell et al. 2001, Maire et al. 2007), heart rates (Widdows 1973) and even ventilation rates (Thompson and Bayne 1972). Using algae concentrations of 1696 (±178 SE) to 4811 cells/ml (±905 SE), starvation effects as probably occurred in the study by Berge et al. (2006) were avoided. Valve gape, on the other hand, was closely correlated with filtration rate (Jørgensen et al. 1988), which, in turn, is also more adjusted to prevailing food concentrations than to temperature (Kittner and Riisgård 2005) or to nutritional needs (Clausen and Riisgård 1996). The energetic growth

model (Riisgård 2001) suggests maximum valve opening and filtration activity at algae concentrations applied in this study (i.e. 1696 to 4811 cells/ml). This is even irrespective of high levels of silt (Riisgård et al. 2003), as was found to enhance clearance rates in other studies (Navarro et al. 1996). Algae concentrations lower than 1000-1500 *Phaeodactylum tricornutum* cells/ml trigger valve closure due to lack of food (Riisgård and Randløv 1981, Riisgård et al. 2003) and higher concentrations than 30,000 trigger valve closure due to satiation of the digestive system (Riisgård and Randløv 1981, Davenport and Woolmington 1982, Riisgård 1991).

To achieve a constant algae supply, a peristaltic pump was used to drip a suspension of DT's Live Marine Phytoplankton to the header tank. Even though this diet had already been approved of in another study by Espinosa and Allam (2006), it should be applied with care since other studies already questioned its nutritious value (Teßmann 2008). Only *Phaeodactylum tricornutum* is a natural food source of blue mussels in the Baltic Sea and has been proven to be completely (100%) retained (Møhlenberg and Riisgård 1978), whereas *Nannochloropsis oculata* is probably of less value due its size, since particle selection depends on the size of the labial palps (Kiørboe and Møhlenberg 1981). Exudates of *Chlorella* sp. have even been shown to cause feeding inhibition (Wilson 1981). The algae cell calculation (equ 2.2) introduced in chapter 2.4.1 including the filtration rate equation (equ. 2.1) by Møhlenberg and Riisgård (1979) should also only be used as an estimate, since the filtration rate equation is only reliable in a dry mass range between 0.11 – 1.36 g and was defined at 10-13 °C and a salinity of 30.

A continuous supply rate of one drop about every 5-10 sec (1 ml/min) was ensured, since Riisgård et al. (2003) found that constant algae concentrations within an optimum concentration ensure maximum filtration rates. Air stones were added in all tanks, including the header and algae tank ensuring water mixing to avoid sedimentation. A disadvantage of introducing the algae cells via the peristaltic pump was that algae cells were trapped in the small diameter tubing at very low flow rates, which led to clogged tubing causing a varying supply rate. Therefore, algae cell concentrations were checked using a coulter counter in the middle of every experiment to adjust food supply. Interestingly, the algae cell concentration in the storage tank was increasing during the experimental period, compensating for the increased clogging of the tubing. Therefore, algae cell concentrations in the aquaria excluding the 4000 ppm treatment were well in the optimum concentration in every experiment, even though great variations occurred. Riisgård and Randløv (1981) showed that filtration rate was independent from algae concentration in between the optimum range. Algae from Kiel Fjord were able to reach the storage tank as a result of

inefficient mechanical filtration systems. The regression line of algae cell concentration in the storage tank even indicated a typical growth curve including the end of the lag phase (end of April to beginning of May), where algae acclimated to the new environment, the exponential growth phase (May to June) and the stationary phase (July), where the number of new algae equal the number of dying algae. For further studies, especially when examining the food consumption more closely, it is recommended to change the filter cartridges of the mechanical filtration units more often (every few days instead of every two weeks).

Interestingly, mussels in the 4000 ppm treatment (corresponding to a calculated pH of 7.2) removed significantly less algae cells than all other mussels. It is concluded that this behaviour is the result of an inhibition of filtration activity. This is in good agreement with literature data, as suppression of feeding activity was found at a pH ≤ 7.2 in *Mytilus edulis* as well as in *Ostrea edulis* and *Crassostrea gigas* independent of size, water temperature or experimental duration (Bamber 1990). Even in *Venerupis decussate,* an inhibited feeding rate was observed at a pH of approximately 7.0 (Bamber 1987). Since Booth et al. (1984) found a haemolymph pH of 7.2 in mussels exposed to air, this pH value might be a stimulus to stop filtering resulting from limited functioning of the involved ATPases. A low pH_e leads to a low pH_i and, hence, to low cell energy charge (Gibb's free energy charge, ΔG). As a consequence, proper functioning of ATPases is restricted (Kammermeier et al. 1982).

But the question arises, if pumping rates and filtration activity are correlated to valve and siphon gape as well as heart rates, why was there no significant decrease in those parameter evident in the 4000 ppm treatment? Even though the high pCO_2 did not affect valve and siphon opening, it probably did affect Na^+/K^+ ATPase activity of the gills, since an insignificant decrease at the highest pCO_2 level was observed (Thomsen et al. unpublished, fig. 4.3). Na^+/K^+-ATPase is a membrane protein that couples the exchange of two extracellular K^+ ions for three intracellular Na^+ ions to the hydrolysis of one molecule of ATP. Its main action is to maintain ion electrochemical gradients across the plasma membrane accounting for 25% of the standard metabolic rate (see review by Lingwood et al. 2005). Since the dynein ATPase in the gill cilia such as any other ATPase is dependent cellular homeostasis for proper functioning, this may indicate that the gills are less active suggesting slower ciliary movement. Further studies on gill ATPases including a higher resolution need to prove this hypothesis.

Heart rates were only affected by feeding if the animals were starved for over 28 days in another study by Widdows (1973) and when fed again, they increased their filtration rate steadily to a control level within 10 days. Fed animals, on the other hand, showed no

response to food additions (Thompson and Bayne 1972). Hence, the period of suppressed food uptake was not sufficient to trigger a response in heart rate during the course of this study.

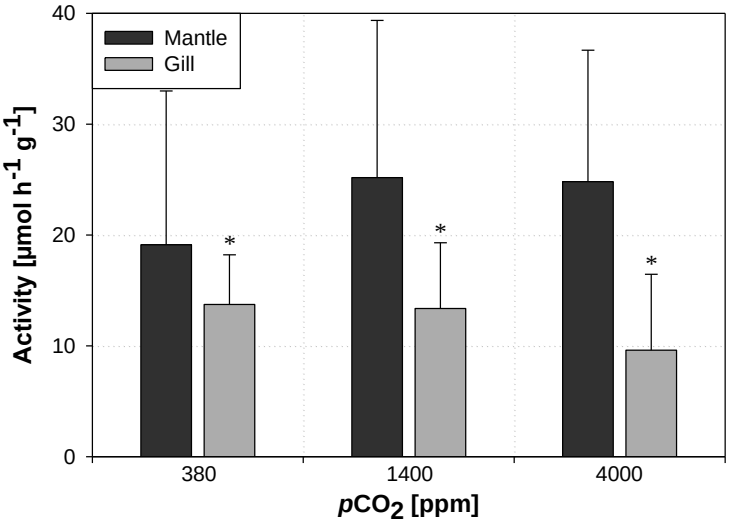

Figure 4.3 Na^+/K^+-ATPase activity [µmol h^{-1} g^{-1}] of Baltic Sea blue mussels at three different pCO_2 levels [ppm]. The same mussels were used as in this study. An asterisk (*) marks a highly significant difference ($p<0.01$; t-test) between mantle and gill ATPases. Thomsen et al. unpublished.

4.1.4 Length and wet mass

Even though sufficient food was supplied, no growth was observed. This was no surprise, since mussels were too old (>5 yr) to significantly grow during the experimental period. In the Kiel Bight *M. Edulis* achieves a maximum length of up to 90 mm after 5 yr (Kautsky 1982a). Mussels were significantly longer (3.5 mm) in the last experiment than in the first. Differences in wet mass were highly significant leading to an increase of up to 14.6 g or 39% between experiment I and III (measurement error accounted for about only about 1.1 mm). This rise in mass up to June/July is characteristic for mussels in Kiel Bight and is related to reproductive system proliferation beginning in early spring (Boje 1965, Kautsky 1982a). Mass loss at spawning accounts for up to 50 to 60% of shell free dry mass (Kautsky 1982b). Hence, formation of gonads already started shortly before the beginning of the first experimental period. Taking the already heavier wet mass into account, the increase of 39% during the study duration fits well the calculated gain in gonad mass. Wet body mass has been shown to strongly influence filtration (Winter 1973) and heart rates (Bayne 1976), but no effects have been observed between the experiments in this study.

4.2 Influencing factors

4.2.1 Carbonate system and pH

To evaluate the findings made above, other influencing factors will be discussed in this section. The coulorimetric method of C_T determination should be preferred over the photometric analysis, since high CO_2 concentrations above 1400 ppm led to equilibration of sample pCO_2 with the atmosphere. C_T in the experimental aquaria increased according to the composition of the introduced gas mixture, while A_T remained constant with increasing gas mixture pCO_2. Therefore, even though overall total dissolved inorganic carbon (C_T) increased, the carbonate alkalinity (CA) was not greatly affected (see equ.4.1). For every mol CO_2 added one mole of carbonate (counting twice for the CA, see chapter 1.1) is converted with water to two moles of bicarbonate and, hence, the CA stayed constant.

Equ. 4.1 Effect of increasing CO_2 concentration on the carbonate system speciation

$$CO_2 + CO_3^{2-} + H_2O = 2HCO_3^-$$

Expected A_T values of 1800 and 2000 µmol kg^{-1} in Kiel Bight (Rodhe 1988) were confirmed in this study. Variation in A_T over time are due to the correlation of A_T to changes in salinity, even though the correlation is weaker in the Baltic Sea than in other ocean caused by influences of the river runoff (Gripenberg 1960), e.g. the river Schwentine near the sampling site may have an influence. Higher A_T values, on the other hand, caused higher C_T values because the sum of $[HCO_3^-]$, $[CO_3^{2-}]$ and $[CO_2]$ makes up C_T (chapter 1.1).

The pCO_2 values in the experimental aquaria were very variable due to fluctuations of the gas mixing facility. No sensor had been applied at that time measuring the output concentration of the facility. But furthermore, a rising trend towards higher pCO_2 became visible especially in the incoming water (the storage tank) corresponding to a concomitant decline in pH and **Ω**. This is consistent with field measurements, where a decline in pH and an increase in salinity were measured. The reason for this is thought to be wind driven upwelling. Hansen et al. (1999) reported aerobic decomposition of organic matter and a concomitant decline in pO_2 in the bottom waters during stratification in the Eckernförde Bay, close to Kiel Bight. Although pCO_2 values were not determined in this study, they must have been high, as respiratory use of $[O_2]$ results in an almost equimolar increase in $[CO_2]$. Surface water is blown away if southern and western winds occur and bottom water, characterized by higher pCO_2 values, lower pH and higher salinity values are being upwelled. Measured pH in this study was strongly correlated (r=0.8) to salinity, further

supporting the upwelling theory. On several days, extremely low pH values were observed being as low as 7.4. All calculated pCO_2 values were above 1000 ppm, peaking at 2345 ppm (238 Pa), which is far above the pCO_2 value of 1900 ppm predicted the year 2300 by Caldeira and Wicket (2003). As the fjord mussel population is being frequently confronted with high pCO_2 levels in their natural habitat, this could explain why CO_2 treatments <2000 ppm in this study were not sufficient to trigger a measurable response in cardiac performance and activity patterns.

The thermocline in the Kiel Bight is stable from April/May to November (Kändler 1959). The decrease in pH should be stopped when the water is mixed again. Therefore, further measurements need to be carried out to confirm the upwelling hypothesis. The carbonate system parameters in Kiel Bight had a strong effect on the experimental setup. The rising pCO_2 between the experiments indicated that the effect was not totally compensated for by vigorously aerating the incoming water with pressurized air in the storage tank.

The characteristic low alkalinity of the Baltic Sea caused low Ω with respect to aragonite in all treatments and with respect to calcite above a pCO_2 of 840 ppm. Increasing pCO_2 in rising treatment level led to lowering of the carbonate concentration and, and hence, a decrease in saturation state (see equ.4.1). But saturation state and shell dissolution are not tightly coupled as zero calcification was not reached before pCO_2 values of 2500-2750 ppm were reached (Heinemann et al. unpublished data). In some species, the rate of calcification and metabolism even increased with increasing pCO_2, but at the cost of reducing muscle tissue, as shown for the brittle star, *Amphiura filiformis* (Wood et al. 2008). Whereas organisms like corals strictly depend on the saturation state (Hoegh-Guldberg 2007), Gazeau et al. (2007) even found bivalve (*M. edulis*) shell dissolution to occur before the water was undersaturated with respect to calcite.

4.2.2 Temperature

The effect of temperature was kept to a minimum using a cooler, since changes heart rates (Bayne 1976, Braby and Somero 2006) and valve opening including filtration rates (Jørgensen et al. 1990) correlated with changes in temperature. Furthermore, temperature influences the dissociation constants of carbonic acid and thus the pH (Howell et al. 1973). But, in the range and at the speed of observed temperature changes, these changes were negligible, since the natural variation measured in the Kiel Bight was greatly more fluctuating.

4.2.3 Salinity

Salinity has been shown to have an effect on heart rates (Stickle and Sabourin 1979, Braby and Somero 2006) as well as filtration rate (Theede 1963) and valve gape (Seed and Suchanek 1991). During the course of the first two experiments, salinity did not vary much if compared to the natural fluctuation, but during experiment III a continuous increase up to 1.3 units/day was observed. Braby and Somero (2006) investigated the effects of salinity on mussel heart rate by reducing the salinity from 28 to S_{crit} (critical salinity at which the heart rate is zero) in 2-3 units/hour steps. They found S_{crit} to be 11 in *M.edulis* acclimated to 22 salinity and 14 °C, whereas S_{crit} decreased with decreasing salinity acclimation. But the salinity change per hour was greater and faster than the change mussels experienced in one day in this study. Therefore, no significant changes in heart rates or heart rate variability were found in correlation with salinity. But the possibility exists that a decrease in cardiac performance due to higher pCO_2 was maybe masked by an increase due to rising salinity.

5 Conclusion and Outlook

Decreasing carbonate saturation states, elevated seawater pCO_2 values and decreased pH as a result of anthropogenic CO_2 emissions have already been observed. Furthermore, recent studies predict an even further rise in atmospheric carbon. Drastic impacts especially on the ecophysiological performance of calcifying organisms are expected.

In this work, physiological parameters, i.e. cardiac performance and activity patterns were monitored in adult specimens of the blue mussel, *Mytilus edulis,* exposed to different seawater pCO_2 values for two weeks. It was shown, that heart rates and valve/siphon opening status were not significantly altered by elevated pCO_2. However, a strong decline in filtration activity was evident in the highest pCO_2 treatment (4000 ppm).

This study demonstrated that adult specimens of the blue mussel, *Mytilus edulis*, are well adapted to cope with elevated seawater pCO_2 values (<1400 ppm) during short-term exposure. Cardiac performance and activity patterns were maintained even at 4000 ppm (405 Pa), a carbon dioxide level higher than predicted by current models of ocean acidification (Caldeira and Wickett 2003). This was reflected by unimpaired cardiac activity and activity patterns in response to carbon dioxide, even though calcification continuously decreased with rising pCO_2 (Heinemann et al. unpublished) and extracellular acid-base balance was constrained at 4000 ppm (Thomsen et al. unpublished). Therefore, short-term exposure to pCO_2 values applied in this work was not sufficient to pose a great enough abiotic stress on the animal to elicit metabolic depression. On the other hand, in the highest treatment (4000 ppm) filtration rate was reduced to a minimum, which suggests that the functional capacity of the organism was significantly restricted. Since Widdows (1973) observed a reduction in heart rates in animals starved for 28 days, a longer CO_2 exposure period is probably necessary to trigger a response due to feeding inhibition.

Modelled future scenarios do not include a value as high as 4000 ppm, but due to the special characteristics of the Baltic Sea, i.e. low buffering capacity, ocean chemistry might be even more altered by carbon dioxide emission than in the high-saline oceans. Furthermore, blue mussels are already frequently being exposed to extraordinarily high pCO_2 values resulting from upwelling in Kiel Fjord. On several days, pCO_2 values higher than the predicted values for the year 2300 have been observed reaching up to 2345 ppm (238 Pa; 7.4 pH). Due to its low buffering capacity, future increases in atmospheric CO_2 are most likely to result in pCO_2 values around 3000 ppm in Kiel Fjord. Since *M. edulis* is an important ecosystem engineer, detrimental physiological changes of elevated pCO_2, e.g.

shell dissolution /reduced calcification will have devastating consequences not only for the species, but also for the whole benthic ecosystem in Kiel Fjord.

Hence, long-term studies need to be carried out to titrate those pCO_2 levels, at which filtration rate starts to be impaired. It is expected that cardiac activity and activity patterns will then be reduced concomitantly in response to starvation. In addition to heart rate, stroke volume and oxygen consumption should be included in future studies in order to calculate the cardiac output at different pCO_2 levels, leading to a complete understanding of cardiac performance. Further, more detailed work on the carbon chemistry in the Baltic Sea and on the effects and causes of upwelling in the Kiel Fjord should be carried out in order to give a better estimation of the impact of future ocean acidification.

6 References

Allen J and Schwartz A (1969) A possible biochemical explanation for the insensitivity of the rat to cardiac glycosides. *J. Pharm. Exp. Ther.* 168: 42-46

Ameyaw-Akumfi C and Naylor E (1987) Temporal patterns of shell-gape in *Mytilus edulis*. *Mar. Biol.* 95: 237-242

Anestis A, Lazou A, Pörtner HO and Michaelidid B (2007) Behavioral, metabolic, and molecular stress responses of marine bivalve *Mytilus galloprovincialis* during long-term acclimation at increasing ambient temperature. *Am. J. Physiol. Regul. Integr. Comp. Physiol.* 293: R911-R921

Bahmet IN, Berger VJ and Halaman VV (2005) Heart rate in the blue mussel *Mytilus edulis* (Bivalvia) under salinity change. *Russ. J. Mar. Biol.* 31: 314-317

Bakhmet IN, Berger VJ and Khalaman VV (2005) The effect of salinity change on the heart rate of *Mytilus edulis* specimens from different ecological zones. *J. Exp. Mar. Biol. Ecol.* 318: 121-126

Bamber RN (1987) The effects of acidic sea water on young carpet-shell clams *Venerupis decussata* (L.) (Mollusca : Veneracea). *J. Exp. Mar. Biol. Ecol.* 108: 241-260

Bamber RN (1990) The effects of acidic sea water on three species of lamellibranch molluscs. *J. Exp. Mar. Biol. Ecol.* 143:181–191

Bayne BL (1976) Physiology: II: Circulation. In: Marine mussels: their ecology and physiology. Cambridge University Press, Cambridge, pp. 207-223

Bayne BL, Bayne CJ, Carefoot TC and Thompson RJ (1975) The Physiological Ecology of *Mytilus californianus* Conrad. 2. Adaptations to low oxygen tension and air exposure. *Oecologia* 22, 229-250

Berge JA, Bjerkeng B, Pettersen O, Schaanning MT and Øxnevad S (2006) Effects of increased sea water concentrations of CO_2 on growth of the bivalve *Mytilus edulis* L. *Chemosphere* 62: 681–687

Berntson GG, Bigger JT, Eckberg DL, Grossman P, Kaufmann PG, Malik M, Nagaraja HN, Porges SW, Saul JP, Stone PH and van der Molen M (1997) Heart rate variability: Origins, methods, and interpretive caveats. *Psychophysiology* 34: 623-648

Bibby R, Widdicombe S, Parry H, Spicer J and Pipe R (2008) Effects of ocean acidification on the immune response of the blue mussel *Mytilus edulis*. *Aquat. Biol.* 2: 67-74

Bøhle B (1972) Effects of adaptation to reduced salinity on filtration activity and growth of mussels (*Mytilus edulis* L.). *J. Exp. Mar. Biol. Ecol.* 10: 41-47

Boje R (1965) Die Bedeutung von Nahrungsfaktoren für das Wachstum von *Myilus edulis* L. in der Kieler Förde und im Nord-Ostsee-Kanal. *Kieler Meeresforsch.* 21: 81-100

Booth CE, McDonald DG and Walsh PJ (1984) Acid-base balance in the sea mussel, *Mytilus edulis*. I: Effects of hypoxia and air-exposure on hemolymph acid-base status. *Mar. Biol. Lett.* 5: 347-358

Boutilier RG (2001) Mechanisms of cell survival in hypoxia and hypothermia. *J. Exp. Biol.* 204(18): 3171-3181

Braby CE and Somero GN (2006) Following the heart: temperature and salinity effects on heart rate in native and invasive species of the blue mussels (genus *Mytilus). J. Exp. Biol.* 209: 2554-2566

Caldeira K and Wickett ME (2003) Anthropogenic carbon and the ocean pH. *Nature* 425:365

Clausen I and Riisgård HU (1996) Growth, filtration and respiration in the mussel *Mytilus edulis*: no regulation of the filter-pump to nutritional needs. *Mar. Ecol. Prog. Ser.* 141, 37-45.

Coleman N and Trueman ER (1971) The effect of aerial exposure on the activity of the mussels *Mytilus edulis* and *Modiolus modiolus. J. Exp. Mar. Biol. Ecol.* 7: 295-304

Crowley TJ and Berner RA (2001) Paleoclimate: Enhanced: CO_2 and climate change. *Science* 292: 870-872

Curtis TM, Williamson R and Depledge MH (2000) Simultaneous, long-term monitoring of valve and cardiac activity in the blue mussel *Mytilus edulis* exposed to copper. *Mar. Biol.* 136: 837-846

Davenport J and Woolmingtin AD (1982) A new method of monitoring ventilator activity in mussels and its use in a study of the ventilator pattern of *Mytilus edulis* L. *J. Exp. Mar. Biol. Ecol.* 62: 55-67

De Zwart D, Kramer KJM, Jenner HA (1995) Practical experiences with the biological early warning system ``Mosselmonitor''. *Envir. Toxic Wat. Qual.* 10: 237-247

Depledge MH, Lundebye A-K, Curtis TM, Aagaard A and Andersen BB (1996) Automated interpulse-duration assessment (AIDA): a new technique for detecting disturbances in cardiac activity in selected macroinvertebrates. *Mar. Biol.* 126: 313-319

Depledge MH (1984) Photoplethysmography – A non-invasive technique for monitoring heart beat and ventilation rate on decapods crustaceans. *Comp. Biochem. Physiol.* 77A:.369-371

Depledge, MH and Andersen BB (1990) A computer-aided physiological monitoring system for continuous, long-term recording of cardiac activity in selected invertebrates. *Comp. Biochem. Physiol.* 96A: 473-477

Dickson AG (1981) An exact definition of total alkalinity and a procedure for the estimation of alkalinity and total inorganic carbon from titration data. *Deep-Sea Res.* 28A: 609-623

Dickson AG (1990) Standard potential of the (AgCl + ½ H_2= Ag + HCl (aq)) cell and the dissociation of bisulfate ion in synthetic sea water from 273.15 to 318.15 K. *J. Chem. Therm.* 22: 113-127

Dickson AG and Millero FJ (1987) A comparison of the equilibrium constants for the dissociation of carbonic acid in seawater media. *Deep-Sea Res.* 34: 1733-1743

Dickson AG, Afghan JD and Anderson GC (2003) Reference materials for oceanic CO_2 analysis: a method for the certification of total alkalinity. *Mar. Chem.* 80: 185-197.

Dickson AG, Sabine CL, and Christian JR (2007) Guide to best practices for ocean CO_2 measurements. *PICES Special Publication* 3

Ellington WR (1993) Studies in intracellular pH regulation in cardiac myocytes from the marine bivalve mollusk, *Mercenaria campechiensis*. *Biol. Bull.* 184: 209-215

Espinosa EP and Allam B (2006) Comparative growth and survival of juvenile hard clams, *Mercenaria mercenaria*, fed commercially available diets. *Zoo Biol.* 25: 513–525

Fabry VJ, Seibel BA, Feely RA and Orr JC (2008) Impacts of ocean acidification on marine fauna and ecosystem processes. *ICES J. Mar. Sci.* 65: 1-19

Feely RA, Sabine CL, Lee K, Berelson W, Kleypas J, Fabry VJ and Millero FJ (2004) Impact of Anthropogenic CO_2 on the $CaCO_3$ System in the Oceans. *Science* 305: 362-366 fishes and invertebrates (mid-Atlantic) -- hard clam. United States Fish and Wildlife Service Office of Biological Services Report No. FWS/OBS-82/11.41, and United States Army Corps of Engineers Report No. TR EL-82-4, Washington D.C

Frederich M, DeWachter B, Sartoris FJ and Pörtner HO (2000) Cold tolerance and the regulation of cardiac performance and hemolymph distribution in *Maja squinado* (Crustacea: Decapoda). *Physiol. Biochem. Zool.* 73: 406-415

Gazeau F, Quiblier C, Jansen JM, Gattuso JP, Middelburg JJ and Heip CHR (2007). Impact of elevated CO_2 on shellfish calcification. *Geophys. Res. Lett.* 34: L07603.

Gran G (1952) Determination of the equivalence point in potentiometric titrations of seawater with hydrochloric acid. *Oceanol. Acta* 5:209-218

Gripenberg S (1960) On the alkalinity of Baltic Waters. *J. Cons. Perm. Int. Explor. Mer.* 26: 5-20

Gruner H-E, Hartmann-Schröder G, Kilias R and Moritz M (1993) Band I: Wirbellose Tiere. 3. Teil: Mollusca, Sipunculida, Echiurida, Annelida, Onychophora Tardigradia, Pentastomida. In: Lehrbuch der Speziellen Zoologie. Gruner H-E (eds), Gustav Fischer Verlag, Jena, p.155

Guppy M (2004) The biochemistry of metabolic depression: a history of perceptions. *Comp. Biochem. Physiol. B* 139: 435-442

Guppy M, Fuery CJ and Flanigan JE (1994) Biochemical principles of metabolic depression. *Comp. Biochem. Physiol. B Biochem. Mol. Biol.* 109: 175-89

Gutiérrez JL, Jones CG, Strayer DL and Iribarne OO (2003) Mollusks as ecosystem engineers: the role of shell production in aquatic habitats. *Oikos* 101:79–90

Hall-Spencer JM, Rodolfo-Metalpa R, Martin S, Ransome E, Fine M, Turner SM, Rowley SJ, Tedesco D and Buia M-C (2008) Volcanic carbon dioxide vents show ecosystem effects of ocean acidification. *Nature* 454: 96-99

Hansen HP, Giesenhagen H, and Behrends G (1999) hydrography – seasonal and long-term control of bottom-water oxygen deficiency in a stratified shallow-water coastal system. *ICES Journal of Marine Science* 56: 65-71

Haugan PM and Drange H (1996) Effects of CO_2 on the ocean environment. *Energy Convers. Mgmt* 37: 1019-1022

Helm MM and Trueman ER (1967) Effect of exposure on heart rate of mussel *Mytilus edulis* L. *Comp. Biochem. Physiol.* 21: 171

Hily (1991) Is the activity of benthic suspension feeders a factor controlling water quality in the Bay of Brest? *Mar. Ecol. Progr. Ser.* 69: 179-188

Hjalmarsson S, Wesslander K, Anderson LG, Omstedt A, Perttilä M, and Mintrop L (2007) Distribution, long-term development and mass balance calculation of total alkalinity in the Baltic Sea. *Cont. Shelf Res.* 28: 593-601

Hoegh-Guldberg O, Mumby PJ, Hooten AJ, Steneck RS, Greenfield P, Gomez E, Harvell CD, Sale PF, Edwards AJ, Caldeira K, Knowlton N, Eakin CM, Iglesias-Prieto R, Muthiga N, Bradbury RH, Dubi A and Hatziolos ME (2007) Coral reefs under rapid climate change and ocean acidification. *Science* 318: 1737-1742

Houghton J, Ding Y, Griggs D, Noguer M, van der Linden P and Xiaosu D (2001) Climate Change 2001: The Scientific *Basis* (Contribution of Working Group I to the Third Assessment Report of the IPCC). *Cambridge University Press*, Cambridge.

Howell BJ, Rahn H, Goodfellow D and Herreid C (1973) Acid-base regulation and Temperature in selected Invertebrates as a function of temperature. *Amer. Zool.* 13: 557-563

Hubbard F, McManus J and Al-Dabbas M (1981) Environmental influences on the shell mineralogy of *Mytilus edulis*. *Geo. Mar. Lett.* 1: 267-269

Irisawa H, Norikazu S and Otani M (1967) Effect of Na^+ and Ca^{2+} on the excitation of the *Mytilus* (Bivalve) heart muscle. *Comp. Biochem. Physiol.* 23: 199-212

Jones HD (1968) Some aspects of heart function in *Patella vulgata* L. *Nature* 217:1170-117

Jørgensen CB, Famme P, Kristensen HS, Larsen PS, Møhlenberg F and Riisgård HU (1986a) The bivalve pump. *Mar. Ecol. Progr. Ser.* 34: 69-77

Jørgensen CB, Larsen PS and Riisgård HU (1990) Effects of temperature on the mussel pump. *Mar. Ecol. Progr. Ser.* 64: 89-97

Jørgensen CB, Larsen PS, Møhlenberg F and Riisgård HU (1988) The bivalve pump: properties and modelling. *Mar. Ecol. Prog. Ser.* 45:205-216

Jørgensen CB, Møhlenberg F and Sten-Knudsen O (1986b) Nature of relation between ventilation and oxygen consumption in filter feeders. *Mar. Ecol. Progr. Ser.* 29: 73-88

Kammermeier H (1987) High energy phosphate of the myocardium: concentration versus free energy change. *Basic Res. Cardiol.* 82: 31-36

Kändler R (1959) Hydrographische Beobachtungen in der Kieler Förde 1952-1957. *Kieler Meeresforsch.* 15: 145-156

Kautsky H and van der Maarel E (1990) Multivariate approaches to the variation in phytobenthic communities and environmental vectors in the Baltic Sea. *Mar. Ecol. Prog. Ser.* 60: 169-184

Kautsky N (1982) Growth and size structure in a baltic *Mytilus edulis* population. *Mar. Biol.* 68: 117-133

Kautsky N and Evans S (1987) Role of biodeposition by *Mytilus edulis* in the circulation of matter and nutrients in a Baltic coastal ecosystem. *Mar. Ecol. Progr. Ser.* 38: 201-212

Kiørboe T and Møhlenberg F (1981) Particle selection in suspension-feeding bivalves. *Mar. Ecol. Progr. Ser.* 5: 291-296

Kittner C and Riisgård HU (2005) Effect of temperature on filtration rate in themussel *Mytilus edulis*: no evidence for temperature compensation. *Mar. Ecol. Progr. Ser.* 305: 147-152

Kleiger RE, Stein PK, Bosner MS and Rottman JN (1995) 3. Time-Domain Measurement of Heart Rate Variability. In: Heart Rate Variability. Malik M (eds.), Blackwell Publishing, Berlin

Kobayashi H, Ishibashi K and Noguchi H (1999) Heart rate variability: An index for monitoring and analyzing human autonomic activites. *Appl. Human Sci.* 18:53-59

Koester J, Dieringer N and Mandelbaum DE (1979) Cellular Neuronal Control of the Molluscan Heart. *Amer. Zool.* 19: 103-116

Kohler I, Meier R, Busato A, Neiger-Aeschbacher G and Schatzmann U (1999) Is carbon dioxide (C02) a useful short acting anaesthetic for small laboratory animals? *Lab. Anim.* 33: 155-161

Kramer KJM, Jenner HA and Zwart de Dick (1989) The valve movement response of mussels: a tool in biological monitoring. *Hydrobiol.* 188/189: 433-443

Krijgsman BJ and Divaris GA (1955) Contractile and pacemaker mechanisms of the heart of mollusks. *Biol. Reviews* 30: 1-39

Kurihara H and Shirayama Y (2004) Effects of increased atmospheric CO_2 on sea urchin early development. *Mar. Ecol. Prog. Ser.* 274:161-169.

Kurihara H, Kato S and Ishimatsu A (2007) Effects of increased seawater pCO_2 on early development of the oyster *Crassostrea gigas* . *Aquat. Biol.* 1:91-98.

Langenbuch M and Pörtner HO (2002) Changes in metabolic rate and N excretion in the marine invertebrate *Sipunculus nudus* under conditions of environmental hypercapnia identifying effective acid-base variables. *J. Exp. Biol.* 205: 1153-1160

Lewis, E and Wallace DWR (1998) Program developed for CO_2 system calculations. ORNL/CDIAC-105. Carbon Dioxide Information Analysis Center, Oak Ridge National Laboratory, U.S. Department of Energy, Oak Ridge, Tennessee

Lindinger MI, Lauren DJ and McDonald DG (1984) Acid-base balance in the sea mussel, *Mytilus edulis*. III: Effects of environmental hypercapnia on intra- and extracellular acid-base balance. *Mar. Biol. Lett.* 5:371-381

Lingwood D, Harauz G and Ballantyne JS (2005) Regulation of fish gill Na^+/K^+ ATPase by selective sulfatideenriched raft partitioning during seawater adaptation. *J Biol. Chem.* 280:36545-36550

Lowe GA and Trueman ER (1972) The heart and water flow rates *Mya arenaria* (Bivalvia: Mollusca) at different metabolic levels. *Comp. Biochem. Physiol.* 41A:487-494

Lundebye AK, Curtis TM, Braven J and Depledge MH (1997) Effects of the organophosphorous pesticide, dimethoate, on cardiac and acetylcholinesterase (AChE) activity in the shore crab *Carcinus maenas*. *Aquat. Tox.* 40: 23-36

Maire OM, Amouroux J-M, Duchêne JC and Grémare A (2007) Relationship between filtration activity and food availability in the Meditterranean mussel *Mytilus galloprovincialis*. *Mar. Biol.* 152: 1293-1307

Marshall DJ, Peter R and Chown SL (2004) Regulated bradycardia in the pulmonate limpet Siphonaria (Gastropoda: Mollusca) during pollutant exposure: implication for biomarker studies. *Comp. Biochem. And Physiol.* 139A: 309-316

Mehrbach C, Culberson C, Hawley J and Pytkowicz R (1973) Measurement of the apparent dissociation constants of carbonic acid in seawater at atmospheric pressure. *Limnol. Oceanogr.* 18: 897-907

Meyer HA and Möbius K (1872) Fauna der Kieler Bucht. In: Die Prosobranchia und Lamellibranchia nebst einem Supplement zu den Opistobranchia. Verlag Wilhelm Engelmann, Leipzig.

Michaelidis B, Ouzounis C, Paleras A and Pörtner HO (2005) Effects of long-term moderate hypercapnia on acid-base balance and growth rate in marine mussels *Mytilus galloprovincialis*. *Mar. Ecol. Prog. Ser.* 293: 109-118

Michaelidis B, Rofalikou E and Grieshaber M (1999) The effects of hypercapnia on the force and rate of contraction and intracellular pH of perfused ventricles from the land snail *Helix lucorum* (L.). *J. Exp. Biol.* 202: 2993-3001

Michaelidis B, Spring A and Pörtner HO (2007) Effects of long-term acclimation to environmental hypercapnia on extracellular acid-base status and metabolic capacity in Mediterranean fish *Sparus aurata*. *Mar. Biol.* 150:1417-1429

Miles H, Widdicombe S, Spicer JI and Hall-Spencer, J. (2007) Effects of anthropogenic seawater acidifcation on acid-base balance in the sea urchin *Psammechinus miliaris*. *Mar. Poll. Bull.* 54: 89-96

Møhlenberg F and Riisgård HU (1979) Filtration rate, using a new indirect technique in thirteen species of suspension-feeding bivalves. *Mar. Biol.* 54: 143-147

Mucci A (1983) The solubility of calcite and aragonite in seawater at various salinities, temperatures, and one atmosphere total pressure. *Am. J. Sci.* 283:780

Navarro E, Iglesias JIP, Camachob AOC and Labarta U (1996) The effect of diets of phytoplankton and suspended bottommaterial on feeding and absorption of raft mussels (*Mytilus galloprovincialis* Lmk). *J. Exp. Mar. Biol. Ecol.* 198: 175-189

Newell CR, Wildish DJ and MacDonald BA (2001) The effects of velocity and seston concentration onthe exhalant siphon area, valve gape and filtration rate of the mussel *Mytilus edulis*. *J. Exp. Mar. Biol. Ecol.* 262: 91-111

Newell RIE (1959) Species profiles: Life histories and environmental requirements of coastal fishes and invertebrates (North and Mid-Atlantic): Blue mussel. *Biol. Report* 82: 11.102

Officer CB, Smayda TJ and Mann R (1982) Benthic filter feeding: A natural eutrophication control. *Mar. Ecol. Progr. Ser.* 9: 203-210

Orr J, Fabry V, Aumont O, Bopp L, Doney S, Feely R, Gnanadesikan A, Gruber N, Ishida A, Joos F, Key RM, Lindsay K, Maier-Reimer E, Matear R, Monray P, Mouchet A, Najjar RG, Plattner G-K, Rodgers KB, Sabine CL, Sarmiento JL, Schlitzer R, Slater RD, Totterdell IJ, Weirug M-F, Yamanaka Y and Yool A (2005) Anthropogenic ocean acidifcation over the twenty-first century and its impact on calcifying organisms. *Nature*, 437:681-686

Petit JR, Jouzel J, Raynaud D, Barkov NI, Barnola J-M, Basile I, Bender M, Chappellaz J, Davis M, Delaygue G, Delmotte M, Kotlyakov VM, Legrand M, Lipenkov VY, Lorius C, Pépin L, Ritz C, Saltzman E and Stievenard M (1999) Climate and atmospheric history of the past 420,000 years from the Vostok ice core, Antarctica. *Nature* 399: 429-436

Pörtner HO, Bock C, and Reipschläger A (2000) Modulation of the cost of pH_i regulation during metabolic depression: a (31) P-NMR study in invertebrate (*Sipunculus nudus*) isolated muscle. *J. Exp. Biol.* 203: 2417–2428

Pörtner HO, Langenbuch M, and Reipschläger A (2004) Biological Impact of Elevated Ocean CO_2 Concentrations: Lessons from Animal Physiology and Earth History. *J. Oceanogr.* 60:705-718

Pörtner HO, Reipschläger A and Heisler N (1998) Metabolism and acid-base regulation in *Sipunculus nudus* as a function of ambient carbon dioxide. *J. Exp. Biol.* 201: 43-55

Prins TC, Smaal AC and Dame RF (1998) A review of the feedbacks between bivalve grazing and ecosystem processes. *Aquat. Ecol.* 31: 349–359

Ragnarsson SA and Raffaelli D (1999) Effects of the mussel *Mytilus edulis* L. on the invertebrate fauna of sediments. *J. Exp. Mar. Biol. Ecol.* 241: 31-43

Ravenswaaij-Arts van CMA, Kollee LAA, Hopman JCW, Stoelinga GBA and van Geijn HP (1993) Heart Rate Variability. *Ann. Int. Med.* 118:436-447

Reipschläger A and Pörtner HO (1996) Metabolic depression during environmental stress: the role of extracellular versus intracellular pH in *Sipunculus nudus*. *J. Exp. Biol.* 199: 1801–1807

Riebesell U, Zondervan I, Rost B, Tortell PD, Zeebe RE, and Morel FMM (2000). Reduced calcification of marine plankton in response to increased atmospheric CO_2. *Nature* 407: 364-367

Riisgård HU (1991) Filtration rate and growth in the blue mussel, *Mytilus edulis* Linneaus 1758: Dependence on algal concentration. *J Shellfish Res.* 10: 29-35

Riisgård HU (2001) On measurement of filtration rates in bivalves–the stony road to reliable data: review and interpretation. *Mar. Ecol. Prog. Ser.* 211: 275– 291

Riisgård HU and Randløv A (1981) Energy budgets, growth and filtration rates in *Mytilus edulis* at different algal concentrations. *Mar. Biol.* 61: 227-234

Riisgård HU, Kittner C and Seerup DF (2003) Regulation of opening state and filtration rate in filter-feeding bivalves (*Cardium edule, Mytilus edulis, Mya arenaria*) in response to low algal concentration. *J. Exp. Mar. Biol. Ecol.* 284:105-127

Rodhe J (1998) The Baltic and the North Seas: a process-oriented review of the Physical Oceanography. In: The Sea. Robinson AR and Brink K (Eds.), Vol. 11, Wiley, New York, pp. 699–732

Rumohr H, Brey T and Ankar S (1987) A compilation of biometric conversion factors for benthic invertebrates of the Baltic Sea. The Marine Biologist Publication No. 9

Sabine CL, Feely R, Gruber N, Key R, Lee K, Bullister J, Wanninkhof R, Wong C, Wallace D, Tilbrook B, Millero FJ, Peng T-H, Kozyr A, Ono T and Rios A (2004) The oceanic sink for anthropogenic CO_2. *Science* 305:367_371.

Schlieper C (1955a) Über die physiologische Wirkung des Brackwassers (Nach Versuchen an der Miesmuschel *Mytilus edulis) Kieler Meereswiss.* 11: 22-33

Schlieper C (1955b) Die Regulation des Herzschlages der Miesmuschel *Mytilus edulis* L. bei geöffneten und bei geschlossenen Schalen. *Kieler Meereforsch.* 11: 139-148

Scott DM and Major CW (1976) The effects of copper (II) on survival, respiration and heart rate in the common blue mussels, *Mytilus edulis*. *Biol. Bull.* 143: 678-688

Seed R (1968) Factors influencing shell shape in the mussel *Mytilus edulis*. *J. Mar. Biol. Assoc. UK* 48: 561-584

Seed R and Suchanek TH (1991) Population and community ecology of *Mytilus*. In *The Mussel Mytilus: Ecology, Physiology, Genetics and Culture*, ed. E. Gosling, pp.87 -169, Elsevier, New York

Shumway SE (1977) Effect of salinity fluctuation on the osmotic pressure and Na^+,Ca^{2+} and Mg^{2+} ion concentrations in the hemolymph of bivalve molluscs. *Mar. Biol.* 41: 153-177

Siegenthaler U and Sarmiento JL (1993) Atmospheric carbon dioxide and the ocean. *Nature* 365: 119-125

Spicer JI, Raffo A and Widdicombe S (2007) Influence of CO_2-related seawater acidifcation on extracellular acid-base balance in the velvet swimming crab *Necora puber*. *Mar. Biol.* 151:1117-1125

Stanley JG (1985) Species profiles: life histories and environmental requirements of coastal

Stickle WB and Sabourin TD (1979) Effects of salinity on the respiration and heart rate of the common mussel, *Mytilus edulis,*and the black chiton, *Katherina tunicate* (Wood). *J. Exp. Biol. Ecol.* 41: 257-268

Stoll M, Bakker K, Nobbe G and Haese R (2001) Continuous-flow analysis of dissolved inorganic carbon content in seawater. *Analyt. Chem.* 73: 4111-4116

Storey KB and Storey JM (2004) Metabolic rate depression in animals: transcriptional and translational controls. *Biol. Rev.* 79: 207-233

Sukhotin AA, Abele D and Pörtner HO (2002) Growth, metabolism and lipid peroxidation in *Mytilus edulis*: age and size effects. *Mar. Ecol. Progr. Ser.* 226: 223-234

Task Force of the European Society of Cardiology and the North American Society of Pacing and Electrophysiology (1996) Heart Rate Variability: Standards of Measurement, Physiological Interpretation, and Clinical Use. *Circulation* 93:1043-1065

Teßmann M (2008) Growth responses of *Mytilus edulis* L. to increased athmospheric CO_2 as a preliminary experiment within the frame of the project Cassiopeia. Semester thesis, University of Kiel

Theede H (1963) Experimentelle Untersuchungen über die Filtrationsleistung der Miesmuschel *Mytilus edulis* (L). *Kieler Meeresforsch.* 19: 20-41

Thompson RJ and Bayne BL (1972) Active metabolism associated with feeding in the mussel *Mytilus edulis* L. *J. Exp. Mar. Biol. Ecol.* 9: 111-124

Thomsen J (unpublished) Ion and acid-base regulation in marine invertebrates in response to altered carbonate system parameters. Diplom thesis, University of Kiel

Walsh PJ, McDonald DG and Booth CE (1984) Acid-base balance in the sea mussel, *Mytilus edulis*. II: Effects of hypoxia and air-exposure on intracellular acid-base status. *Mar. Biol. Lett.* 5: 359-369

Wedderburn J, McFadzen I, Sanger RC, Beesley A, Heath C, Hornsby M and Lowe D (2000) The field application of cellular and physiological biomarkers in the mussel *Mytilus edulis*, in conjunction with early life stage bioassays and adult histopathology. *Mar. Poll. Bull.*40: 257-267

Weiss RF (1974). Carbon dioxide in water and seawater: the solubility of a non-ideal gas. *Mar. Chem.* 2: 203-215

Widdows J (1973) Effect of temperature and food on the heart beat, ventilation and oxygen uptake of *Mytilus edulis*. *Mar. Biol.* 20: 269-276

Widdows J and Bayne BL (1971) Temperature acclimation of Mytilus edulis with reference to its energy budget. *J. Mar. Biol. Ass. UK* 51: 827-843

Widdows J and Brinsley M (2002) Impact of biotic and abiotic processes on sediment dynamics and the consequences to the structure and functioning of the intertidal zone. *J. Sea Res.* 48: 143-156

Wilbur KM (1972) Shell formation in mollusks. In: Chemical Zoology. Florkin M and Scheer BT (Eds.), Vol. 2: Mollusca, Academic Press, London

Wilson DP (1981) An experimental search for phytoplanktonic algae producing external metabolites which condition natural sea waters. *J. mar. Biol. Ass. U.K.* 61: 585-607

Wilson R, Reuter P and Wahl M (2005) Musceling in on mussels: new insights into bivalve behavior using vertebrate remote-sensing technology. *Mar. Biol.* 147: 1165-1172

Winter JE (1973) The filtration rate of *Mytilus edulis* and its dependence on algal concentration, measured by a continuous automatic recording apparatus. *Mar. Biol.* 22: 317-328

Wood HL, Spicer JI and Widdicombe S (2008) Ocean acidification may increase calcification rates, but at a cost. *Proc. R. Soc. B* 275: 1767–1773

Woortmann KD (1926) Beiträge zur Nervenphysiologie von *Mytilus edulis*. *Z. vergl. Physiol.* 4: 488-527

Zeebe, RE and Wolf-Gladrow DA (2001) CO_2 in seawater: Equilibrium, kinetics, isotopes. Elsevier Oceanography Series, 65, Amsterdam, pp. 346

Zwaan de A and Wijsmann HE (1976) Anaerobic metabolism in Bivalvia (Mollusca): characteristics of anaerobic metabolism. *Comp. Biochem. Physiol.* 54: 313-324

Acknowledgement/Danksagung

Thanks to: / Ich danke:

Prof. Dr. Frank Melzner für die Betreuung der Diplomarbeit und der stetigen Unterstützung. Besonders möchte ich mich dafür bedanken, dass er in allen Lagen immer ein offenes Ohr für mich hatte.
Dr. Stefan Forster für die freundliche Übernahme des Erstgutachters und die konstruktive Hilfe.
Jörn Thomsen für die tolle Zusammenarbeit bei der Durchführung der Experimente und die wirklich hilfreiche Unterstützung in allen Phasen der Diplomarbeit. Wir waren doch ein super „Dynamisches Duo".
Martin Bielke für die technische Hilfe bei der Installation der Webcams und bei Computer Problemen. Ohne ihn wäre die Arbeit so nicht möglich gewesen.
Steffi Syré für die Hilfe bei der Auswertung der HRV. Danke, dass du so schnell noch ein springen konntest, ansonsten wäre die Auswertung nicht so ausführlich geworden.
Ulrike Panknin für die tatkräftige Hilfe bei der Sektion. Besonders möchte ich mich bei ihr für ihre fröhliche und aufgeschlossene Art bedanken und die geselligen Stunden in ihrem Garten.
Catriona Clemmesen für die Zusammenarbeit im Kühlraum und an der CO_2 Anlage
Susan Grobe für die coulorimetrische Bestimmung von C_T und der Messung von A_T in den letzten beiden Versuchen.
Andrea Ludwig und Michael Meyerhöfer für die Benutzung der Alkalinitätsanlage und für die photometrische Messung von C_T im ersten Versuch.
Peter Wiebe für die Einführung in die Alkalinitätsanalage.
Ferdi Oberheinrich für die kräftige und schnelle Unterstützung bei AD Instruments.
Frank Sommer für die geschenkten Vorratstanks.
Helgi Mempel für das Eis.
Magda Gutowska, Marian Yong-An Hu, Katja Trübenbach und Martina Langenbuch danke für das tolle Arbeitsklima und die seelische Unterstützung.
Agnes Heinemann für die freundliche Bereitstellung ihrer Daten und die zahlreiche Unterstützung.
Meike Stumpp erstmal für ihre wirkliche sehr wertvollen Tipps und Ratschläge sowohl zur Versuchsdurchführung als auch zum Manuskript. Aber ein besonderer Dank gilt an ihre fröhliche Art, die mich oft durch Tiefs bei der Arbeit hinweg half und auf andere Gedanken brachte.
Meinen Freunden Sarah Sokoll, Judith Ficker, Jennifer Nietzke, Robert Grädener, Verena Hanke, Steffi Jaskulke, Svenja Kaden, Marlene Schmiedek und alle die ich vergessen habe für die wunderschöne Studienzeit, ohne euch wäre es bestimmt viel schwerer geworden.
Lennart Bach für die schöne gemeinsame Zeit und die Hilfe bei der Fertigstellung.
Meiner Oma Ilse Saphörster dafür, dass es sie gibt. Danke, dass du immer für mich da bist.
Meiner Schwester Henrike Saphörster dafür dass wir uns immer wieder vertragen. Ich freu mich, dass ich dich habe.

Zu guter Letzt ein ganz besonderer Dank an **meine Eltern Bärbel und Horst**, für Alles, was sie mir bisher ermöglicht haben.

Selbstständigkeitserklärung

Hiermit versichere ich, dass ich die vorliegende Arbeit selbständig verfasst und keine anderen als die angegebenen Quellen (siehe § 25, Abs. 7 der Diplomprüfungsordnung Biologie 2000) und Hilfsmittel verwendet habe.

Mir ist bekannt, dass gemäß § 8, Abs. 3 der Diplomprüfungsordnung Biologie 2000 die Prüfung wegen einer Pflichtwidrigkeit (Täuschung u.ä.) für nicht bestanden erklärt werden kann.

Kiel, den

Julia Saphörster